AD-A121 283 DEVELOPMENT OF A NUMERICAL MODELING CAPABILITY FOR THE COMPUTATION OF UNS.. (U) ARMY ENGINEER WATERWAYS EXPERIMENT STATION VICKSBURG MS HYDRA.. B H JOHNSON 1/2

UNCLASSIFIED AUG 82 WES-TR-HL-82-20 F/G 8/8 NL

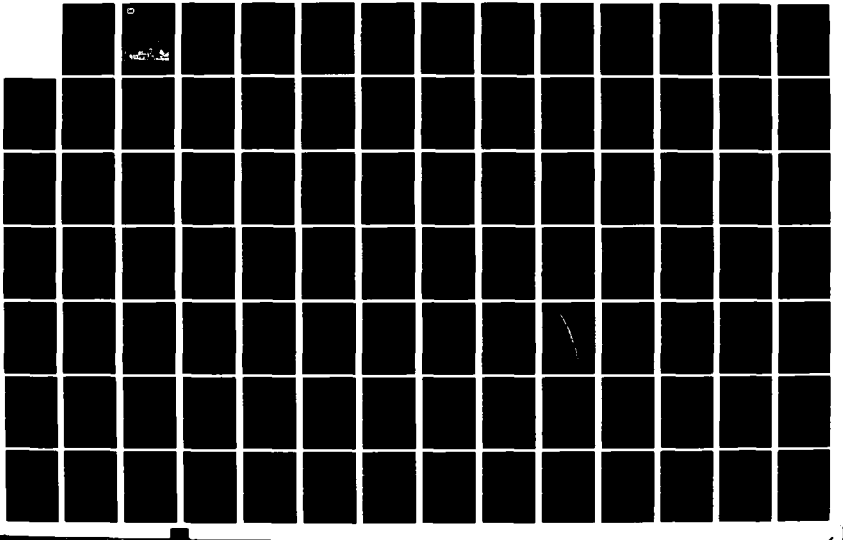

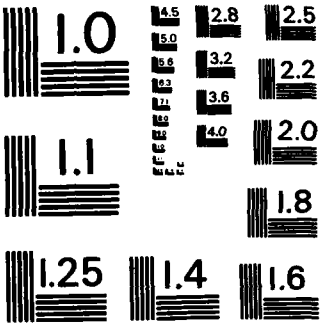

MICROCOPY RESOLUTION TEST CHART
NATIONAL BUREAU OF STANDARDS-1963-A

12

TECHNICAL REPORT HL-82-20

DEVELOPMENT OF A NUMERICAL MODELING CAPABILITY FOR THE COMPUTATION OF UNSTEADY FLOW ON THE OHIO RIVER AND ITS MAJOR TRIBUTARIES

by

Billy H. Johnson

Hydraulics Laboratory
U. S. Army Engineer Waterways Experiment Station
P. O. Box 631, Vicksburg, Miss. 39180

August 1982
Final Report

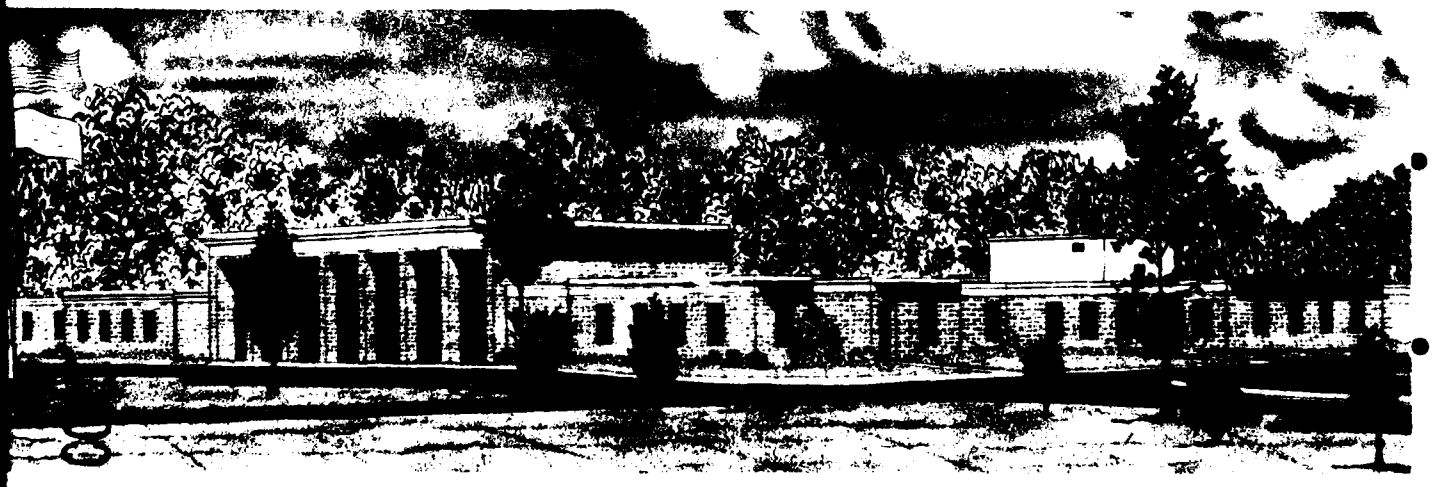

Prepared for U. S. Army Engineer Division, Ohio River
Cincinnati, Ohio 45201

Destroy this report when no longer needed. Do not return it to the originator.

The findings in this report are not to be construed as an official Department of the Army position unless so designated by other authorized documents.

The contents of this report are not to be used for advertising, publication, or promotional purposes. Citation of trade names does not constitute an official endorsement or approval of the use of such commercial products.

Unclassified

SECURITY CLASSIFICATION OF THIS PAGE (When Data Entered)

REPORT DOCUMENTATION PAGE		READ INSTRUCTIONS BEFORE COMPLETING FORM
1. REPORT NUMBER Technical Report HL-82-20	2. GOVT ACCESSION NO.	3. RECIPIENT'S CATALOG NUMBER
4. TITLE (and Subtitle) DEVELOPMENT OF A NUMERICAL MODELING CAPABILITY FOR THE COMPUTATION OF UNSTEADY FLOW ON THE OHIO RIVER AND ITS MAJOR TRIBUTARIES		5. TYPE OF REPORT & PERIOD COVERED Final report 6. PERFORMING ORG. REPORT NUMBER
7. AUTHOR(s) Billy H. Johnson		8. CONTRACT OR GRANT NUMBER(s)
9. PERFORMING ORGANIZATION NAME AND ADDRESS U. S. Army Engineer Waterways Experiment Station Hydraulics Laboratory P. O. Box 631, Vicksburg, Miss. 39180		10. PROGRAM ELEMENT, PROJECT, TASK AREA & WORK UNIT NUMBERS
11. CONTROLLING OFFICE NAME AND ADDRESS U. S. Army Engineer Division, Ohio River P. O. Box 1159 Cincinnati, Ohio 45201		12. REPORT DATE August 1982 13. NUMBER OF PAGES 154
14. MONITORING AGENCY NAME & ADDRESS(if different from Controlling Office)		15. SECURITY CLASS. (of this report) Unclassified 15a. DECLASSIFICATION/DOWNGRADING SCHEDULE

16. DISTRIBUTION STATEMENT (of this Report)

Approved for public release; distribution unlimited.

17. DISTRIBUTION STATEMENT (of the abstract entered in Block 20, if different from Report)

18. SUPPLEMENTARY NOTES

Available from National Technical Information Service, 5285 Port Royal Road, Springfield, Va. 22151

19. KEY WORDS (Continue on reverse side if necessary and identify by block number)

20. ABSTRACT (Continue on reverse side if necessary and identify by block number)

The U. S. Army Engineer Division, Ohio River, directs the operation of flood-control reservoirs as well as navigation locks and dams on the Ohio River and its tributaries. A one-dimensional mathematical model, FLOWSED, for predicting flow conditions on the Ohio River as a result of these activities is discussed. The basic numerical technique used in the

(Continued)

DD FORM 1 JAN 73 1473 EDITION OF 1 NOV 65 IS OBSOLETE

Unclassified

SECURITY CLASSIFICATION OF THIS PAGE (When Data Entered)

20. ABSTRACT (Continued)

model is an extension of work by Y. H. Chen on the upper Mississippi River. As the name implies, FLOWSED computes flow conditions as well as sediment movement. The work reported herein emphasizes the flow computations with coefficients selected to make the sediment transport negligible. FLOWSED is an implicit finite difference model that provides the capability of modeling a system containing any number of tributaries. In addition, FLOWSED models the influence of locks and dams in the system as well as levee overtopping. The system modeled herein consists of the complete Ohio River from Pittsburgh, Pa., through its junction with the Mississippi River plus 12 tributaries. Applications to various portions of the system using observed 1964, 1972, and 1976 flood data have been made and results are presented.

PREFACE

The work described herein and the preparation of this report were conducted during portions of 1978-81 for the U. S. Army Engineer Division, Ohio River (ORD), by the U. S. Army Engineer Waterways Experiment Station (WES) under the general supervision of Messrs. H. B. Simmons, Chief of the Hydraulics Laboratory, and M. B. Boyd, Chief of the Hydraulic Analysis Division (HAD).

Dr. B. H. Johnson, HAD, conducted the study and prepared this report. Mr. Ron Yates, Chief of the Reservoir Control Center, ORD, provided valuable guidance and aided in the data preparation.

Commanders and Directors of WES during the conduct of this study and the preparation and publication of this report were COL John L. Cannon, CE, COL Nelson B. Conover, CE, and COL Tilford C. Creel, CE. Technical Director was Mr. F. R. Brown.

CONTENTS

CONVERSION FACTORS, U. S. CUSTOMARY TO METRIC (SI) UNITS OF MEASUREMENT

U. S. customary units of measurement used in this report can be converted to metric (SI) units as follows:

Multiply	By	To Obtain
cubic feet per second	0.02831685	cubic metres per second
feet	0.3048	metres
miles (U. S. statute)	1.609344	kilometres

DEVELOPMENT OF A NUMERICAL MODELING CAPABILITY FOR THE COMPUTATION OF UNSTEADY FLOW ON THE OHIO RIVER AND ITS MAJOR TRIBUTARIES

PART I: INTRODUCTION

Purpose

1. The U. S. Army Engineer Division, Ohio River (ORD), is responsible for the multipurpose operation of many reservoirs in the Ohio River Basin. During periods of flooding on the lower Ohio and lower Mississippi Rivers, the Division Office issues specific instructions for the operation of Barkley and Kentucky Reservoirs on the Cumberland and Tennessee Rivers, respectively. The primary objective of flood-control regulation by such reservoirs is to reduce the frequency and magnitude of flooding of lands along the Ohio River and its tributaries. In addition, ORD also maintains and operates navigation locks and dams on the Ohio River. At the present time, these structures are operated only for navigation purposes; however, studies are being considered to assess the feasibility of utilizing the pools for hydropower. Obviously, a mathematical model capable of computing unsteady flows on the Ohio River and its major tributaries for different tributary inputs while allowing for the influence of the operation of the navigation locks and dams on the Ohio River would be a useful tool to aid in these activities. The development of such a modeling capability for the ORD was the objective of this study.

Background

2. The study reported herein was in essence an extension of a modeling study that began in 1971. At its twenty-seventh meeting on 19 May 1970, the Mississippi Basin Model (MBM) Board authorized a study to develop computer programs for unsteady flow computations along reaches of the Mississippi River and its larger tributaries. At the

thirty-second meeting on 7 January 1971, in a joint effort with ORD, the U. S. Army Engineer Waterways Experiment Station's area of responsibility was determined to be the lower Ohio River from Louisville, Kentucky, to the junction with the Mississippi River at Cairo, Illinois. Results from this effort were reported by Johnson and Senter (1973) and illustrated the applicability of a finite-difference representation of the unsteady flow equations applied to the lower Ohio River.

3. At the conclusion of the study by Johnson and Senter, it was decided that in order to provide ORD with a model capable of being used to predict stages at Cairo for given release schedules at Barkley and Kentucky Reservoirs, the Cumberland and Tennessee Rivers should be treated as dynamic branches of the system (see Figure 1 for a schematic of the modeled region). In the earlier study, these flows were treated as lateral inflows into the Ohio; therefore, a study was initiated to improve the modeling capability to allow for the modeling of flows in multijunction systems. In addition, it was also considered necessary to obtain more accurate geometric data from the MBM. The one-dimensional mathematical model that resulted from this study was an extension of a model developed at the Tennessee Valley Authority (TVA) by Garrison, Granju, and Price (1969). A brief discussion of the model (called SOCHMJ from Simulation of Open Channel Hydraulics in Multi-Junction Systems) and results from the study are presented by Johnson (1974).

4. As a result of the success enjoyed from the use of SOCHMJ as an aid in determining the operation of Barkley and Kentucky Reservoirs during periods of flooding on the lower Ohio and Mississippi Rivers, ORD then initiated a project to extend the modeling limits to McAlpine Lock and Dam on the Ohio, with the Green and Wabash Rivers being treated as dynamic branches of the system. This effort required developing a capability in SOCHMJ for handling the high-lift locks and dams at Cannelton, Newburgh, and Uniontown as illustrated in Figure 2. Results and a discussion of the lock and dam routine as well as other modifications to SOCHMJ are presented by Johnson (1977).

5. The extension of SOCHMJ to McAlpine Lock and Dam resulted in a

model which simulated approximately 750 river miles,* and computation costs suggested that this size system approached the economic limit for the numerical scheme used in SOCHMJ. This stems from the fact that SOCHMJ utilizes an explicit finite-difference scheme to solve the governing equations. As a result, the computational time-step Δt is restricted by the stability criterion

$$\left(V + \sqrt{g \frac{A}{B}}\right) \frac{\Delta t}{\Delta x} \leq 1 - \frac{gn^2 |V| \Delta t}{2.21 R^{4/3}}$$

where all variables are defined in Appendix C. For values of Δx of 3 to 5 miles on the Ohio River, the time-step is restricted to a maximum of perhaps 5 min. With such a small computational step, computational costs for a larger system would become excessive.

6. After the extension of SOCHMJ to McAlpine Lock and Dam, the ORD expressed an interest in developing a modeling capability for the complete Ohio River from Pittsburgh, Pennsylvania, through its junction with the Mississippi River. Based upon results from the previous study, it was obvious that the use of SOCHMJ was not economically feasible. Therefore, the development of a new modeling capability that would not contain such a restrictive stability criterion was required.

Scope

7. When employing the method of finite differences to solve the governing equations there are two general types of schemes, either an explicit or an implicit scheme. As previously noted, explicit schemes are conditionally stable, whereas implicit schemes are not. In other words, much larger computational time-steps may be employed with an implicit scheme, which of course in general reduces the cost of computations.

8. A one-dimensional, implicit finite-difference model developed

---

* A table of factors for converting U. S. customary units of measurement to metric (SI) units is presented on page 4.

by Chen (1973) and applied to a segment of the upper Mississippi River by Simons et al. (1975) was selected as the base from which an efficient modeling capability for the complete Ohio River Basin (Figure 3) could be developed and provided to ORD. Necessary modifications included the development of input/output routines, the generalization of the basic code to handle a system containing an unlimited number of branches and junctions, and the incorporation of a technique similar to that programmed in SOCHMJ to handle the many high-lift locks and dams in the system. The resulting computer code is called FLOWSED to reflect the fact that both sediment movement and flow are computed. The work reported herein emphasizes the flow computations with coefficients selected to make the sediment transport negligible.

9. In addition to the work required on the basic computer program furnished by Chen (1973) to convert it into an efficient model for use on the Ohio River and its major tributaries, necessary geometry data had to be constructed. These data were constructed from storage volume data collected from the MBM, topographic maps and cross-sectional information furnished by ORD. To convert the data obtained from the latter two sources into the form required by FLOWSED, a computer program called GEOM was written.

10. After the generation of the required tables of geometry data, historical flood data from 1964, 1972, and 1976 were used to calibrate various portions of the system. Such a calibration requires the manipulation of Manning's n and/or geometry data until recorded and computed elevations and discharges are in reasonable agreement.

11. PART II of this report presents a discussion of the governing equations to be solved and underlying assumptions made in their derivation, along with the particular solution technique developed by Chen (1973). In addition, special features such as the handling of navigation dams and levee overtopping are also discussed. A general description of the computer code with special emphasis on the computational cycle and input requirements is presented in PART III. In PART IV, details of the complete Ohio River system and construction of the required geometry data base are presented. PART V presents results from

the calibration effort, while PART VI summarizes the modeling effort and offers recommendations for additional work needed. A listing of the input cards required by FLOWSED is given in Appendix A; Appendix B presents an example of FLOWSED output.

PART II: THEORETICAL DISCUSSIONS

Governing Equations

12. In the case of one-dimensional open-channel flows within rigid boundaries, the flow behavior can be adequately described by the Saint Venant partial differential equations of unsteady flow. These equations are derived by considering the conservation principle for mass and for the momentum of the flows. For mobile boundary channels, three equations are needed to describe the sediment-water mixture: continuity and momentum of the mixture and conservation of mass of the sediment. A detailed derivation of these equations is presented by Chen (1973). Some of the more important features are discussed below.

13. The governing equations are derived for nonprismatic channels with irregular cross sections. The flow field under consideration is assumed to be one-dimensional and the pressure field varies in the vertical direction in a hydrostatic manner. These assumptions imply that the river reach to be modeled should be reasonably straight with the free surface taken to be a horizontal line across the section and that vertical accelerations are negligible. In addition, the density of the water-sediment mixture is homogeneous in the vertical direction.

Sediment continuity equation

14. Considering Figures 4a and 4b, let Q_s be the total volume of sediment transported by the riverflow per unit time, where Q_s is a function of both the longitudinal distance, x, and time, t. Let q_s be the unit rate of volume of sediment entering the river because of lateral inflows into the river as a result of small tributaries or overland flow, where q_s is expressed in volume of sediment per unit length and unit time. Equating the change in the mass of sediment stored within the control volume presented in Figure 4b during the time interval Δt to the difference between the sediment entering and the sediment leaving results in the sediment continuity equation, a statement of which is

Sediment entering - Sediment leaving = Change in sediment stored (1)

15. The change in the storage of sediment within the control volume is effected in two ways; by the deposition or scour of sediment on the riverbed and by the change in the suspended sediment concentration. Assuming that the deposition or scour occurs uniformly over the whole bed area, the mass of sediment per computational cell in a bed layer of thickness ΔZ is $\rho_s(P\Delta Z\Delta x)p$ where ρ_s is density of sediment, P is the wetted perimeter at the section where the control volume is located, and p is the porosity of the bed layer, i.e. the volume of sediment per unit volume of the bed layer. The change in sediment storage due to the change in the suspended sediment concentration taken as an average over the control volume can be expressed as $\rho_s(\partial/\partial t)(A\Delta x C_s)\Delta t$, where A is the cross-sectional flow area and C_s is the suspended sediment concentration.

16. Assuming that $\Delta Z = (\partial Z/\partial t)\Delta t$, the sediment continuity equation expressed as Equation 1 becomes

$$\frac{\partial Q_s}{\partial x} + P\frac{\partial Z}{\partial t}p + \frac{\partial AC_s}{\partial t} = q_s \qquad (2)$$

where Z is the elevation of the channel bed.

Continuity equation for
sediment-water mixture

17. In this case, both the mass of water and sediment are considered together. As for the sediment continuity, the basic equation is expressed over the control volume as

(Sediment-water mixture entering) - (Sediment-water mixture leaving)
= Change in storage of sediment-water mixture (3)

It can be shown that if Q is the total discharge, A is the total cross-sectional area, and q_ℓ is the unit lateral inflow and if Equation 2 is utilized, then the mathematical representation of Equation 3 becomes

$$\frac{\partial Q}{\partial x} + \frac{\partial A}{\partial t} + P \frac{\partial Z}{\partial t} = q_\ell \tag{4}$$

Momentum equation for sediment-water mixture

18. For the control volume in Figure 4a, the equation for the conservation of momentum of the sediment-water mixture can be written as

Net rate of momentum flux into the control volume + Sum of forces
= Rate of accumulation of momentum within the control volume (5)

Once again referring to Chen, the above equation can be written in mathematical terms as

$$\frac{\partial}{\partial t} (\rho Q) \Delta x = - \frac{\partial}{\partial x} \left(\beta \rho \frac{Q^2}{A} \right) \Delta x - \rho q_\ell \frac{Q}{A} \Delta x + \sum \text{forces} \tag{6}$$

where the forces acting on the control volume are gravity, pressure, and frictional resistance, ρ is the density of the sediment-water mixture, and β is the momentum correction factor.

Gravity force

19. The force due to gravity is the weight of the fluid mixture within the control volume. If S_x is the slope of the control volume bottom, then the component of this force along the flow direction becomes

$$\rho g A \Delta x S_x \tag{7}$$

if the flow within the control volume is uniform.

Pressure force

20. The net pressure force along the direction of flow is composed of the pressure forces acting on the two ends of the control volume and the pressure forces in the direction of the flow on the banks due to widening or narrowing along the length of the nonprismatic channels.

Assuming a hydrostatic pressure distribution, it can be shown that the net pressure force acting on the control volume is

$$-\rho g A \frac{\partial Y}{\partial x} \Delta x \tag{8}$$

where Y is the flow depth.

Frictional force

21. The frictional force resisting the motion of the sediment-water mixture acts along the solid boundaries of the channel and is expressed as $-(\tau_o P \Delta x)$, where τ_o is the shear stress and P is the wetted perimeter. Assuming that the expression for the shear stress in steady flow applies in unsteady flows, the frictional force along the direction of flow acting on the control volume can be expressed as

$$-\rho g A S_f \Delta x \tag{9}$$

where S_f is the friction slope. An eddy loss term S_e similar to the friction slope S_f has been added to Chen's basic equation to account for head losses in addition to those due to boundary friction. These losses are due to large-scale eddies formed in the flow at rather abrupt changes in the cross sections along the channel. The eddy loss slope is evaluated using an expression taken from Fread (1976):

$$S_e = \frac{K_e}{2g} \left| \frac{\partial V^2}{\partial x} \right| \tag{10}$$

in which K_e is a nondimensional coefficient of contraction and expansion. Cross sections contracting abruptly in the direction of flow have K_e values ranging from 0 to 0.4, while abruptly expanding cross sections have K_e values ranging from 0.5 to 1.0. The larger coefficients are associated with the more abrupt contractions and expansions of the cross section.

22. Considering Figure 4a, the flow cross-sectional area is given by

$$A = \int_0^Y \xi(x,\eta)\, d\eta \tag{11}$$

Using the Leibnitz rule, one can then compute the time and spatial derivative of A in Equations 2, 4, and 6 as

$$\frac{\partial A}{\partial t} = \int_0^Y \frac{\partial}{\partial t} \xi \, d\eta + \xi(x,Y) \frac{\partial Y}{\partial t} = B \frac{\partial Y}{\partial t} \tag{12}$$

and

$$\frac{\partial A}{\partial x} = \int_0^Y \frac{\partial}{\partial x} \xi \, d\eta + \xi(x,Y) \frac{\partial Y}{\partial x} = A_x^Y + B \frac{\partial Y}{\partial x} \tag{13}$$

where B is the top width of the channel and A_x^Y is the rate of change of area with respect to x with the flow depth Y held constant.

23. Substituting the expressions for the gravity, pressure, and frictional forces as well as the expression for $\partial A/\partial x$ into Equation 6, the conservation of momentum equation for the sediment-water mixture becomes

$$\frac{\partial}{\partial t}(\rho Q) + V \frac{\partial}{\partial x}(\beta \rho Q) + \beta \rho V \frac{\partial Q}{\partial x} - \beta \rho V^2 B \frac{\partial Y}{\partial x}$$

$$+ gA \frac{\partial}{\partial x}(\rho Y) = \rho g A (S_x - S_f - S_e) + \beta \rho V^2 A_x^Y \tag{14}$$

24. Equations 2, 4, and 14 are the equations governing the motion of a sediment-water mixture in open channels in a one-dimensional sense. These equations involve six unknowns; namely, the flow discharge Q, the flow depth Y, the bed elevation Z, the sediment transport rate Q_s, the frictional slope S_f, and the density of the sediment-water mixture, ρ. Other variables such as the lateral inflows, bed porosity,

and geometry data are expected to be known. To achieve closure of the system, three additional relations are required. These are provided by a sediment transport function given as

$$Q_s = C_1 V^{C_2} Y^{C_3} Q \tag{15}$$

Manning's equation which relates the friction slope to the flow and channel characteristics, and an equation of state for the density of the sediment-water mixture given as

$$\rho = \rho_w + C_s(\rho_s - \rho_w) \tag{16}$$

With these additional relations one can then solve for the basic unknowns Q , Y , and Z .

Special Features

Locks and dams

25. To account for the effect of navigation locks and dams, the following equations are utilized to simulate the sediment-water mixture through the locks and dams:

$$Q_{s_{us}} = Q_{s_{ds}} \tag{17}$$

$$Q_{us} = Q_{ds} \tag{18}$$

$$Y_{us} = f(t) \tag{19}$$

where the subscripts us and ds refer to the cells immediately upstream and downstream of the structure. The normal procedure is to input a constant water-level elevation upstream of a lock and dam to reflect the pool elevation the lock operator is expected to maintain, i.e. $f(t)$ = constant . With such a procedure, the flow required to be passed through the structure in order to maintain the upstream elevation

is computed. Theoretically, the operator could then use gate rating curves to make the gate adjustments required to pass the computed flow. In hydropower feasibility studies, one may wish to specify some time variation of a particular pool rather than prescribing a constant value.

Junctions

26. The interaction between the main river and a tributary being handled in a dynamic fashion as opposed to being treated as lateral inflow is simulated by the following continuity and energy equations:

$$Q_3 = Q_2 + Q_1 \tag{20}$$

$$Q_{s_3} = Q_{s_2} + Q_{s_1} \tag{21}$$

$$Z_2 + Y_2 + \frac{V_2^2}{2g} = Z_3 + Y_3 + \alpha_2 \frac{V_3^2}{2g} + (S_f \Delta x)_2 \tag{22}$$

$$Z_1 + Y_1 + \frac{V_1^2}{2g} = Z_3 + Y_3 + \alpha_1 \frac{V_3^2}{2g} + (S_f \Delta x)_1 \tag{23}$$

in which α is the energy correction factor, $S_f \Delta x$ is the energy head loss and subscripts 1, 2, 3, as illustrated below, refer to sections above the confluence on the tributary and main river and below the confluence on the main river.

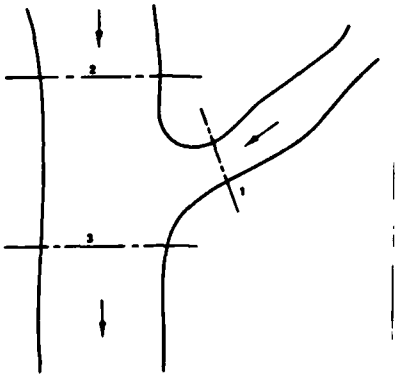

Levees

27. To handle the effect of levee overtopping, the weir equation

$$q = \frac{2}{3} H\Delta x \sqrt{\frac{2}{3} gH} \tag{24}$$

where H is the height of water over the levee, is invoked to compute the unit lateral outflow from the channel whenever the water-surface elevation exceeds the height of the levee. A basic assumption in the current handling of levees is that flow which leaves the channel as a result of levee overtopping is lost from the system.

Overbanks

28. The lateral inflow q_ℓ consists of two components, q_{ℓ_1} and q_{ℓ_2}, induced by the handling of floodplains and tributaries, respectively. For overbank flow on floodplains, q_{ℓ_1} is computed from

$$q_{\ell_1} = - \frac{A_f}{\Delta x \Delta t} \Delta h \tag{25}$$

where A_f is the surface area of the floodplain and Δh is the change over a time period Δt of the water-surface elevation. Similarly, the unit lateral inflow of sediment is also composed of two parts. As the water surface rises, flow onto the floodplain carries sediment along with it. The coarse material is deposited along the riverbank, resulting in an increase of the height of the natural levee. Chen assumes a triangular-shaped natural levee with bottom angles of 30 (face to the main channel) and 15 deg. The increase in height of the natural levee over a time Δt can then be computed from

$$\Delta Z_f = \left\{ \frac{-2 \sum \left(q_{s_1} \Delta t \right)}{P(\cot 15^\circ + \cot 30^\circ)} \right\}^{1/2} \tag{26}$$

where the sediment concentration near the riverbank is assumed to be five times larger than the average concentration C_s. Therefore, the

lateral sand flow associated with overbank flow is determined from

$$q_{s_1} = 5 q_{\ell_1} C_s \tag{27}$$

on the rising side of the hydrograph, but is set to zero on the falling limb as water returns to the channel.

29. In addition to the movement of sandy material, the stream also carries a wash load composed of mainly clays and silts. Chen has selected the following expression for the wash-load discharge on the upper Mississippi River,

$$Q_{WL} = 3.53 \times 10^{-13} Q^{2.752} \tag{28}$$

The deposition of silts and clays on the floodplain is then computed from

$$\Delta Z_{WL} = - \frac{2\left(\sum q_{\ell_1} \Delta t C_{WL}\right)\Delta x}{PA_f} \tag{29}$$

where $C_{WL} = Q_{WL}/Q$ for $q_{\ell_1} < 0$ but is set to zero when $q_{\ell_1} > 0$. Additional discussion of the manner in which sediment deposition on overbank areas is handled is provided by Simons et al. (1975).

Boundary Conditions

30. The governing Equations 2, 4, and 14 constitute a set of first order hyperbolic partial differential equations. As long as the flow regime is subcritical, i.e.

$$V < \sqrt{gY} \tag{30}$$

the following boundary conditions are possible for a well-posed problem.

At an upstream open boundary, either the flow discharge or the water-surface elevation may be prescribed as a function of time. In addition, the sediment discharge hydrograph must either be specified or can be computed internally from the given transport function. At a downstream boundary, either the flow discharge, water-surface elevation, or a rating curve relating the flow discharge and elevation must be prescribed. Unless the downstream boundary coincides with a control structure, the normal procedure is to employ a rating curve as the downstream boundary condition.

Initial Conditions

31. As previously noted, the equations to be solved constitute a hyperbolic system and initial values of the dependent variables must be prescribed to begin the time marching of the solution. A steady-flow profile or perhaps a transient profile from previous computations can be used. The specification of initial conditions is flexible due to the characteristic of hyperbolic equations that the solution becomes independent of initial conditions after a sufficient length of time.

Finite-Difference Representation

32. The governing equations expressing the conservation of sediment and the conservation of mass and momentum of the sediment-water mixture do not in general possess analytic solutions. One must therefore rely upon numerical techniques such as finite differences to obtain solutions. The finite-difference approximations selected by Chen to express the values and the partial derivatives of a function ϕ , where ϕ represents the dependent variables Q , Y , Z , are given as

$$\phi \cong \frac{\phi_i^n + \phi_{i+1}^n}{2} \tag{31}$$

$$\frac{\partial \phi}{\partial x} \cong \frac{\phi_{i+1}^{n+1} - \phi_i^{n+1}}{\Delta x} \tag{32}$$

$$\frac{\partial \phi}{\partial t} \cong \frac{1}{2\Delta t} \left[\left(\phi_i^{n+1} - \phi_i^n \right) + \left(\phi_{i+1}^{n+1} - \phi_{i+1}^n \right) \right] \tag{33}$$

Figure 5 illustrates the positioning of the derivatives in a computational cell.

33. Constructing difference equations from the governing differential equations through use of the finite-difference approximations above results in a linear-implicit finite-difference scheme in which the difference form of the governing equations written over a computational cell formed by sections i and i+1 take the form

$$K_{k1}^n Q_i^{n+1} + K_{k2}^n Y_i^{n+1} + K_{k3}^n Z_i^{n+1} + K_{k4}^n Q_{i+1}^{n+1} + K_{k5}^n Y_{i+1}^{n+1} + K_{k6}^n Z_{i+1}^{n+1} = E_k^n \tag{34}$$

$$K_{\ell 1}^n Q_i^{n+1} + K_{\ell 2}^n Y_i^{n+1} + K_{\ell 3}^n Z_i^{n+1} + K_{\ell 4}^n Q_{i+1}^{n+1} + K_{\ell 5}^n Y_{i+1}^{n+1} + K_{\ell 6}^n Z_{i+1}^{n+1} = E_\ell^n \tag{35}$$

$$K_{m1}^n Q_i^{n+1} + K_{m2}^n Y_i^{n+1} + K_{m3}^n Z_i^{n+1} + K_{m4}^n Q_{i+1}^{n+1} + K_{m5}^n Y_{i+1}^{n+1} + K_{m6}^n Z_{i+1}^{n+1} = E_m^n \tag{36}$$

where $k = 3i$, $\ell = 3i+1$, $m = 3i+2$, and the coefficients K's and E's are functions of known variables from the previous time line.

34. In casting the difference equations into the form shown, it might be noted that the sediment transport function Q_s and the friction slope S_f are expanded in a first order Taylor series, i.e.

$$Q_s^{n+1} \cong Q_s^n + \left(\frac{\partial Q_s}{\partial Q} \right)^n \left(Q^{n+1} - Q^n \right) + \left(\frac{\partial Q_s}{\partial Y} \right)^n \left(Y^{n+1} - Y^n \right) + \left(\frac{\partial Q_s}{\partial Z} \right)^n \left(Z^{n+1} - Z^n \right)$$

$$S_f^{n+1} \cong S_f^n + \left(\frac{\partial S_f}{\partial Q} \right)^n \left(Q^{n+1} - Q^n \right) + \left(\frac{\partial S_f}{\partial Y} \right)^n \left(Y^{n+1} - Y^n \right) + \left(\frac{\partial S_f}{\partial Z} \right)^n \left(Z^{n+1} - Z^n \right)$$

where the partial derivatives are computed by differentiating the analytic expressions for Q_s and S_f. The friction slope is taken at the (n+1) time level in the momentum equation to assure the stability of the scheme.

35. Before briefly discussing the solution technique employed by Chen for solving the algebraic system of equations resulting from Equations 34-36, the manner in which boundary conditions are handled is discussed. Assume that the flow discharge is specified at an upstream boundary, i.e.

$$Q_i = f(t)$$

this equation can be cast into the form

$$K^n_{k4} Q^{n+1}_i + K^n_{k5} Y^{n+1}_i + K^n_{k6} Z^{n+1}_i = E^{n+1}_k \qquad (37)$$

where $K^n_{k4} = 1$, $K^n_{k5} = K^n_{k6} = 0$, and $E^{n+1}_k = f(t)$. The subscript k has the value $k = 3(i-1) + 1$ and thus will be equal to 1 at the first upstream section. As can be seen, Equation 37 is in a form similar to the difference Equations 34-36. Thus, it should be obvious that boundary conditions can be set as part of the overall solution scheme merely by setting the proper coefficients equal to either one, zero, or the proper time varying function on the right-hand side.

36. When specifying a sediment discharge hydrograph at an upstream boundary, i.e.

$$Q_{s_i} = g(t)$$

once again a Taylor series expansion is utilized to cast the equation into the form of the difference Equations 34-36. Therefore,

$$g^{n+1}_i \cong g^n_i + \left(\frac{\partial Q_s}{\partial Q}\right)^n_i \left(Q^{n+1}_i - Q^n_i\right) + \left(\frac{\partial Q_s}{\partial Y}\right)^n_i \left(Y^{n+1}_i - Y^n_i\right) + \left(\frac{\partial Q_s}{\partial Z}\right)^n_i \left(Z^{n+1}_i - Z^n_i\right)$$

is rearranged as

$$K_{\ell 4}Q_i + K_{\ell 5}Y_i + K_{\ell 6}Z_i = E_\ell \qquad (38)$$

in which the subscript i takes on its value at the upstream boundary and $\ell = 3(i-1) + 2$.

37. At a downstream boundary where a rating curve is prescribed, a Taylor series expansion once again enables one to obtain the proper form of the equation. Assuming

$$Q_i \approx f_1(h_i)$$

where i takes its value at the downstream boundary and $h_i = Y_i + Z_i$ is the water-surface elevation, one can write

$$Q_i^{n+1} = Q_i^n + \left(\frac{\partial f_1}{\partial Y}\right)_i^n \left(Y_i^{n+1} - Y_i^n\right) + \left(\frac{\partial f_1}{\partial Z}\right)_i^n \left(Z_i^{n+1} - Z_i^n\right)$$

which can be rearranged as

$$K_{m1}Q_i + K_{m2}Y_i + K_{m3}Z_i = E_m \qquad (39)$$

with $m = 3i$. If the elevation rather than a rating curve is specified, one would set $K_{m1} = 0$ and $K_{m2} = K_{m3} = 1$ with E_m being set to the particular time variation specified.

Solution Technique

38. The solution technique developed by Chen is what is commonly called the double sweep algorithm. To demonstrate the procedure, consider the following problem

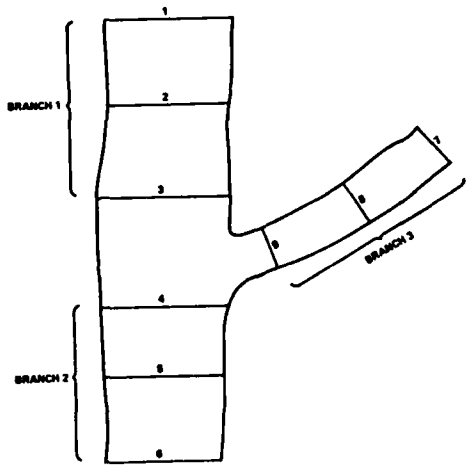

composed of a main river and one tributary. The set of linear equations for branch 1 becomes

$$K_{1,4}Q_1 + K_{1,5}Y_1 + K_{1,6}Z_1 = E_1 \tag{40}$$

$$K_{2,4}Q_1 + K_{2,5}Y_1 + K_{2,6}Z_1 = E_2 \tag{41}$$

$$K_{3,1}Q_1 + K_{3,2}Y_1 + K_{3,3}Z_1 + K_{3,4}Q_2 + K_{3,5}Y_2 + K_{3,6}Z_2 = E_3 \tag{42}$$

$$K_{4,1}Q_1 + K_{4,2}Y_1 + K_{4,3}Z_1 + K_{4,4}Q_2 + K_{4,5}Y_2 + K_{4,6}Z_2 = E_4 \tag{43}$$

$$K_{5,1}Q_1 + K_{5,2}Y_1 + K_{5,3}Z_1 + K_{5,4}Q_2 + K_{5,5}Y_2 + K_{5,6}Z_2 = E_5 \tag{44}$$

$$K_{6,1}Q_2 + K_{6,2}Y_2 + K_{6,3}Z_2 + K_{6,4}Q_3 + K_{6,5}Y_3 + K_{6,6}Z_3 = E_6 \tag{45}$$

$$K_{7,1}Q_2 + K_{7,2}Y_2 + K_{7,3}Z_2 + K_{7,4}Q_3 + K_{7,5}Y_3 + K_{7,6}Z_3 = E_7 \tag{46}$$

$$K_{8,1}Q_2 + K_{8,2}Y_2 + K_{8,3}Z_2 + K_{8,4}Q_3 + K_{8,5}Y_3 + K_{8,6}Z_3 = E_8 \tag{47}$$

and for branch 3

$$K_{19,4}Q_7 + K_{19,5}Y_7 + K_{19,6}Z_7 = E_{19} \tag{48}$$

$$K_{20,4}Q_7 + K_{20,5}Y_7 + K_{20,6}Z_7 = E_{20} \quad (49)$$

$$K_{21,1}Q_7 + K_{21,2}Y_7 + K_{21,3}Z_7 + K_{21,4}Q_8 + K_{21,5}Y_8 + K_{21,6}Z_8 = E_{21} \quad (50)$$

$$K_{22,1}Q_7 + K_{22,2}Y_7 + K_{22,3}Z_7 + K_{22,4}Q_8 + K_{22,5}Y_8 + K_{22,6}Z_8 = E_{22} \quad (51)$$

$$K_{23,1}Q_7 + K_{23,2}Y_7 + K_{23,3}Z_7 + K_{23,4}Q_8 + K_{23,5}Y_8 + K_{23,6}Z_8 = E_{23} \quad (52)$$

$$K_{24,1}Q_8 + K_{24,2}Y_8 + K_{24,3}Z_8 + K_{24,4}Q_9 + K_{24,5}Y_9 + K_{24,6}Z_9 = E_{24} \quad (53)$$

$$K_{25,1}Q_8 + K_{25,2}Y_8 + K_{25,3}Z_8 + K_{25,4}Q_9 + K_{25,5}Y_9 + K_{25,6}Z_9 = E_{25} \quad (54)$$

$$K_{26,1}Q_8 + K_{26,2}Y_8 + K_{26,3}Z_8 + K_{26,4}Q_9 + K_{26,5}Y_9 + K_{26,6}Z_9 = E_{26} \quad (55)$$

Equations 40 and 41 as well as Equations 48 and 49 have the form of the upstream boundary Equations 37 and 38, whereas Equations 42-47 and 50-55 are interior equations of the form of Equations 34-36.

39. Equations 40 and 41 with three unknowns can be reduced to

$$Q_1 = L_{1,2} + L_{1,3}Z_1 \quad (56)$$

$$Y_1 = L_{2,2} + L_{2,3}Z_1 \quad (57)$$

in which the coefficient L's are functions of K's and E's. Substituting Equations 56 and 57 into Equations 42-44 then yields

$$L_{3,3}Z_1 + L_{3,4}Q_2 + L_{3,5}Y_2 + L_{3,6}Z_2 = M_3 \quad (58)$$

$$Q_2 = L_{4,2} + L_{4,3}Z_2 \quad (59)$$

$$Y_2 = L_{5,2} + L_{5,3}Z_2 \quad (60)$$

The same procedure is then used to reduce Equations 45-47 to

$$L_{6,3}Z_2 + L_{6,4}Q_3 + L_{6,5}Y_3 + L_{6,6}Z_3 = M_6 \quad (61)$$

$$Q_3 = L_{7,2} + L_{7,3}Z_3 \quad (62)$$

$$Y_3 = L_{8,2} + L_{8,3}Z_3 \quad (63)$$

by substituting Equations 58-60 into Equations 45-47.

40. The same procedure is now followed on branch 3 to yield first

$$Q_7 = L_{19,2} + L_{19,3}Z_7 \quad (64)$$

$$Y_7 = L_{20,2} + L_{20,3}Z_7 \quad (65)$$

then

$$L_{21,3}Z_7 + L_{21,4}Q_8 + L_{21,5}Y_8 + L_{21,6}Z_8 = M_{21} \quad (66)$$

$$Q_8 = L_{22,2} + L_{22,3}Z_8 \quad (67)$$

$$Y_8 = L_{23,2} + L_{23,3}Z_8 \quad (68)$$

and finally

$$L_{24,3}Z_8 + L_{24,4}Q_9 + L_{24,5}Y_9 + L_{24,6}Z_9 \quad (69)$$

$$Q_9 = L_{25,2} + L_{25,3}Z_9 \quad (70)$$

$$Y_9 = L_{26,2} + L_{26,3}Z_9 \quad (71)$$

41. Before proceeding with the forward sweep in branch 2, the junction must be handled. The confluence Equations 20-23 are written as

$$P_{28}Q_4 + P_{29}Q_3 + P_{30}Q_9 = P_1 \quad (72)$$

$$P_{31}Q_4 + P_{32}Y_4 + P_{33}Z_4 + P_{34}Q_3 + P_{35}Y_3$$

$$+ P_{36}Z_3 + P_{37}Q_9 + P_{38}Y_9 + P_{39}Z_9 = P_2 \quad (73)$$

$$P_{14}Q_3 + P_{15}Y_3 + P_{16}Z_3 + P_{17}Q_4 + P_{18}Y_4 + P_{19}Z_4 = P_{20} \quad (74)$$

$$P_{21}Q_9 + P_{22}Y_9 + P_{23}Z_9 + P_{24}Q_4 + P_{25}Y_4 + P_{26}Z_4 = P_{27} \quad (75)$$

in which the P's are functions of known variables. With the Equations 62, 63, 70, 71, 72, 73, 74, and 75 a set of eight linear equations in nine unknowns is formed. Two equations of the form

$$Q_4 = L_{9,2} + L_{9,3}Z_4 \quad (76)$$

$$Y_4 = L_{10,2} + L_{10,3}Z_4 \quad (77)$$

can then be derived. The forward sweep continues on branch 2 just as performed previously on branches 1 and 3 to finally yield

$$L_{14,3}Z_5 + L_{14,4}Q_6 + L_{14,5}Y_6 + L_{14,6}Z_6 = M_9 \quad (78)$$

$$Q_6 = L_{15,2} + L_{15,3}Z_6 \quad (79)$$

$$Y_6 = L_{16,2} + L_{16,3}Z_6 \quad (80)$$

42. Equations 79 and 80 along with the equation for the downstream boundary of the form of Equation 39 enables one to compute Q_6^{n+1} Y_6^{n+1}, Z_6^{n+1}. The unknown variables at the other nodes are then computed by sweeping backward, e.g. knowing Q_6, Y_6, Z_6 one can compute Z_5 from Equation 78. After computing Q_4, Y_4, Z_4, Equation 74 along with Equations 62 and 63 form a set of three equations and three unknowns from which Q_3, Y_3, Z_3 can be computed. Similarly, Equation 75 along with Equations 70 and 71 enables the computation of Q_9, Y_9, Z_9. The backward sweep can then be continued on each branch until all unknown

variables have been computed. All the coefficients L's and M's in the equations can be computed from recurrence equations and therefore can be easily programmed on a digital computer.

43. As noted by Chen, the double-sweep method offers the following advantages: (a) the computations do not involve any of the many zeros in the coefficient matrix which saves considerable computing time and (b) the computer storage required is reduced from that required for a 3(IMAX) × 3(IMAX) matrix to that of a 3(IMAX) × 6 matrix where IMAX is the total number of nodes.

PART II: DISCUSSION OF THE COMPUTER CODE

44. As previously noted, the computer model is called FLOWSED to reflect the fact that both flow and sediment movement are computed. The basic equations solved in FLOWSED are expressions of the conservation of sediment mass and the conservation of mass and momentum of the sediment-water mixture. Therefore, the dependent variables computed are the flow discharge and depth and the bed elevation, while the independent variables are time and the distance along the channel. The basic solution scheme is an implicit finite-difference scheme in which the resulting system of linear algebraic equations are solved using the double-sweep algorithm.

Input Required

45. With its present structure, all input is read from cards except the geometry data which can be read from a disk file if the user desires. The input data can be broken into 10 groups; namely, general control parameters, plotting, branch information, junction information, locks and dams, coefficients in the sediment transport function and eddy head loss term, initial conditions, information on levees, geometric tables, and boundary conditions. Each is briefly discussed below. A detailed list of the input data is presented in Appendix A.

General control information

46. Several parameters that describe the system being modeled and determine the various forms of output must be input. These include the number of net points, branches, junctions, and locks and dams as well as the numbers of the net points at which printed output is desired. Output can be requested at two different time-step intervals through the specification of a large and small print interval. The small print interval, of course, only occurs for some specified length of time during the computations.

Plotting data

47. CALCOMP plots at as many as 20 net points can be requested.

These plots can consist of only a water-surface elevation, discharge, or velocity time series or various combinations of the three.

Branch information

48. With its present dimension statements, FLOWSED can be applied to a system composed of as many as 29 branches containing a total of less than 400 net points. For each branch, one must input the first and last net points on that branch as well as information related to the type of boundary condition to be applied if the branch contains an open boundary. It is important to note that all branches and corresponding net points on the main river must be numbered before numbering the first tributary. An example of the proper numbering sequence is given below for a system composed of 5 branches and 29 net points.

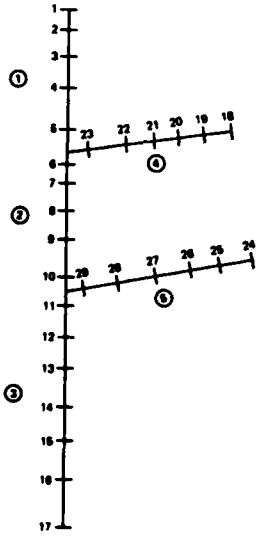

Junction information

49. FLOWSED is currently dimensioned to handle 14 junctions corresponding to the maximum of 29 branches. At each junction one must input the numbers of the three branches composing that junction. Once again it is important to remember the numbering sequence of the branches.

Locks and dams

50. As many as 25 locks and dams can be handled by the current version of FLOWSED. A descriptive title plus the pool elevation to be maintained and the net point immediately upstream must be input. In

addition, through an input parameter one specifies whether either time-varying water-surface elevations or a rating curve will be prescribed later.

Coefficients

51. Coefficients required in the sediment transport function and the eddy head loss term can be prescribed as spatially varying data or can be set equal to constant values if desired. The role of these coefficients can be seen from the expressions presented for S_e and Q_s in Equations 10 and 15.

Initial conditions

52. Initial values of the water-surface elevation, flow discharge, and bed elevation must be input at each net point. Simons et al. (1975) indicate that the bed elevation specified on the upper Mississippi River application corresponded to the deepest 1000-ft width of river channel. Initial values of the discharge and depth are not extremely crucial since their effect is flushed from the system fairly quickly. The time required for a free surface wave traveling at a speed of $\sqrt{gY}$ to traverse the system twice is a good rule of thumb for the time required for initial effects to die out. If lateral inflows are specified, they must also be initially prescribed.

Levee information

53. One can specify that certain reaches contain levees that will be overtopped. The average elevation of the levee top and the upstream net point of the levee must be input. Lateral outflow is then computed from Equation 24.

Geometry data

54. The geometric tables constitute the majority of the input data required by FLOWSED. At each net point in the system a geometric table consisting of three parts must be input. First, a descriptive title, the river mileage, and the bank and bed elevations must be input. Next, the flow area, top width, and Manning's n versus elevation are input for the channel. Finally, the floodplain cross-sectional area and Manning's n versus elevation are input for elevations above the top of the channel. It might be noted that the river mileage of a tributary

must be zero at its junction with the main river. Mileage information is used to compute the computational spatial steps, Δx's .

Boundary conditions

55. If a branch has been specified as one having an open boundary, a boundary condition must be prescribed. At upstream boundaries, the flow and sediment discharge must be specified, although one can request that the sediment discharge be computed internally. At the downstream boundary of the main river, either a rating curve or water-surface elevations must be input. Other required input data are lateral inflows and time-varying pool elevations. At each time-step, the check on time-varying input data follows the order below,

- lateral inflows
- all upstream boundaries
- main river downstream boundary
- pool elevations

Description of Subroutines

56. FLOWSED is composed of a main program that controls the flow of computations and 16 subroutines that perform various functions. A brief description of the role of each is presented below.

LOCKDAM - Sets the coefficients in the equations applied over a computational reach containing a navigation lock and dam. For example, to force the flow discharge to be the same upstream and downstream of a dam the coefficients in the equation

$$C_{\ell,1}Q_i + C_{\ell,2}Y_i + C_{\ell,3}Z_i + C_{\ell,4}Q_{i+1} + C_{\ell,5}Y_{i+1} + C_{\ell,6}Z_{i+1} = E_\ell$$

are set to

$$C_{\ell,1} = 1 \ , \quad C_{\ell,4} = -1 \ , \quad C_{\ell,2} = C_{\ell,3} = C_{\ell,5} = C_{\ell,6} = E_\ell = 0 \ .$$

LINEAR - Linearly interpolates for the flow area, top width, and Manning's n from the geometric tables for a particular water-surface elevation. LINEAR is called many times during the computations.

SEDAREA - Computes the change in the flow area as the result of either erosion or deposition.

FLOOD - Determines the surface area of the floodplain used in computing q_{ℓ_1}

INITIAL - Initializes computations. Various minor computations are performed, e.g. the floodplain area which is input as a cross-sectional area is changed to surface area and the spatial computational steps are computed.

JOINTFR - Joins results from the forward sweep on the main river and a tributary with the confluence equations so that the forward sweep on the main river can then continue.

COEFFIT - As noted in the discussion of the solution scheme, the coefficients in the system of linear algebraic equations are dependent upon information known from the previous time line. These coefficients are computed in COEFFIT.

FORWARD - Computes the coefficients in the forward sweep of the double-sweep solution algorithm.

BACKWARD - Completes the double-sweep algorithm by computing the unknown variables.

NEWFLOW - Called at the end of each time-step to update flow conditions to initiate computations on the next time line.

DAMRC - Computes pool elevations upstream of a lock and dam from a rating curve at the structure.

DOWNCOD - The rating curve at the downstream end of the main river must be cast into the form of the difference Equation 39. This is accomplished by breaking the rating curve up into linear segments. Each linear segment is then defined by specifying the discharge and corresponding elevation at the end of the segment as well as where the segment crosses the elevation axis. From this information the difference coefficients are computed in DOWNCOD.

BRYCAL - Inputs time-dependent boundary data. Either linearly interpolated data or data that have just been read are returned from BRYCAL.

LATERAL - Performs the same function as BRYCAL except that lateral inflows instead of open-boundary data are returned.

COPOUT - Performs the function of grouping output together as well as controlling the punching of restart cards.

PLTOUT - Generates CALCOMP plots, if time-history plots of elevation, flow discharge, or flow velocity are desired.

Computation Cycle

57. As noted, FLOWSED is composed of a main program and 16 subroutines. The main program controls the computational cycle with the various subroutines performing the tasks outlined above. After all input data, except for the time-history of lateral inflows and boundary conditions, have been read and INITIAL has been called, the basic loop in the unsteady flow computations is entered in the main program. Checks are then made to determine if and what type of output is to be printed.

Once the print and/or plot controls have been exercised, LATERAL is called to return updated lateral inflows with a subsequent call to BRYCAL to return new boundary conditions.

58. The next step in the computational cycle is either the specification or computation of the coefficients in the difference equations. Some coefficients are specified in the main program while those influenced by a lock and dam are specified through a call to LOCKDAM. The vast majority of the coefficients are, of course, computed from known conditions through a call to COEFFIT.

59. Once all coefficients have been determined, the double-sweep algorithm is initiated. FORWARD is called for the first branch on the main river and then for the first tributary. JOINTFR is then called to combine the results from the two forward sweeps with the difference form of the confluence equations. FORWARD is then called for the main river branch downstream of the confluence. This procedure is repeated until the downstream end is reached. The backward sweep is then initiated by calling BACKWARD for the last branch on the main river and then the branch on the main river upstream of the last confluence. BACKWARD is then called for the last tributary. This procedure continues until the upstream end of the main river is reached.

60. The final sequence of steps in the computational cycle is the calling of NEWFLOW and a subsequent updating of the velocity, discharge, water depth, etc., arrays in the code. Control is then transferred to the beginning of the computational cycle and the steps outlined above are repeated for the next time-step. After all computations are completed, COPOUT and PLTOUT are called for the handling of output.

Output Furnished

61. Both printed output and time series plots can be obtained from FLOWSED. In the printed output, either a limited form of the output consisting of basically the water-surface elevation, flow discharge and velocity, bed elevation, and sediment discharge at each net point requested is provided or a more detailed listing of output in

which much of the geometric data are listed can be obtained. As previously discussed, time-history plots at as many as 20 net points can be obtained. These plots may consist of elevations and/or discharges and/or velocities. Figure 6 is an example of the form of the plots that can be obtained from FLOWSED, while an example of printed output at one time-step from the limited output mode is presented in Appendix B.

Limitations

62. FLOWSED is a one-dimensional unsteady flow-sediment implicit finite-difference model that can be applied to a fairly general system of open channels containing navigation locks and dams. However, there are limitations to its applicability. FLOWSED can only be applied to a simply connected system, i.e. closed loops within the system cannot be handled. This is illustrated below.

Can be applied

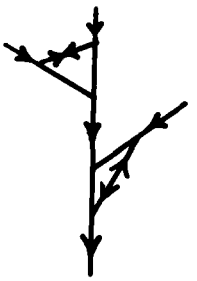

Cannot be applied

63. An additional limitation is that the modeled system must contain at least one tributary. Another restriction on the physical region is that there can only be one downstream boundary. For example, in its present form, FLOWSED cannot be directly applied to a region such as the Mississippi River near the Gulf of Mexico where flow enters the Gulf through several distributaries.

64. A major limitation of the sediment routing capability of FLOWSED is that no provision for a grain-size distribution is allowed. The particular sediment transport function incorporated into FLOWSED was adopted by Chen for use on the upper Mississippi River and has not been

changed. If ORD becomes more interested in the sediment routing capability of FLOWSED, this is an area that deserves additional investigation.

65. In its present form, there is some limitation on the specification of boundary conditions. At an upstream boundary, only flow discharges can be prescribed; whereas at a downstream boundary, either a rating curve or water-surface elevations may be specified. Mathematically, one can specify elevations at an upstream boundary and/or discharges at a downstream boundary but some additional coding would be required to provide these options in FLOWSED. For ORD's use of the model, these options were not needed. It might be noted that all of the limitations discussed could probably be removed without an excessive effort being required except for the incapability of handling closed loops, which would be a major undertaking.

PART IV: DEVELOPMENT OF MODEL INPUT FOR THE OHIO RIVER SYSTEM

Schematization of Physical Region

66. As noted in PART I, a computer model called SOCHMJ has been applied to the lower Ohio River system in previous studies. The first application was to the system shown in Figure 1, whereas a later application extended the model limits to those shown in Figure 2. The Ohio River system to be modeled by FLOWSED included the previous area as well as the remainder of the Ohio River up to Pittsburgh, Pennsylvania, and portions of the Kentucky, Great Miami, Licking, Scioto, Big Sandy, Kanawha, and Muskingham Rivers as routed tributaries. Figure 7 presents a schematic of the total system to be modeled, including the location of the navigation locks and dams. Table 1 presents a description of the branches comprising the system while Table 2 lists the pool elevations maintained by the locks and dams in Figure 7. It should be noted that the locks and dams shown represent the system as it existed in 1981. In the applications to be presented later which use historical data, some of the structures had not been constructed and thus were not included in those applications. For example, the status of the system in May 1974 is illustrated in Figure 8.

Development of Geometry Data

67. The geometric tables required by FLOWSED were constructed using data from the Mississippi Basin Model and cross-sectional data furnished by ORD. The bulk of the data downstream from McAlpine Lock and Dam were storage volume data collected from the MBM during the early 1970's. These data were collected by partitioning the river into small reaches through the use of sheet-metal dividers. Water was then released into the individual segments at a known rate for a known length of time with subsequent measurements of the elevation and water-surface top widths. Knowing the length of the segment, along with an estimate

of the top of the bank elevation, tables of both channel and floodplain geometry could then be constructed.

68. While the majority of the tables on the lower Ohio River were constructed from MBM data, those above McAlpine Lock and Dam were constructed from cross-sectional data cards furnished by ORD. To convert these data into the tabular form required by FLOWSED, a computer program called GEOM was written. The rationale behind GEOM can best be illustrated by considering the figure below

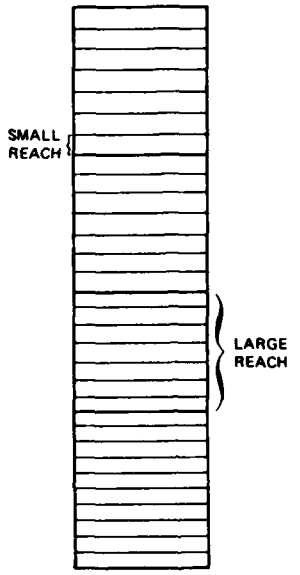

Assume that cross-sectional data have been provided at each of the sections bounding what is referred to as a small reach above. Furthermore, assume that one wishes to generate tabular data that are an average over a large reach. GEOM uses the trapezoidal rule to compute the channel area at various elevations for each cross section. This area multiplied by the length of the channel yields the channel volume in a small reach at a particular elevation. Similarly, GEOM also computes the overbank areas and associated overbank volume at particular elevations in the floodplain for each small branch. These computations begin at the downstream end and proceed up the river until the last small reach is encountered.

69. GEOM then checks to determine the limits of each large reach. Within each large reach, the small reach volumes are summed at the

elevation entries associated with the extreme downstream section of the large reach. This of course normally requires interpolation among the elevation entries of each small reach. The total channel and overbank volumes are then divided by the length of the large reach to yield the average cross-sectional data of the large reach at particular elevations.

70. As shown in Table 1, 12 tributaries are modeled in the Ohio system. It should be noted, however, that much of the geometry data on the upper tributaries was constructed from crudely estimated cross sections that were often considered as small rectangular channels.

71. The complete Ohio system schematized in Figure 7 covers in excess of 1,600 river miles and consists of 25 branches, 12 junctions, 20 navigation locks and dams, and 352 net points. These points are irregularly spaced and are separated by distances ranging from perhaps 10 miles on the lower Ohio and Mississippi Rivers to 5 miles in the upper portions of the model. Of course, the net points surrounding locks and dams and tributary-main river junctions are much closer together.

Lateral Inflow Points

72. Lateral inflows were furnished by ORD as either gaged or ungaged data. The gaged flows represent flow from small rivers such as the Little Kanawha which are not handled as routed branches. The ungaged data are normally given as flow to be distributed over relatively large reaches of the Ohio River, e.g. the Pittsburgh to Wheeling reach. Based upon an inspection of navigation maps showing natural drainage lines into the Ohio River, the distribution of ungaged lateral inflows presented in Table 3 has been prescribed. The gaged inflow points are shown in Table 4.

PART V: APPLICATIONS OF FLOWSED TO THE OHIO RIVER SYSTEM

73. FLOWSED has been applied to the complete Ohio River system in a calibration mode. Calibration runs were made for historical floods in 1964, 1972, and 1976. The applications have been made in a segmented fashion using data furnished by ORD for different reaches of the system. In each of these applications, the values for the friction coefficient, i.e. Manning's n, were varied along the channel as well as with water-surface elevation until sufficient agreement between recorded and computed water-surface elevations and flow discharges was realized. The final n values generally ranged between 0.025 to 0.035, and tended to decrease with stage. In all applications, the coefficient C_1 in the sediment transport function given by Equation 15 was taken to be 1/10 of the value used by Chen on the Mississippi River to minimize the effect of the sediment computations on the flow. This was done because at the present time the primary interest in FLOWSED is as a flow model.

Application from Pittsburgh to Parkersburg Using 1972 Data

74. Figure 9 shows that portion of the Ohio River system extending from Pittsburgh to Parkersburg on a larger scale than shown in Figure 7. As can be seen, neither the Hannibal nor the Willow Island Locks and Dams had been constructed and thus the low-lift Locks and Dams 12-17 shown had to be considered. Table 5 lists the pool elevations maintained by these structures.

75. In analyzing the 1972 data, it was observed that after control was expected to have been lost at Emsworth and Dashields Locks and Dams, the difference in the upstream and downstream elevations at each structure indicated that the flow could not be treated as being free. In discussions with personnel from ORD it was suggested that internal rating curves be used at these structures. These are presented in Table 6.

76. Figure 10 is a plot of the inflow hydrographs prescribed at Pittsburgh and McConnelsville along with the lateral inflow, while

Figure 11 reflects the elevation hydrograph prescribed at Parkersburg. Initial conditions were a steady-state condition obtained by applying FLOWSED with the boundary conditions occurring on 20 June held constant.

77. Results from the application are presented in Figures 12-27 in which a comparison of recorded and computed water-surface elevations are shown. In general, agreement to within 1 ft is realized. Again, it should be stressed that these results were obtained after several runs were made in which Manning's n was varied from one run to the next. The computational time-step for all applications was 1 hr.

Application from Parkersburg to Huntington Using 1964 Data

78. Figure 28 is a location map of the Parkersburg to Huntington reach. As can be seen from a comparison of Figures 7 and 28, of the current high-lift locks and dams only Gallipolis existed in 1964. In addition to Gallipolis, Lock and Dam 22 with a pool elevation of 551.4 ft and Winfield Lock and Dam on the Kanawha River with an upstream pool elevation of 566.0 ft were also in the system.

79. The boundary inflow hydrographs at Parkersburg and at Charleston on the Kanawha River are presented in Figure 29 while Figure 30 shows the lateral inflow. The lateral inflow data were varied substantially during the calibration effort in order to obtain better matching of the recorded and computed water-surface elevations or discharges presented in Figures 31-36. ORD personnel have indicated that such a variation is hydrologically acceptable. Recorded elevations were prescribed as the downstream boundary condition at Huntington. Agreement between computed and recorded elevations is generally in the 1-ft range. However, as illustrated in Figure 36, poor agreement was realized in the peak discharge at Huntington.

Application from Huntington to McAlpine Using 1964 Data

80. The Parkersburg to McAlpine reach, for which 1964 data were available, was broken into two reaches for calibration purposes with the

belief that perhaps the calibration effort could be accomplished more easily by treating each reach separately. Figure 37 is a location map for the Huntington-McAlpine reach. Meldahl Lock and Dam was not included because the recorded elevations showed that the normal Meldahl pool elevation of 485 ft was not maintained and thus the flow was not controlled.

81. Because this application was essentially coupled with that of the Parkersburg to Huntington reach, computed flow discharges at Huntington were taken from the previous application and prescribed as the upstream boundary condition on the Ohio. Recorded discharges were input on the Big Sandy, Scioto, Licking, Great Miami, and Kentucky Rivers. The boundary inflow hydrographs are presented in Figure 38 while the downstream boundary elevations at McAlpine are given in Figure 39. As shown in the lateral inflow hydrographs in Figures 40-43, the ungaged lateral inflows were varied as in the previous application in order to increase the matching of the computed and recorded water-surface elevations and discharges presented in Figures 44-58. As in the upstream applications discussed above, computed and recorded elevations generally agree to within 1 ft. The one exception is at the gage upstream of Meldahl Lock and Dam. As observed at Huntington, poor agreement in peak discharge was realized at Cincinnati and at McAlpine Lock and Dam.

Application from McAlpine to Caruthersville Using 1976 Data

82. The lower Ohio River from McAlpine Lock and Dam through its junction with the Mississippi River to Caruthersville, Missouri, was calibrated using 1976 data. The location map in Figure 59 shows that the Green, Wabash, Cumberland, Tennessee, and upper Mississippi Rivers were all handled as routed tributaries. All locks and dams that currently exist except Smithland were in place in 1976 and thus were considered in the application.

83. Recorded flow discharges were input as the boundary conditions at all upstream boundaries while the rating curve given in Table 7 was

prescribed as the downstream boundary at Caruthersville. The boundary inflow hydrographs are presented in Figure 60 while the lateral inflow hydrographs are given in Figures 61-65. Once again the lateral flows were adjusted to achieve better matching. Results from the calibration exercise are presented in Figures 66-78. Generally, agreement between recorded and computed results is not as good as in the upstream reaches. A major reason is probably the effect of the large floodplains that are encountered in the lower Ohio River.

Tributary Results

84. All results presented up to now for each of the applications have been only at gages on the Ohio River. Results obtained on the tributaries were quite dependent on the quality of the geometry data. For tributaries such as the Big Sandy, Cumberland, Tennessee, and upper Mississippi Rivers on which relatively good geometry data were available, results were comparable to those obtained on the Ohio River, e.g. see Figures 79-82. However, on tributaries such as the Scioto River where the geometry data were quite crude, results were not as good, e.g. see Figure 83. In addition to the geometry problem, average daily values of inflow are not sufficient on most of the tributaries to properly represent the inflow hydrograph.

PART VI: SUMMARY AND RECOMMENDATIONS

Summary

85. Using a computer code developed by Chen for use on the upper Mississippi River as the base, a one-dimensional model for open-channel unsteady flow computations on the complete Ohio River system has been developed. As the name FLOWSED implies, computations for both flow and sediment movement are made by employing a sediment transport function that is dependent upon the flow velocity and depth. FLOWSED is a relatively general implicit finite-difference model that can be applied to a system containing any number of tributaries as well as navigation locks and dams.

86. The major limitation in FLOWSED's use is that it can only be applied to simply connected systems. In other words, multiple connected systems containing closed loops cannot be handled, nor can distributary channels. Other limitations such as those imposed by the particular form of the sediment transport function exist but could be removed without excessive effort as the need arises.

87. FLOWSED has been applied to the complete Ohio River system, broken into four separate segments, in a calibration mode. Historical data from three separate floods (1964, 1972, 1976) were utilized. The results on the Ohio River were excellent at some gages and encouraging at others. However, results on some of the tributaries where crude geometry data were employed were rather poor.

Recommendations

88. The normal procedure in the development of a numerical model for use as a predictive tool is to apply the model first in a calibration effort using data that represent the system as it currently exists. After the model has been calibrated, a separate set of data is then utilized in a verification application. This procedure has not been accomplished in this study. Therefore, it is recommended that two sets

of historical data for the complete Ohio River system be assembled. These data should reflect flows in the system as it currently exists if possible. In addition, it should be noted that based upon the calibration effort to date, daily averaged inflows on the tributaries as well as at the upper limit of the Ohio River at Pittsburgh are inadequate (i.e., flows should be given a shorter time interval, preferably hourly).

89. After assembling the two sets of historical data, FLOWSED should be recalibrated using one set of data and verified using the second set. If refined geometry data are available on the tributaries, these should be employed. In this effort it is suggested that FLOWSED be applied to the complete system rather than in a segmented fashion as was done in the present study.

90. Other recommendations center around suggested improvements to the computer code. To better handle flows through river bends and floodways, e.g. the New Madrid Floodway near the Ohio-Mississippi junction, work done at SOGREAH in France (1978) should be investigated. Such work centers around the use of two-dimensional cells in floodplains which are connected with the normal one-dimensional channel computations. In addition, minor limitations of the current version of the model such as forcing the modeled system to contain at least one tributary should be removed.

REFERENCES

Chen, Y. H. 1973 (Mar). "Mathematical Modeling of Water and Sediment Routing in Natural Channels," Ph. D. Dissertation at Colorado State University, Fort Collins, Colo.

Fread, D. L. "Theoretical Development of Implicit Dynamic Routing Model," presented at Dynamic Routing Seminar, Lower Mississippi River Forecast Center, Slidell, La., 13-17 Dec 1976.

Garrison, M. J., Granju, J.-P., and Price, T. J. 1969 (Sep). "Unsteady Flow Simulation in Rivers and Reservoirs--Applications and Limitations," Journal, Hydraulics Division, American Society of Civil Engineers, Vol 95, No. HY5, p 1559; presented at ASCE Hydraulics Division Specialty Conference; Cambridge, Mass., 21-23 Aug 1968.

Johnson, B. H. 1974 (Sep). "Unsteady Flow Computations on the Ohio-Cumberland-Tennessee-Mississippi River System," Technical Report H-74-8, U. S. Army Engineer Waterways Experiment Station, CE, Vicksburg, Miss.

_____. 1977 (Oct). "A Mathematical Model for Unsteady-Flow Computations Through the Complete Spectrum of Flows on the Lower Ohio River," TR-77-18, U. S. Army Engineer Waterways Experiment Station, CE, Vicksburg, Miss.

Johnson, B. H., and Senter, P. K. 1973 (Jun). "Flood Routing Procedure for the Lower Ohio River," MP-H-73-3, U. S. Army Engineer Waterways Experiment Station, CE, Vicksburg, Miss.

Simons, D. B., et al. 1975 (Jul). "Environmental Inventory and Assessment of Navigation Pools 24, 25, and 26, Upper Mississippi and Lower Illinois Rivers," CR-Y-75-3, U. S. Army Engineer Waterways Experiment Station, CE, Vicksburg, Miss.

SOGREAH Consulting Engineers. 1978 (Oct). "Modelling of Unsteady Flow in River and Flood Plain Networks Using the CARIMA System," In-house report, France.

Table 1

Schematization of the Ohio System

Branch No.	First Net Point	Last Net Point	Description
1	1	63	Ohio R. from Pittsburgh to Muskingham R.
2	64	85	Ohio R. from Muskingham R. to Kanawha R.
3	86	100	Ohio R. from Kanawha R. to Big Sandy R.
4	101	111	Ohio R. from Big Sandy R. to Scioto R.
5	112	140	Ohio R. from Scioto R. to Licking R.
6	141	145	Ohio R. from Licking R. to Great Miami R.
7	146	157	Ohio R. from Great Miami R. to Kentucky R.
8	158	194	Ohio R. from Kentucky R. to Green R.
9	195	205	Ohio R. from Green R. to Wabash R.
10	206	217	Ohio R. from Wabash R. to Cumberland R.
11	218	220	Ohio R. from Cumberland R. to Tennessee R.
12	221	230	Ohio R. from Tennessee R. to Mississippi R.
13	231	243	Lower Mississippi R. to Caruthersville, Mo.
14	244	257	Muskingham R.
15	258	271	Kanawha R.
16	272	280	Big Sandy R.
17	281	295	Scioto R.
18	296	305	Licking R.
19	306	315	Great Miami R.
20	316	324	Kentucky R.
21	325	331	Green R.
22	332	338	Wabash R.
23	339	342	Cumberland R.
24	343	346	Tennessee R.
25	347	352	Upper Mississippi R.

Table 2

Locks and Dams in Ohio System

Lock and Dam	Pool Elevation ft NGVD	Upstream Net Point
Emsworth	710.0	4
Dashields	692.0	9
Montgomery	682.0	17
New Cumberland	664.5	25
Pike Island	644.0	33
Hannibal	623.0	46
Willow Island	602.0	58
Belleville	582.0	70
Racine	560.0	78
Gallipolis	538.0	89
Greenup	515.0	108
Meldahl	485.0	133
Markland	455.0	153
McAlpine	420.0	167
Cannelton	383.0	182
Newburgh	358.0	190
Uniontown	342.0	202
Smithland	320.0	214
Lock & Dam 52	302.0	225
Winfield	566.0	263

Table 3

Ungaged Lateral Inflow Distribution

Net Point	Ungaged Reach	Percent of Flow
3	Pittsburgh-Wheeling	5
8	Pittsburgh-Wheeling	5
10	Pittsburgh-Wheeling	5
13	Pittsburgh-Wheeling	5
16	Pittsburgh-Wheeling	7
20	Pittsburgh-Wheeling	13
24	Pittsburgh-Wheeling	13
28	Pittsburgh-Wheeling	17
32	Pittsburgh-Wheeling	30
		100
36	Wheeling-St. Mary	18
40	Wheeling-St. Mary	13
45	Wheeling-St. Mary	16
51	Wheeling-St. Mary	30
55	Wheeling-St. Mary	23
		100
67	St. Mary-Pomeroy	10
68	St. Mary-Pomeroy	10
73	St. Mary-Pomeroy	30
76	St. Mary-Pomeroy	20
77	St. Mary-Pomeroy	10
79	St. Mary-Pomeroy	20
		100
81	Pomeroy-Huntington	20
83	Pomeroy-Huntington	10
84	Pomeroy-Huntington	10
87	Pomeroy-Huntington	10
91	Pomeroy-Huntington	20
97	Pomeroy-Huntington	30
		100
105	Huntington-Maysville	30
114	Huntington-Maysville	10
120	Huntington-Maysville	30
124	Huntington-Maysville	30
		100
129	Maysville-Cincinnati	30
132	Maysville-Cincinnati	40
138	Maysville-Cincinnati	30
		100
147	Cincinnati-Markland	20
151	Cincinnati-Markland	80
		100
160	Markland-McAlpine	50
165	Markland-McAlpine	50
		100
174	McAlpine-Evansville	22
177	McAlpine-Evansville	12
180	McAlpine-Evansville	33
189	McAlpine-Evansville	33
		100
201	Evansville-Golconda	50
210	Evansville-Golconda	50
		100
213	Golconda-Metropolis	14
215	Golconda-Metropolis	14
219	Golconda-Metropolis	14
223	Golconda-Metropolis	58
		100
225	Metropolis-Cairo	50
228	Metropolis-Cairo	50
		100
347	Thebes-Cairo	50
349	Thebes-Cairo	50
		100

Table 4

Gaged Inflow Points

Net Point	Description of Inflow
13	Beaver River
66	Little Kanawha River
69	Hocking River
96	Guyandot River
99	Twelve Pole Creek
106	Little Sandy River
111	Little Scioto River
140	Little Miami River
171	Salt River

Table 5

Pool Elevations Maintained by Low-Lift Structures in Pittsburgh-Parkersburg Reach

Structure	Pool Elevation Maintained ft NGVD
Lock & Dam 12	626.5
Lock & Dam 13	616.2
Lock & Dam 14	610.7
Lock & Dam 15	602.3
Lock & Dam 16	594.3
Lock & Dam 17	586.9

Table 6

Rating Curves Applied at Emsworth and Dashields

EMSWORTH		DASHIELDS	
Elevation ft NGVD	Discharge cfs	Elevation ft NGVD	Discharge cfs
707.7	37,500	695.25	32,500
709.2	56,000	698.1	110,000
711.3	175,000	700.5	170,000
721.5	385,000	713.5	385,000
715.0	280,000	708.0	300,000
713.0	222,000	703.75	215,000
711.6	180,000	700.3	160,000
710.0	152,500	699.3	140,000
709.9	130,000	695.25	32,500
709.0	117,500		
708.0	100,000		
707.75	75,000		

Table 7

Rating Curve Employed at Caruthersville*

Elevation ft NGVD	Discharge cfs
255.0	200,000
257.0	320,000
259.0	440,000
261.00	575,000
263.0	700,000
265.0	820,000
267.0	940,000
269.0	1,050,000
271.0	1,170,000
273.0	1,290,000
275.0	1,410,000
277.0	1,550,000
279.0	1,710,000
281.0	1,920,000
283.0	2,240,000
285.0	2,900,000

* Obtained from data provided by the U. S. Army Engineer District, Memphis.

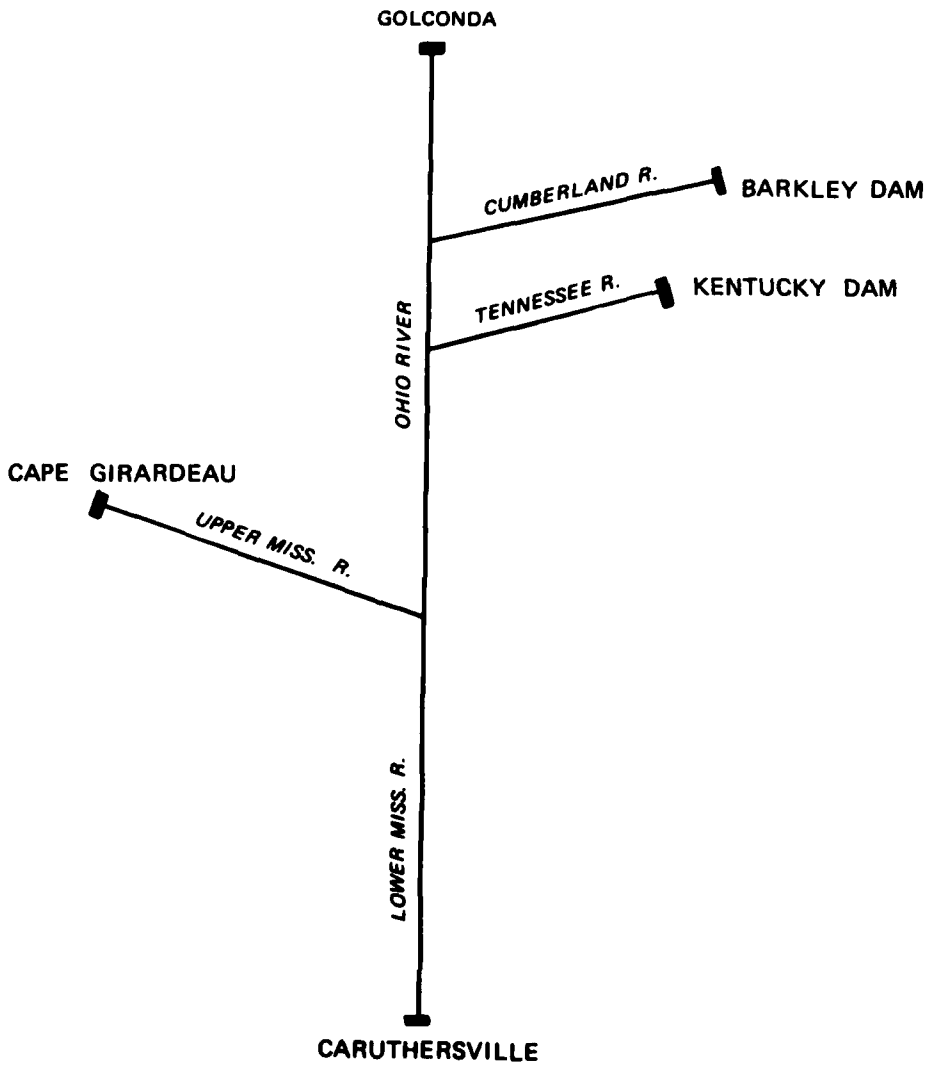

Figure 1. Physical limits of first application of SOCHMJ

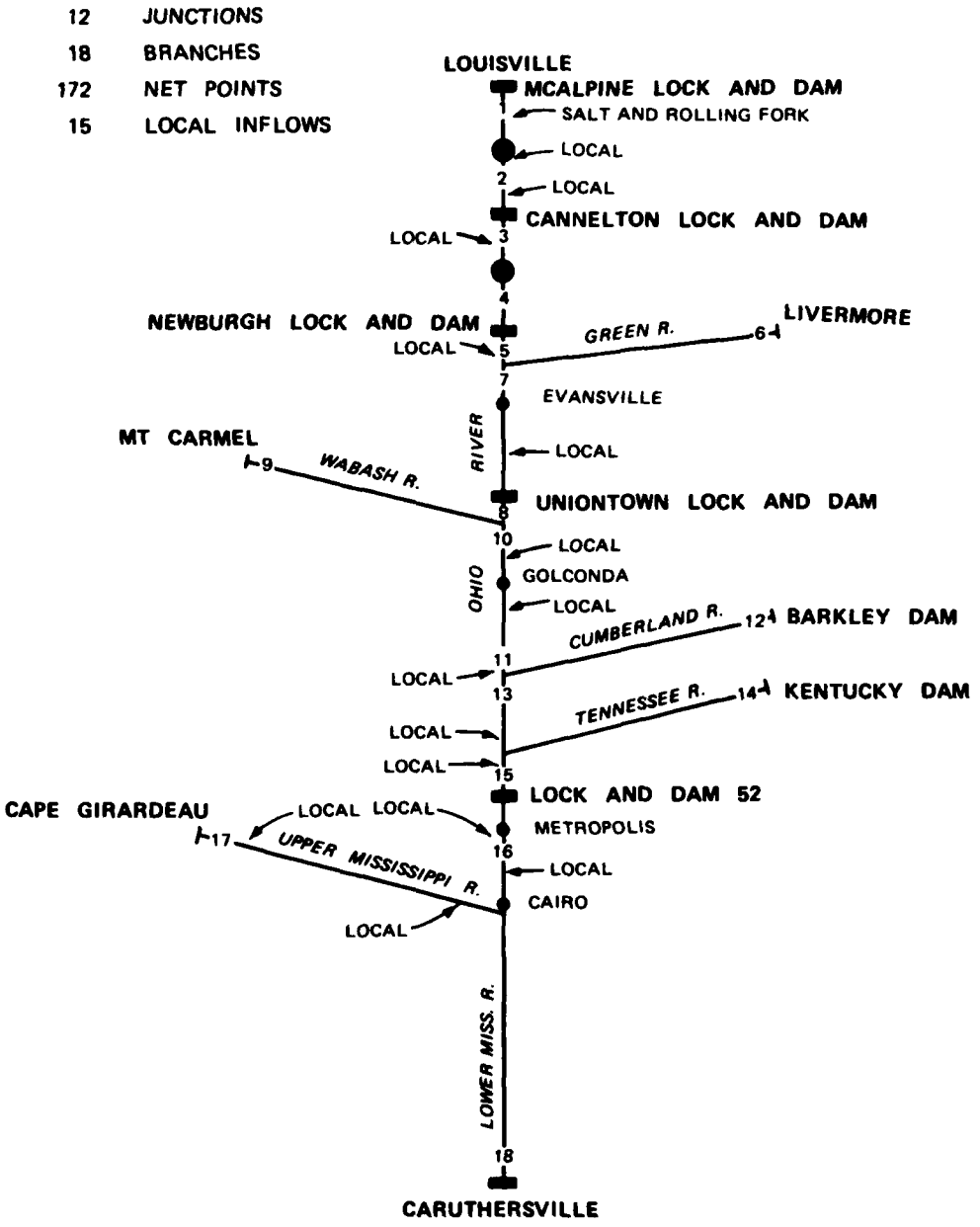

Figure 2. Physical limits of second application of SOCHMJ

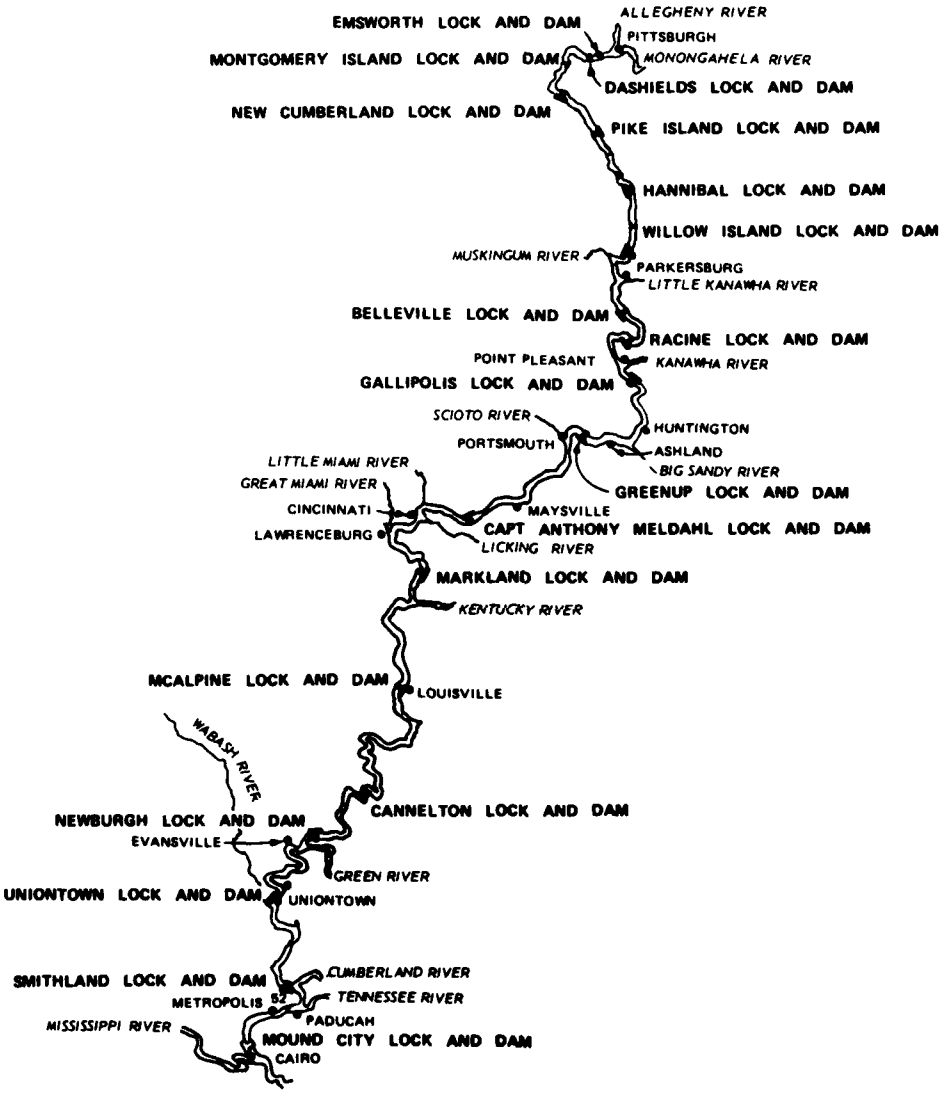

Figure 3. Ohio River Basin

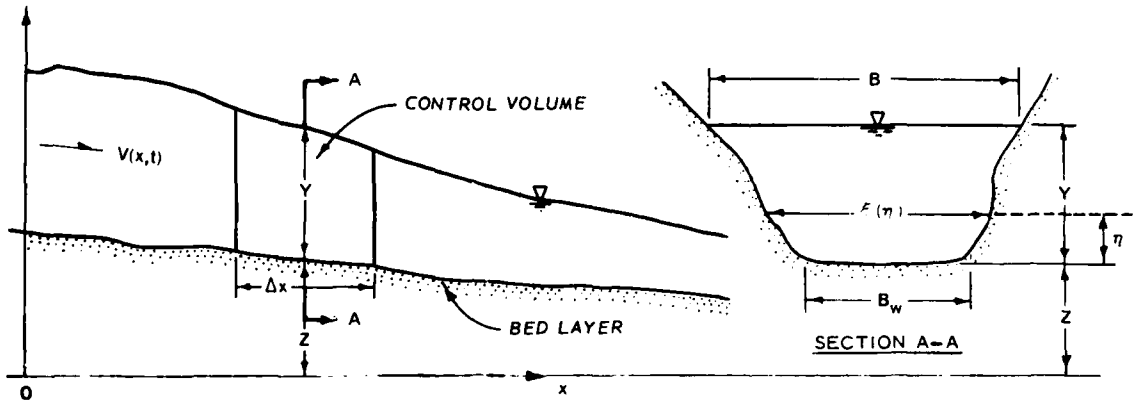

a.

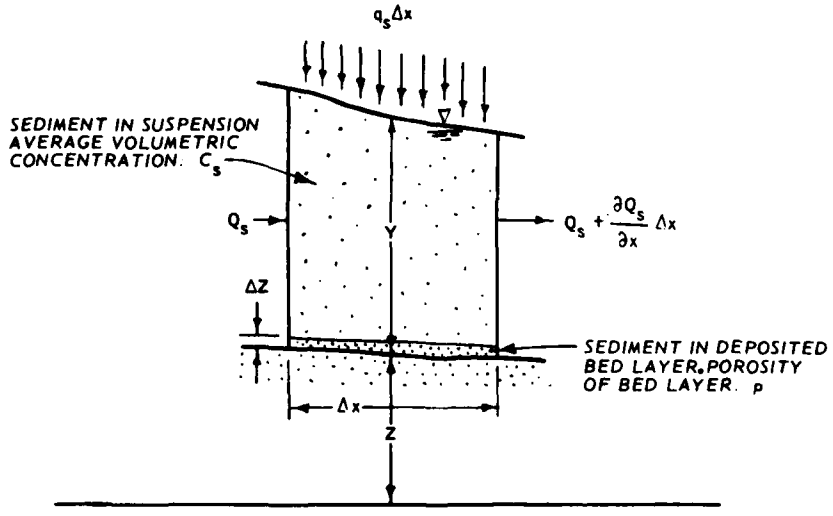

b.

Figure 4. Control volumes used in deriving the governing equations

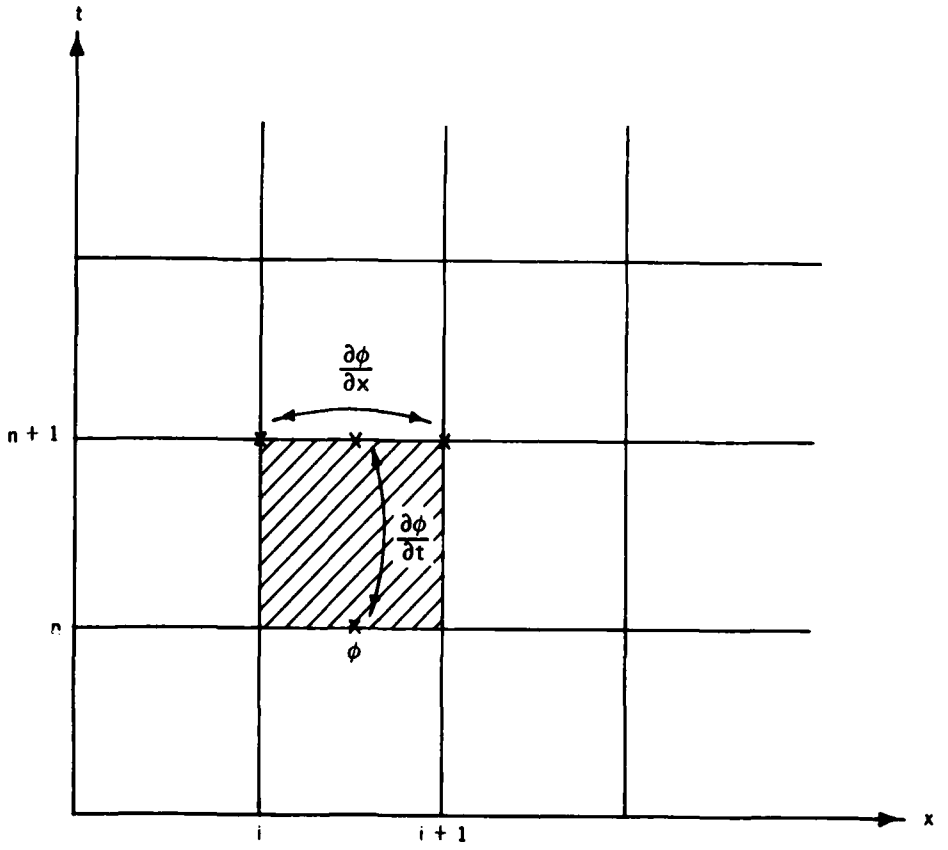

Figure 5. Positioning of derivatives in a computational cell

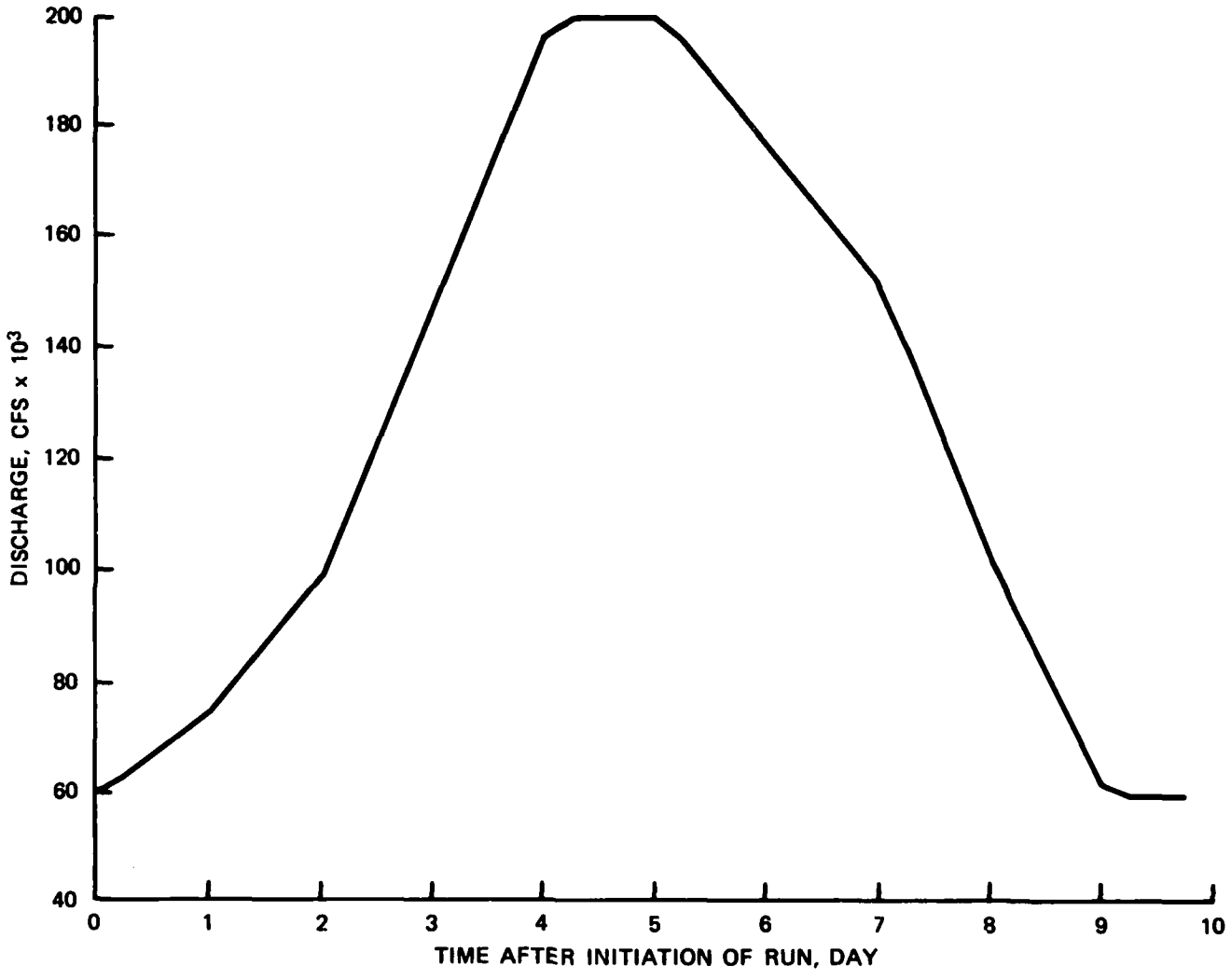

Figure 6. Typical example of FLOWSED's plotting capability

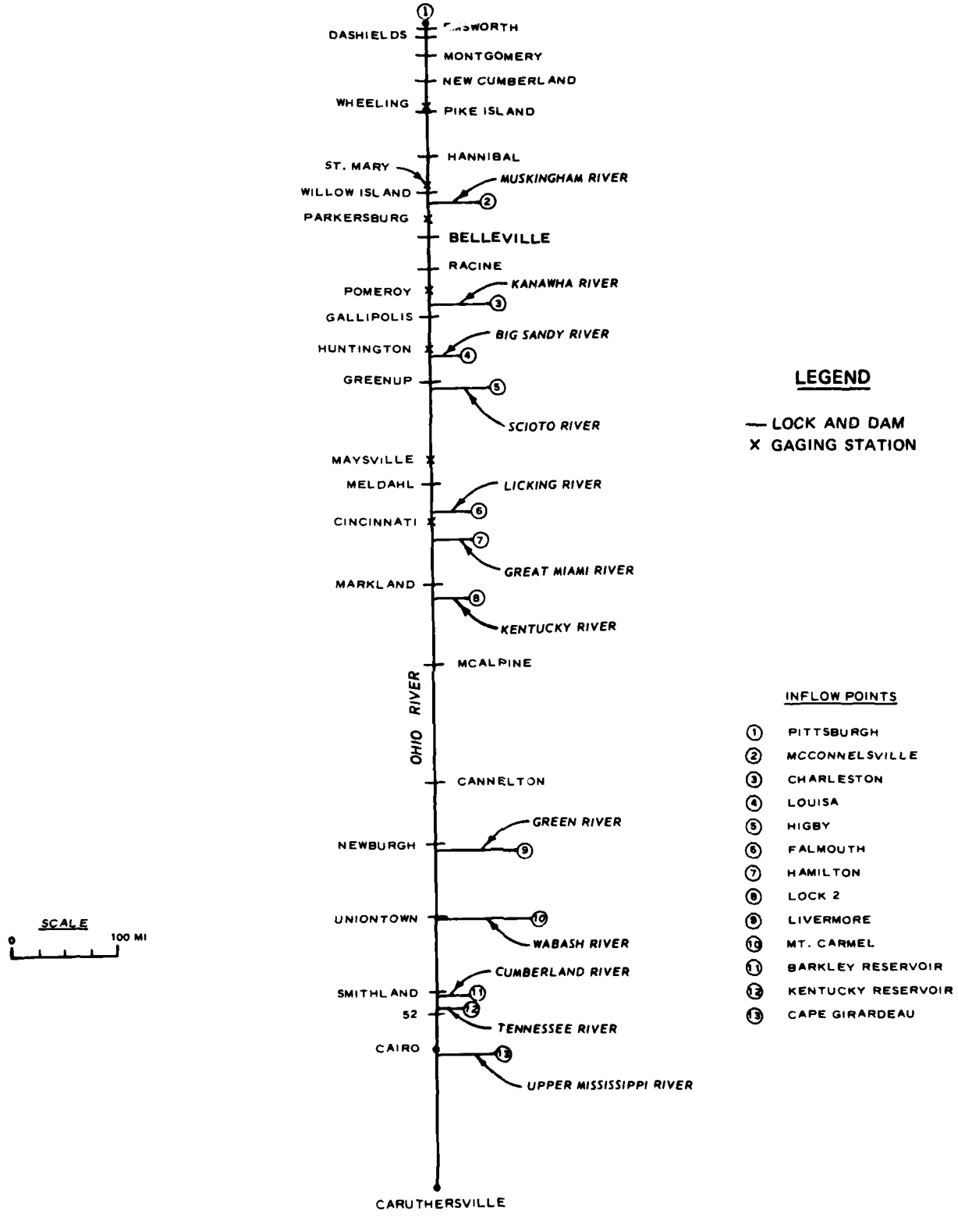

Figure 7. Location map for tributaries, and locks and dams on the Ohio River model

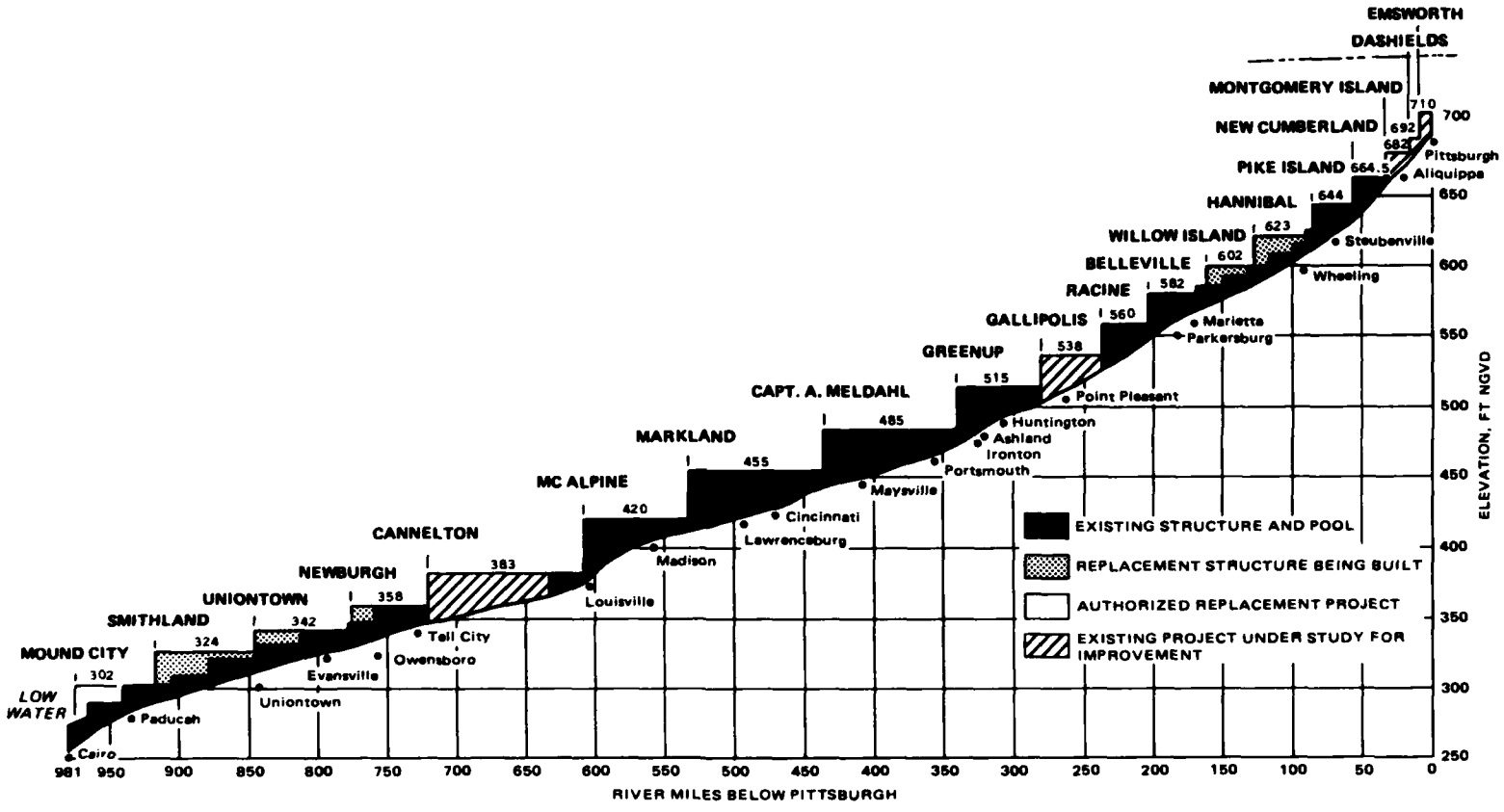

Figure 8. Status of lock and dam construction on the Ohio River, May 1974

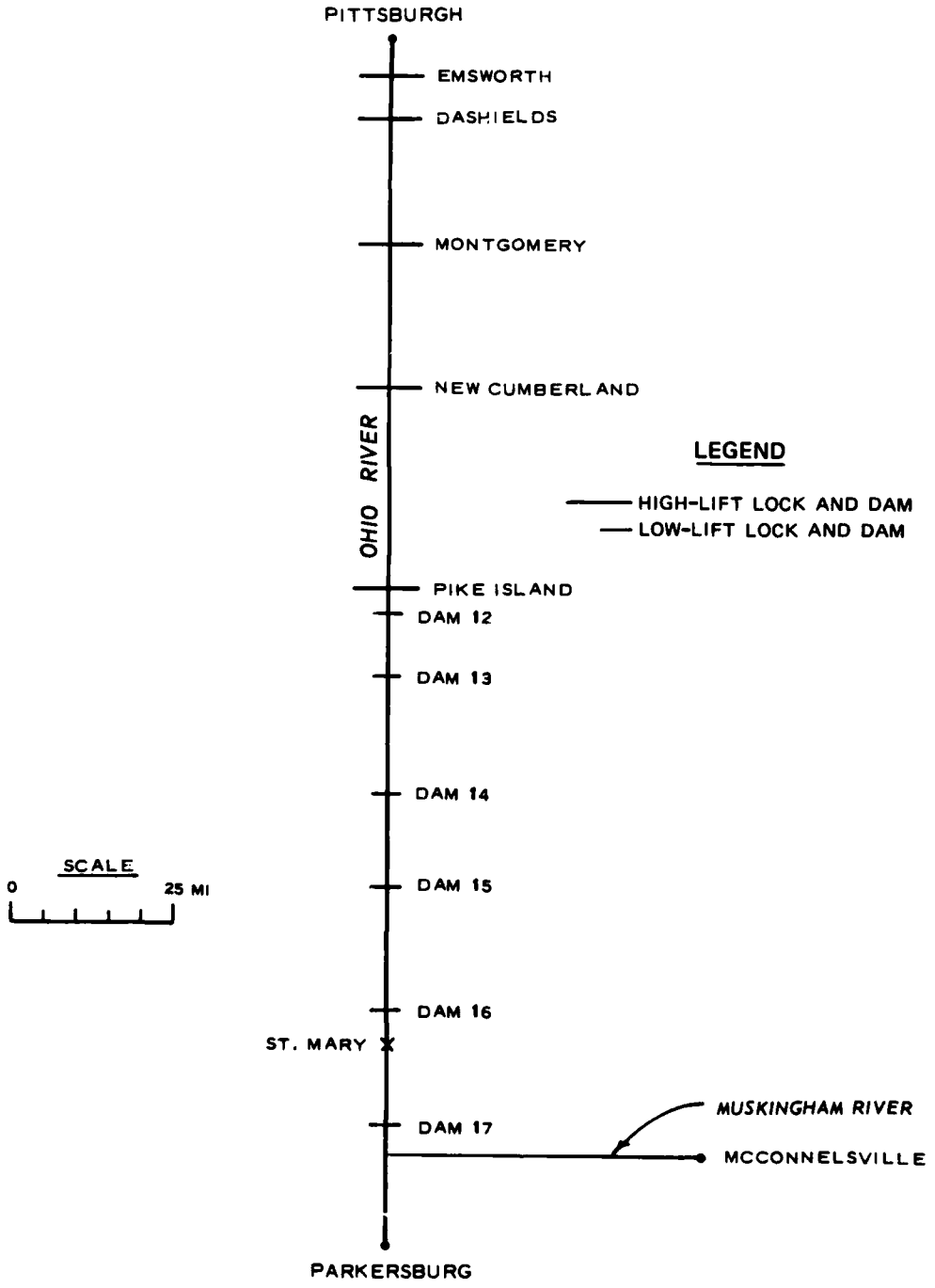

Figure 9. Location map for Pittsburgh-Parkersburg reach

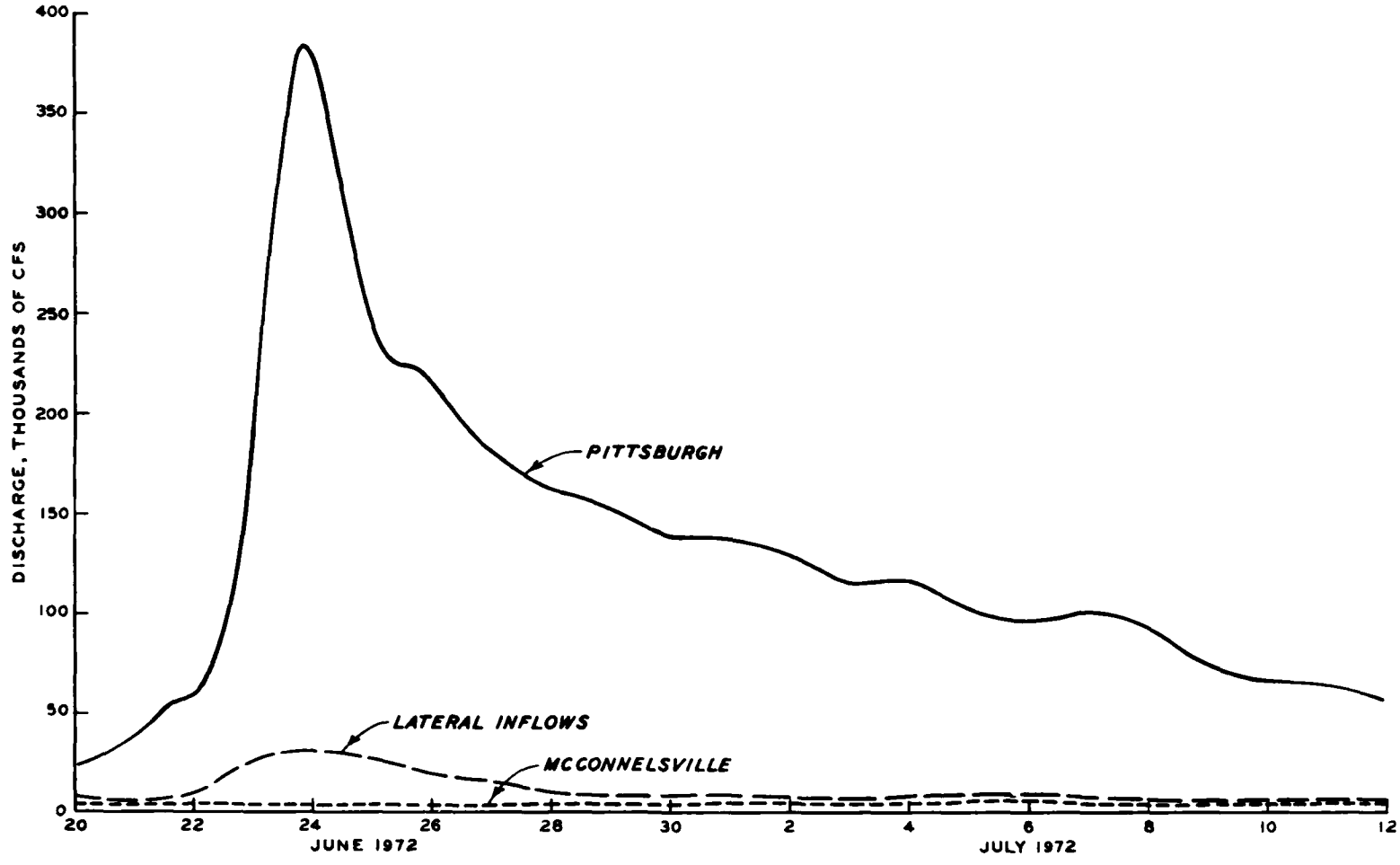

Figure 10. Inflow hydrographs for Pittsburgh to Parkersburg application

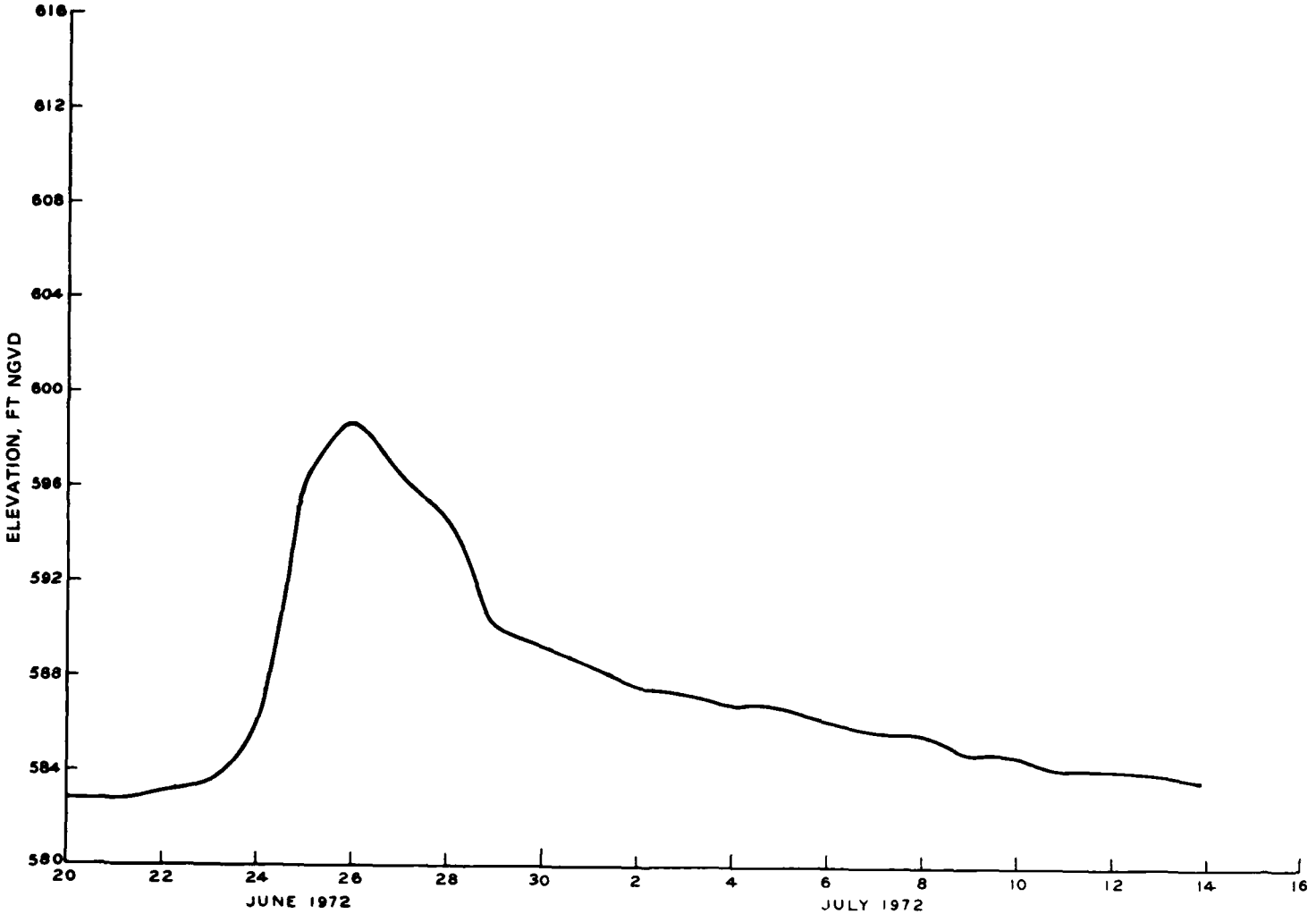

Figure 11. Boundary elevations prescribed at Parkersburg in Pittsburgh-Parkersburg application

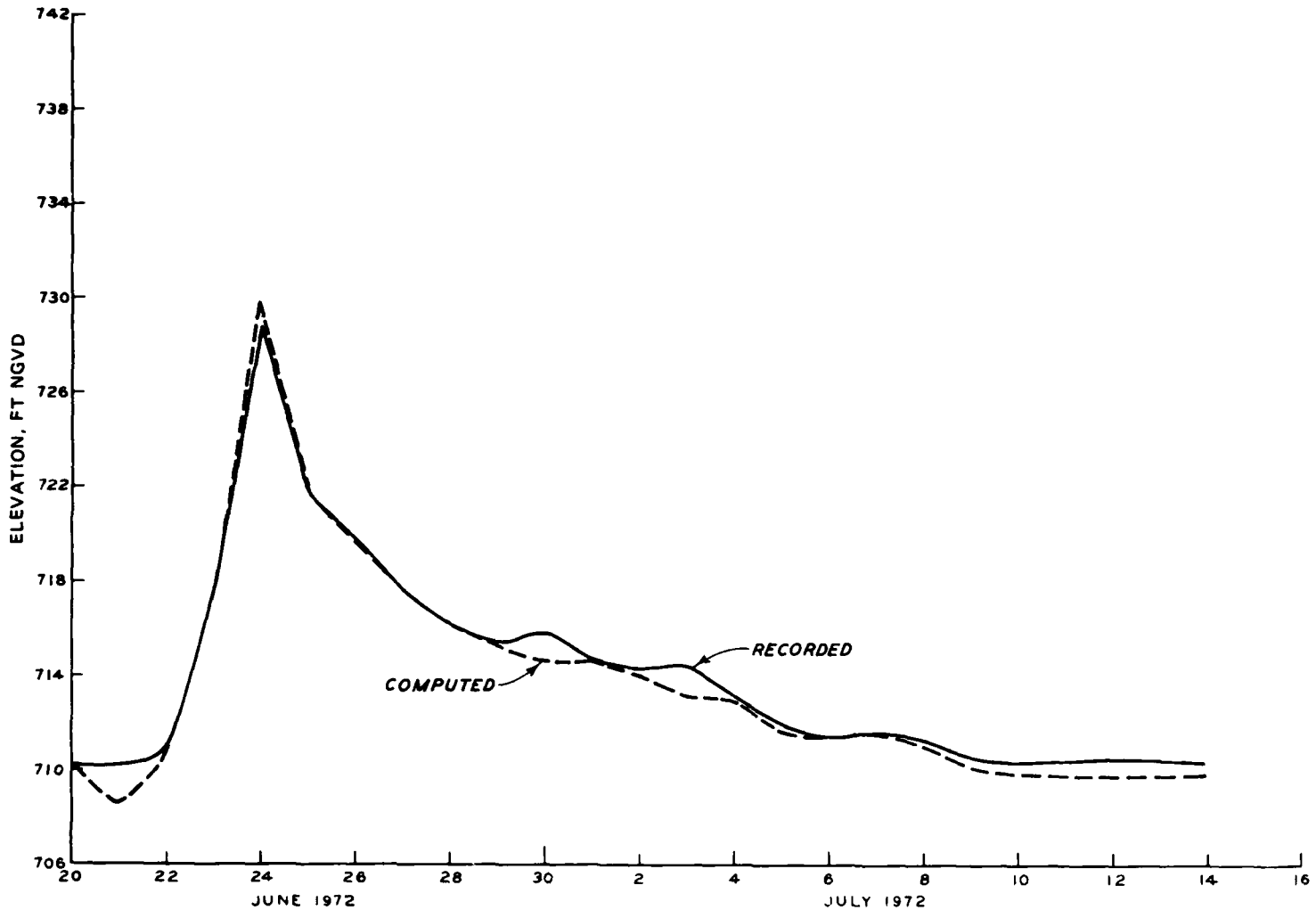

Figure 12. Recorded versus computed elevations at Pittsburgh

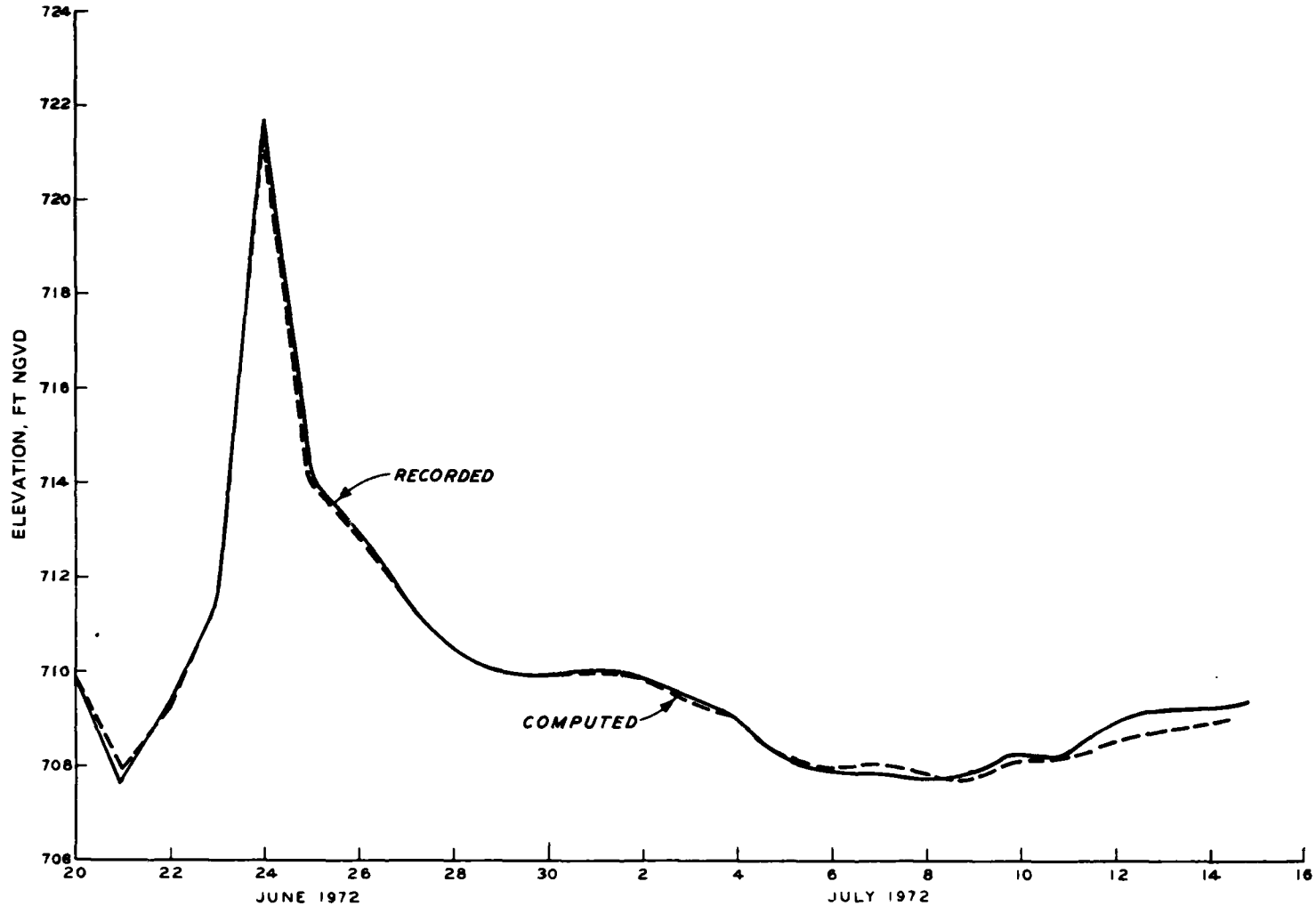

Figure 13. Recorded versus computed elevations at Emsworth L&D, upper gage

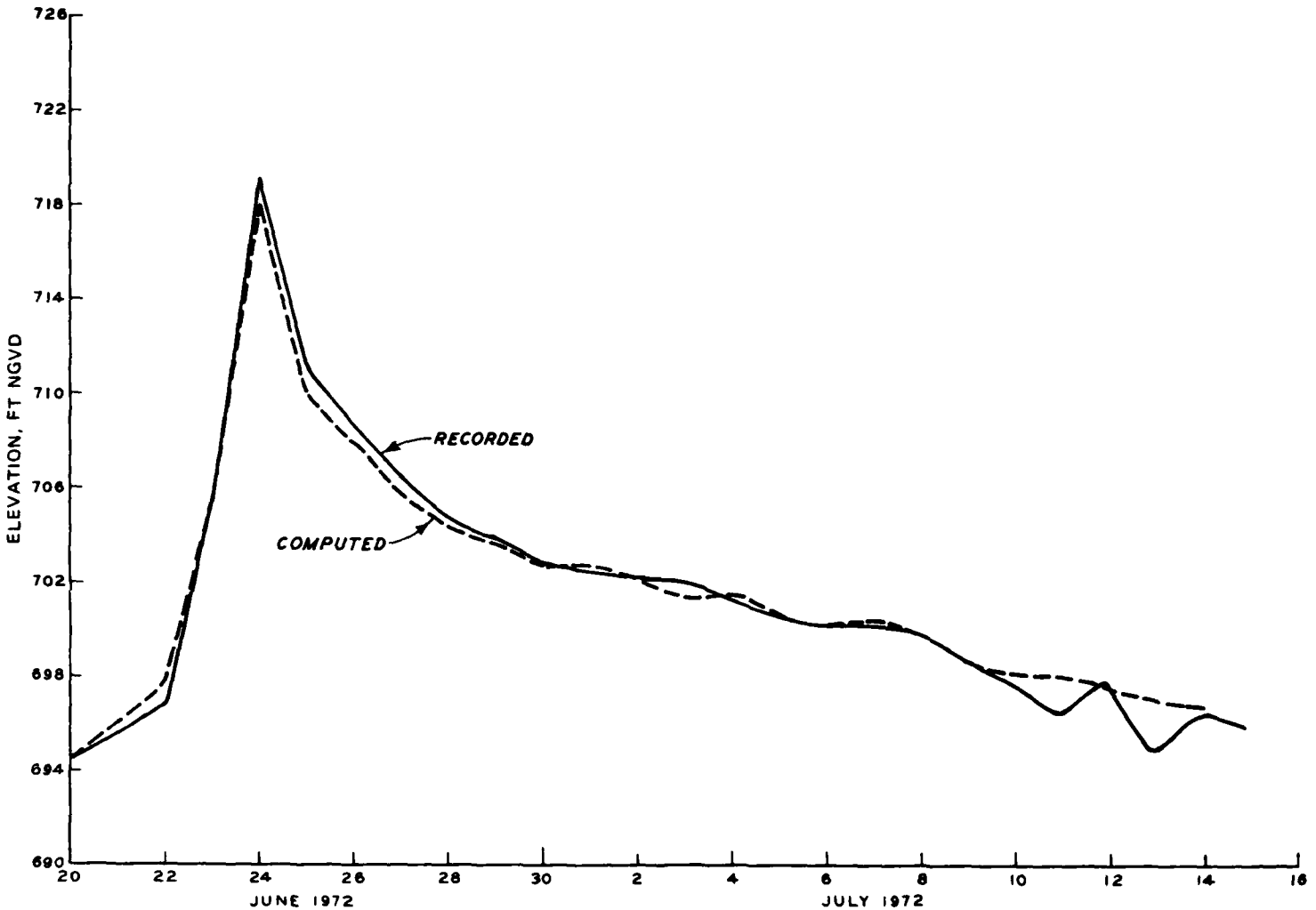

Figure 14. Recorded versus computed elevations at Emsworth L&D, lower gage

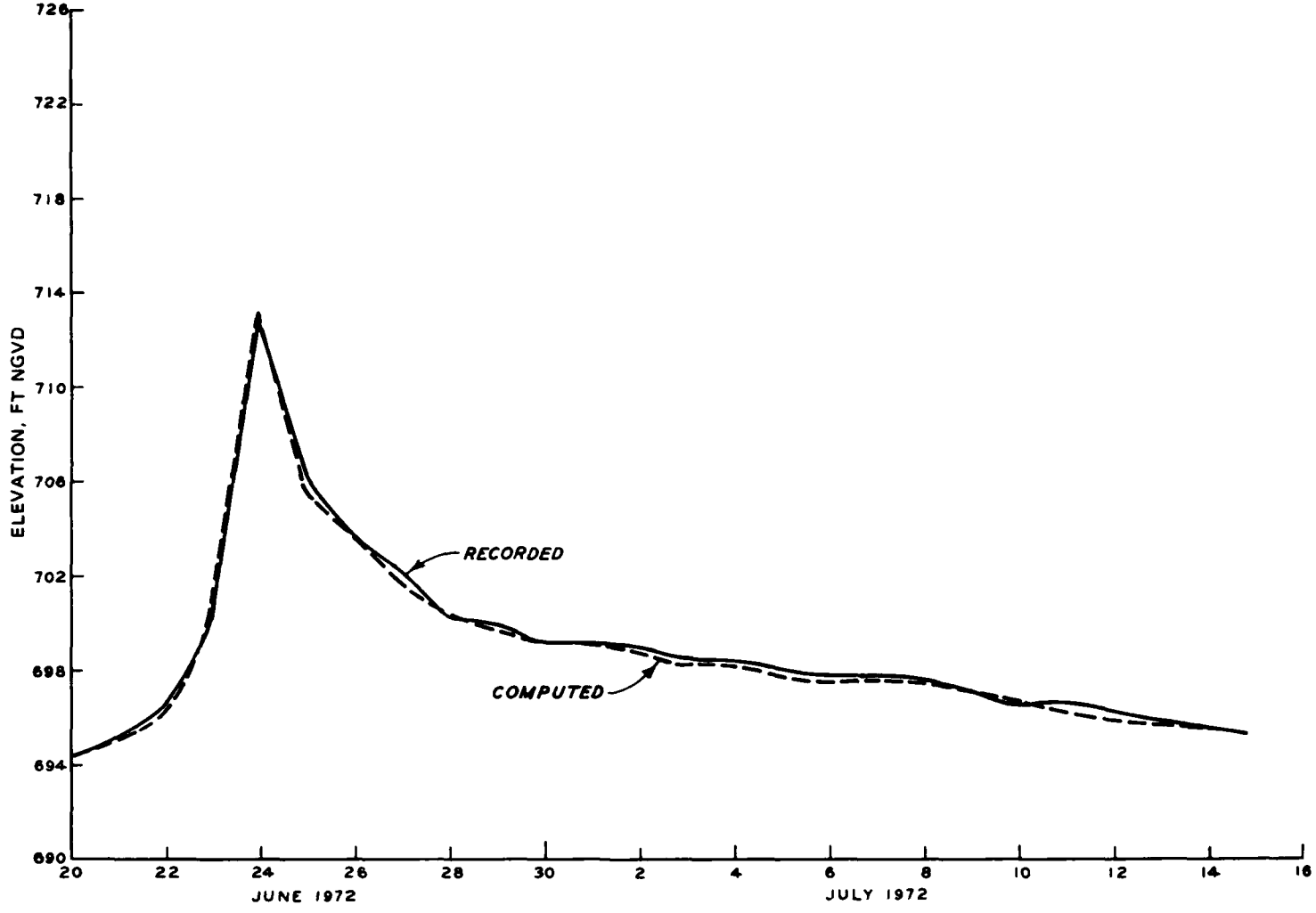

Figure 15. Recorded versus computed elevations at Dashields L&D, upper gage

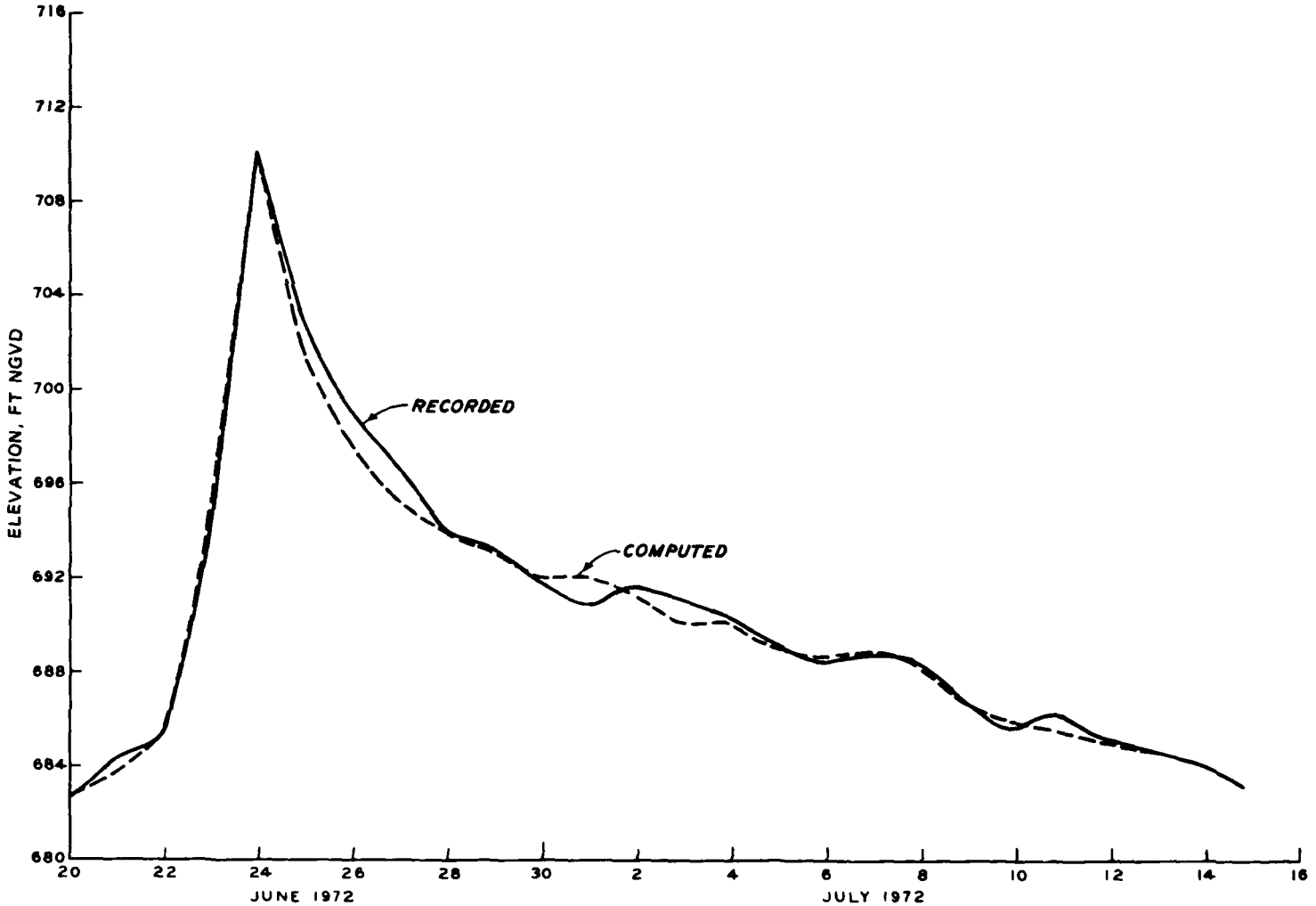

Figure 16. Recorded versus computed elevations at Dashields L&D, lower gage

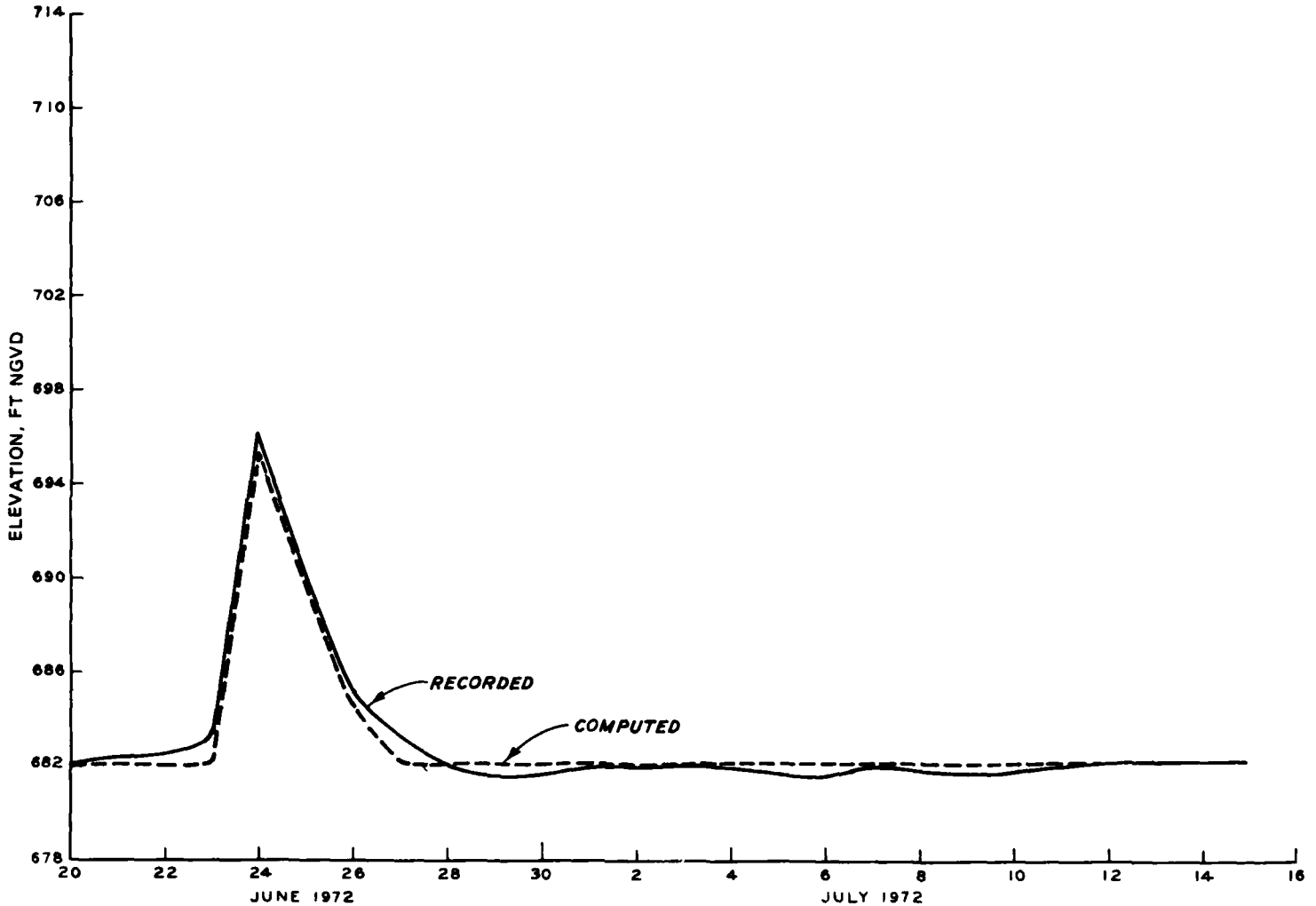

Figure 17. Recorded versus computed elevations at Montgomery L&D, upper gage

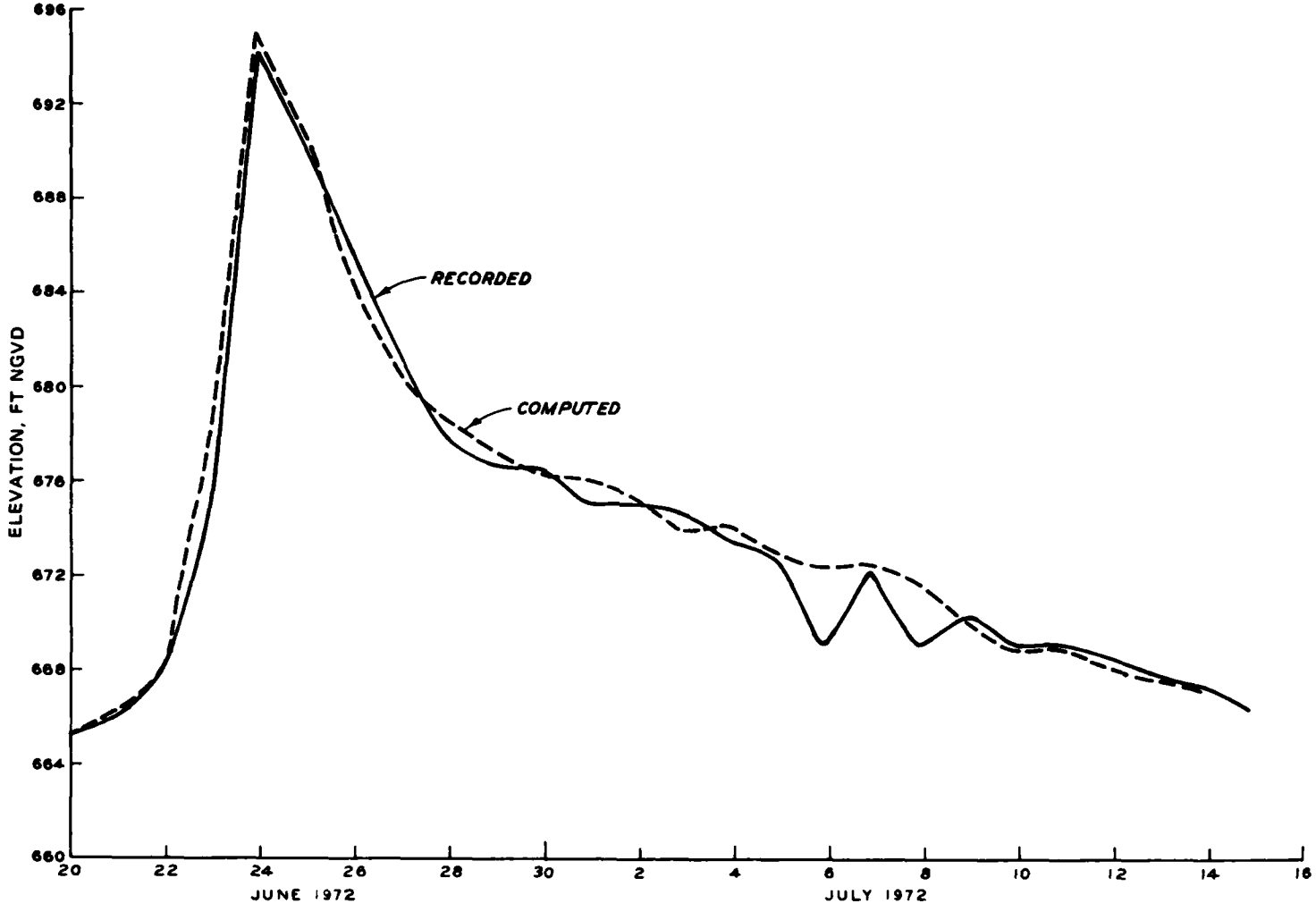

Figure 18. Recorded versus computed elevations at Montgomery L&D, lower gage

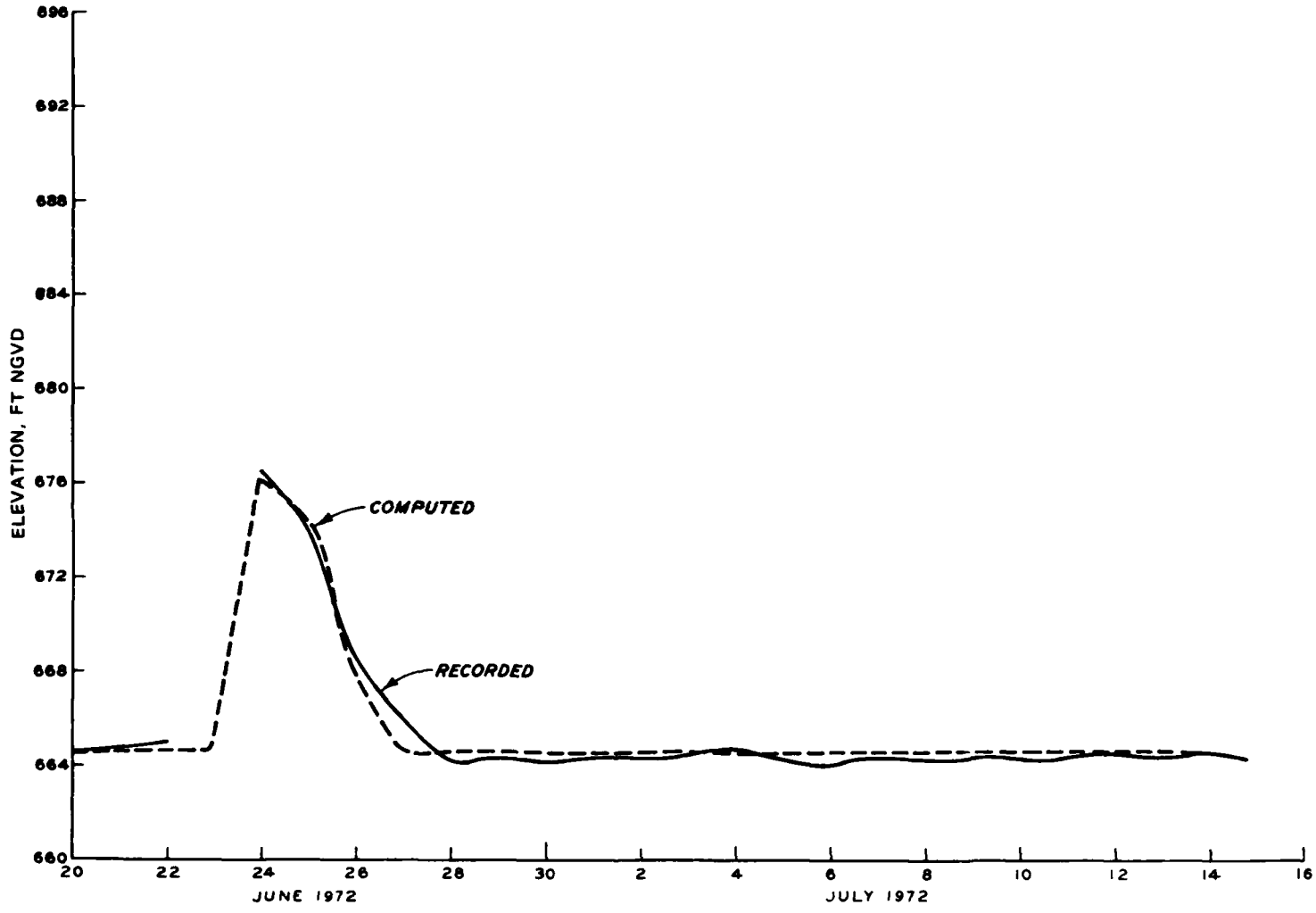

Figure 19. Recorded versus computed elevations at New Cumberland L&D, upper gage

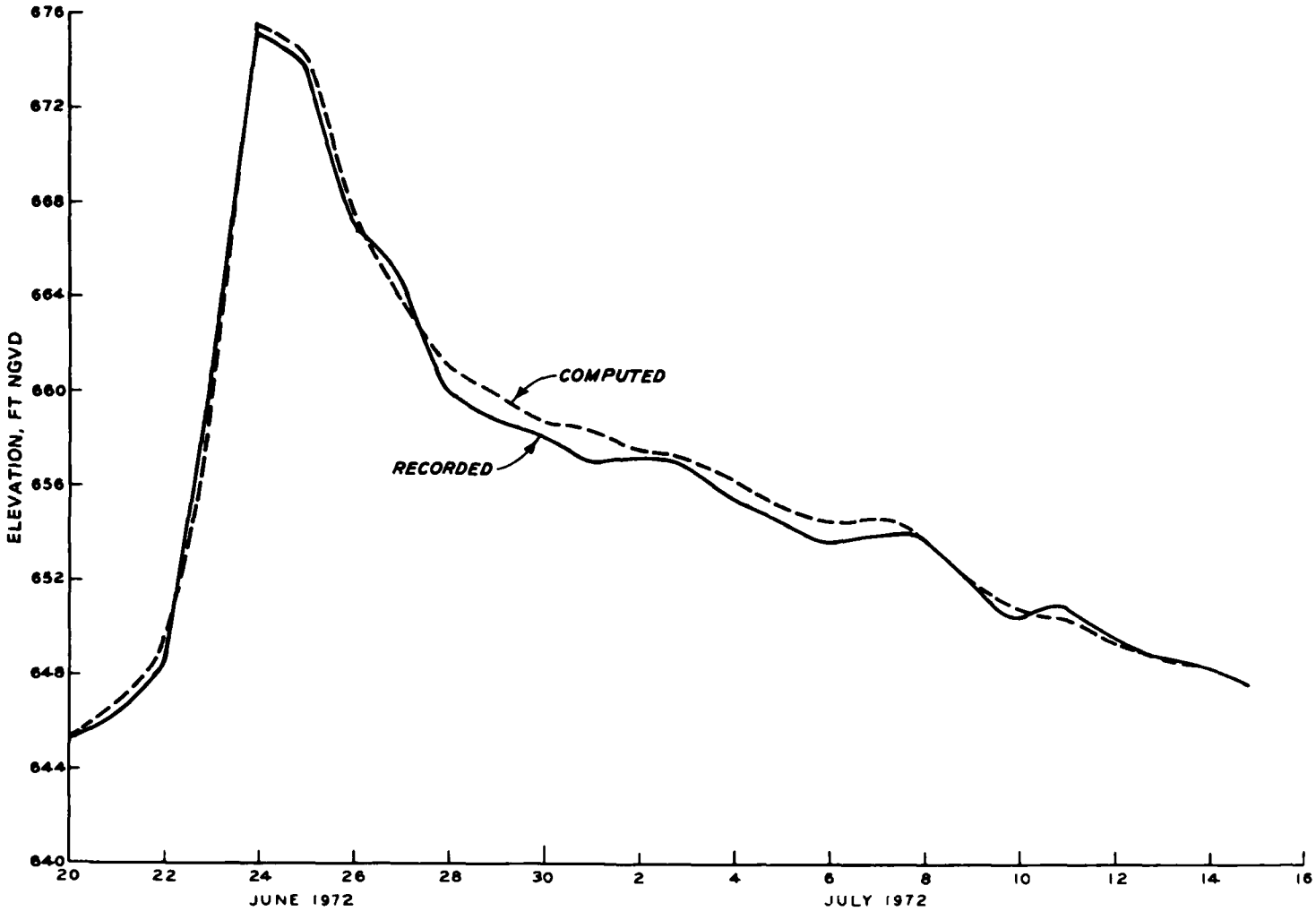

Figure 20. Recorded versus computed elevations at New Cumberland L&D, lower gage

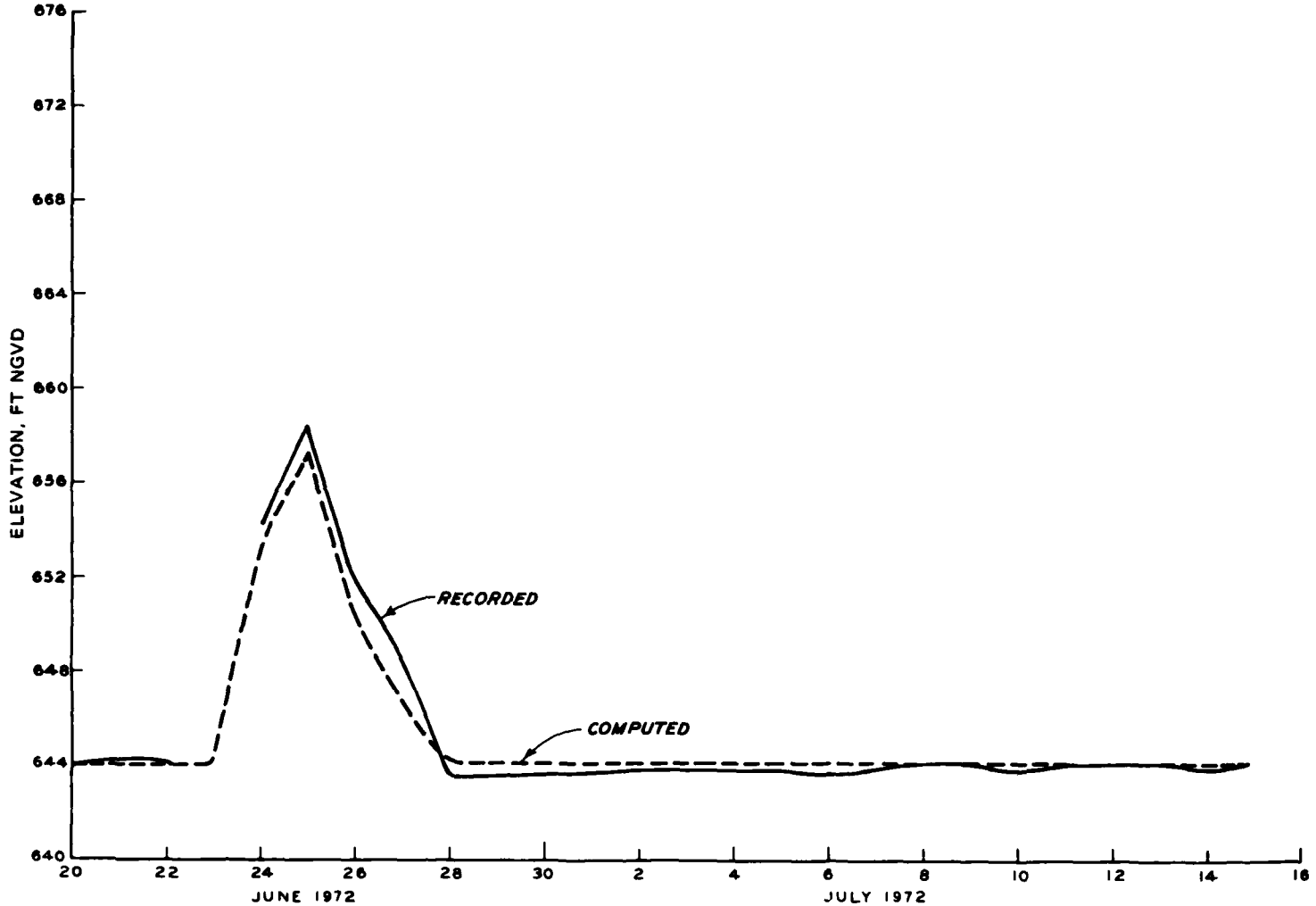

Figure 21. Recorded versus computed elevations at Pike Island L&D, upper gage

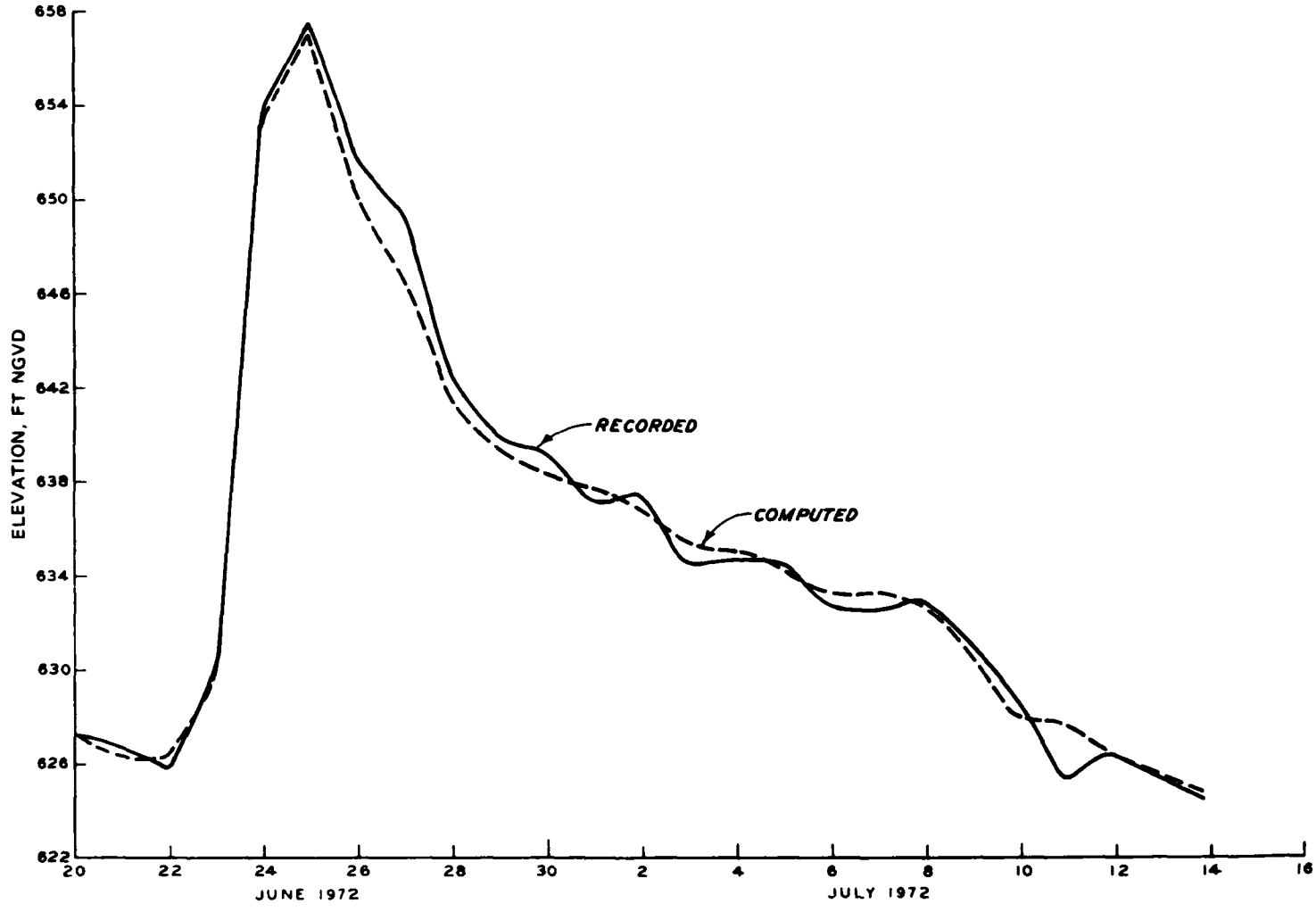

Figure 22. Recorded versus computed elevations at Pike Island L&D, lower gage

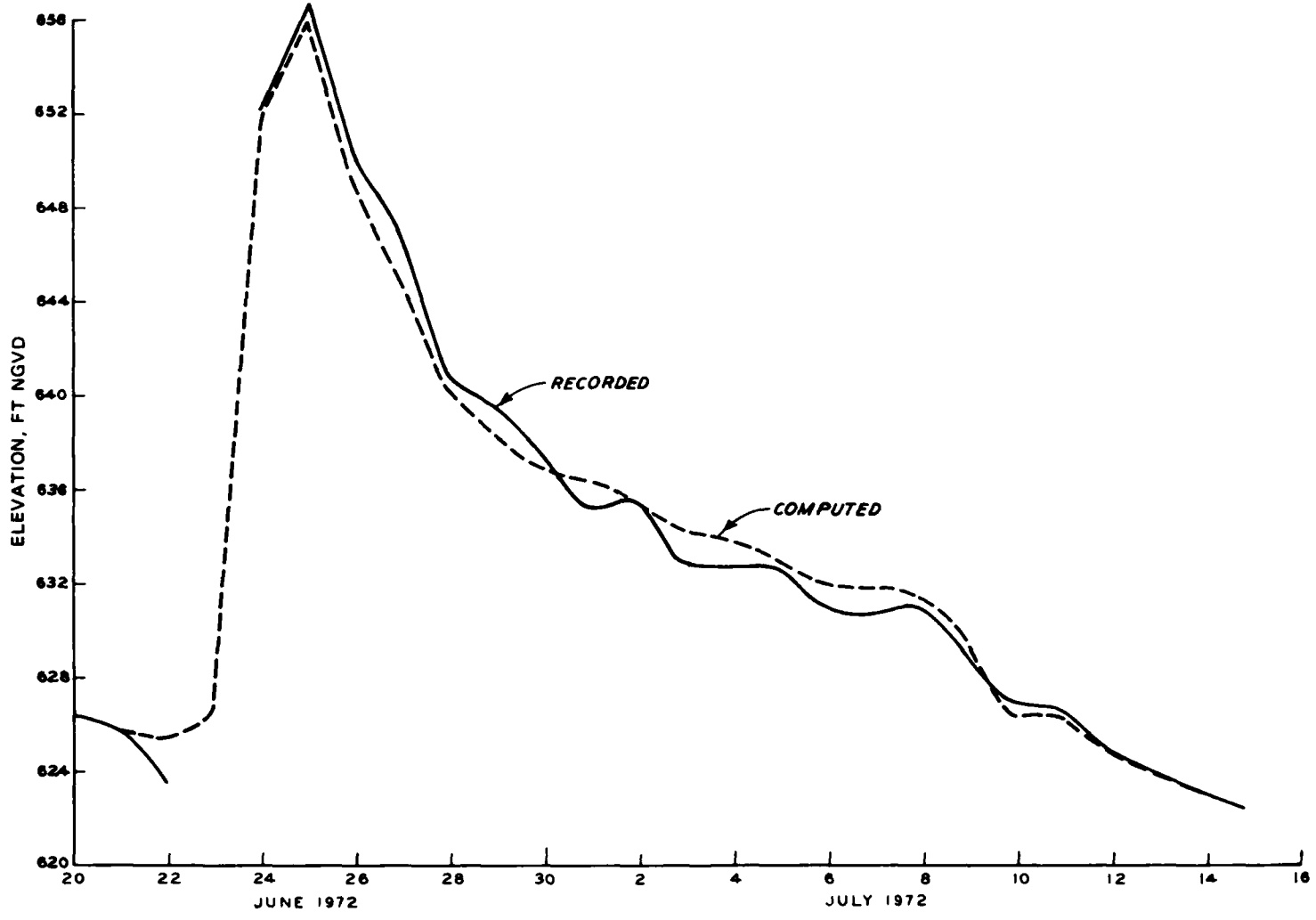

Figure 23. Recorded versus computed elevations at L&D 12, upper gage

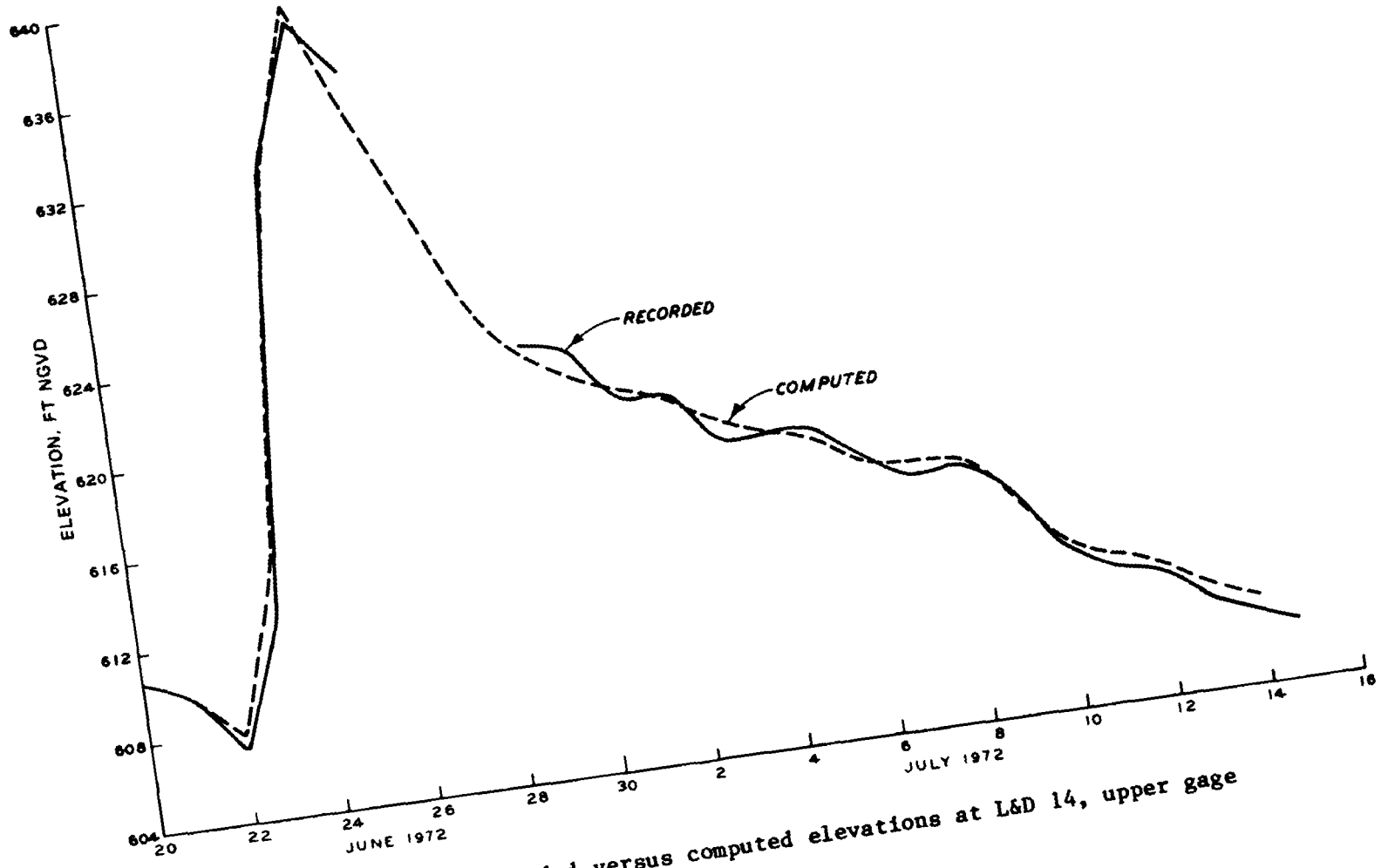

Figure 24. Recorded versus computed elevations at L&D 14, upper gage

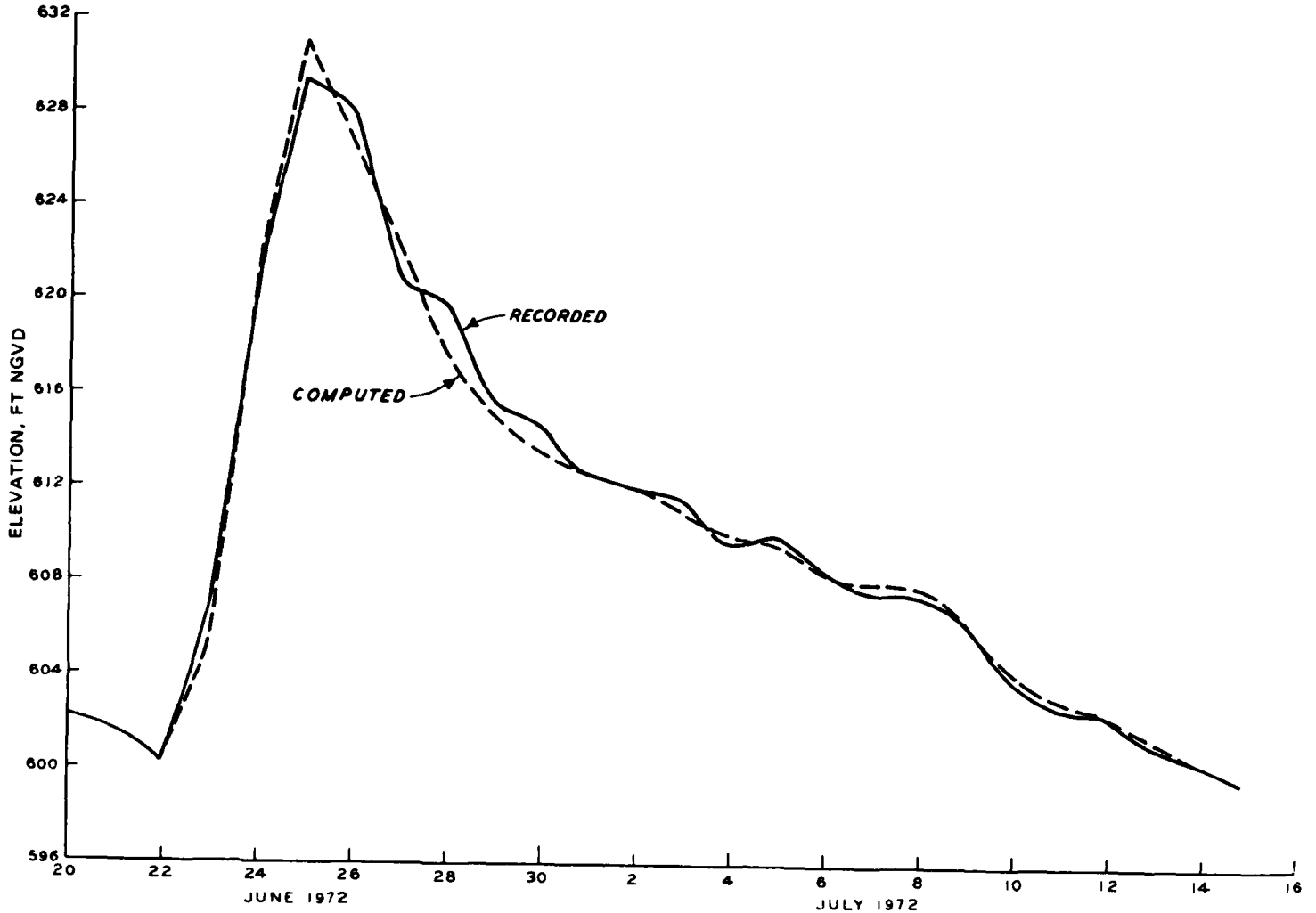

Figure 25. Recorded versus computed elevations at L&D 15, upper gage

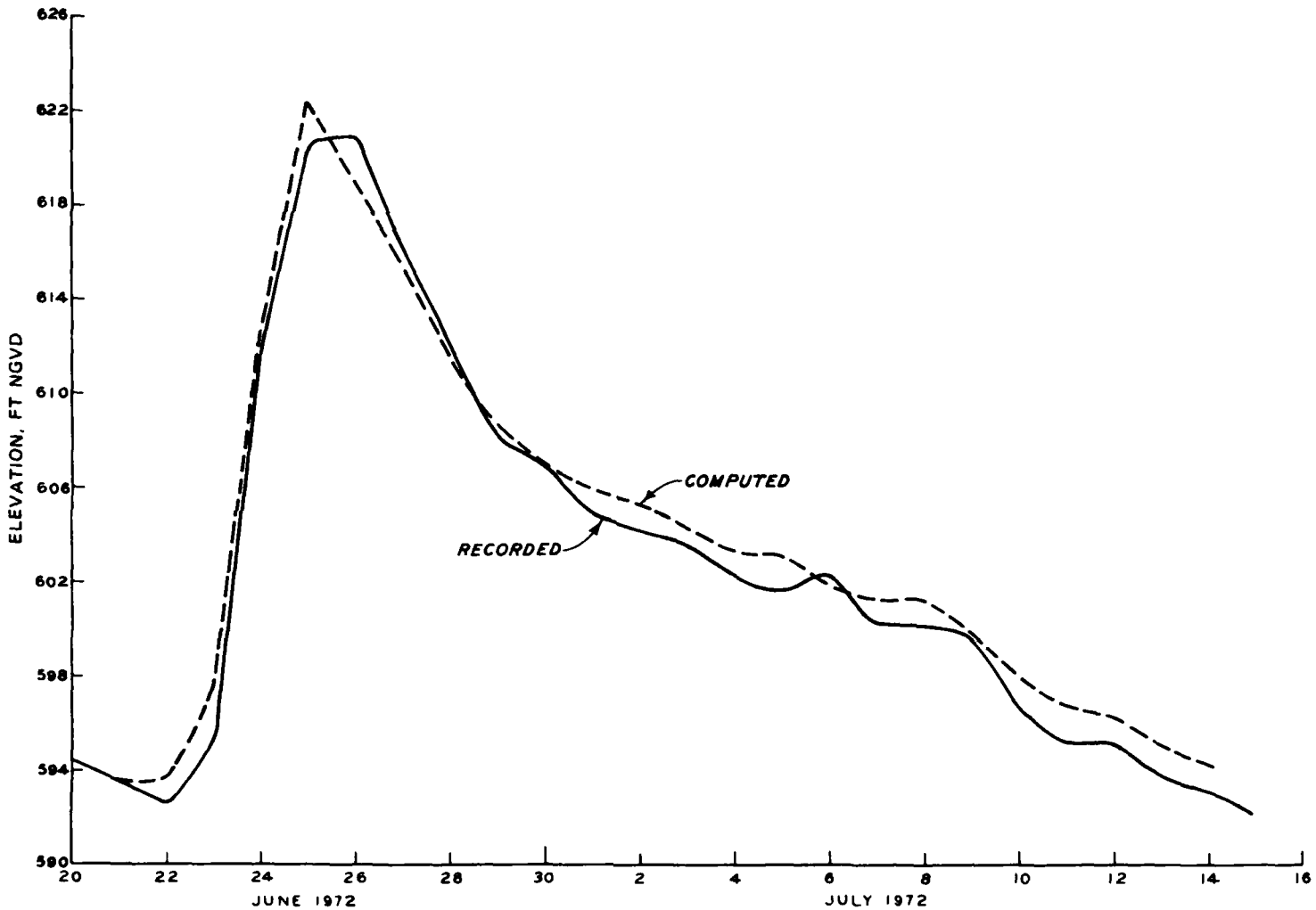

Figure 26. Recorded versus computed elevations at L&D 16, upper gage

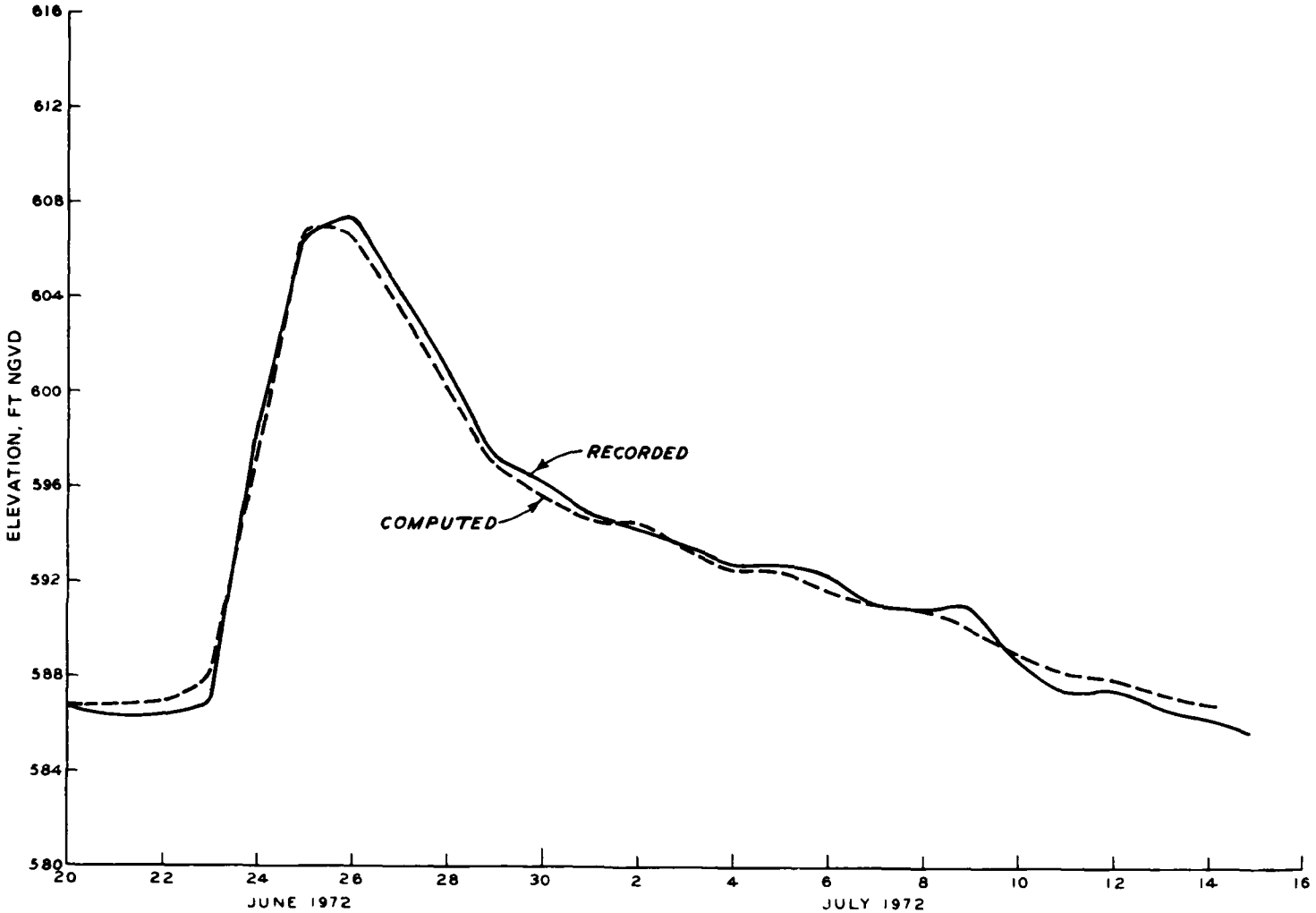

Figure 27. Recorded versus computed elevations at L&D 17, upper gage

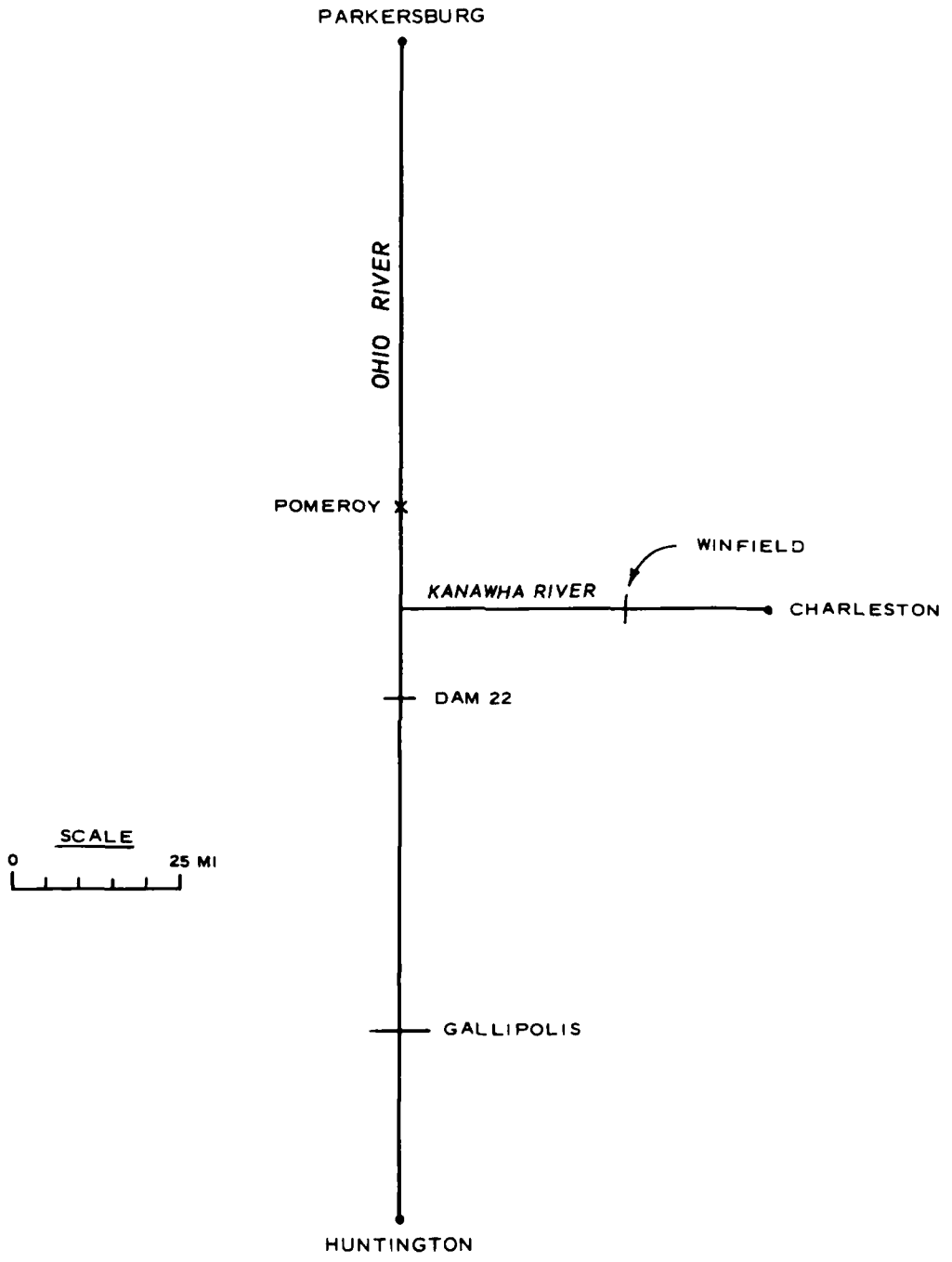

Figure 28. Location map for Parkersburg to Huntington reach

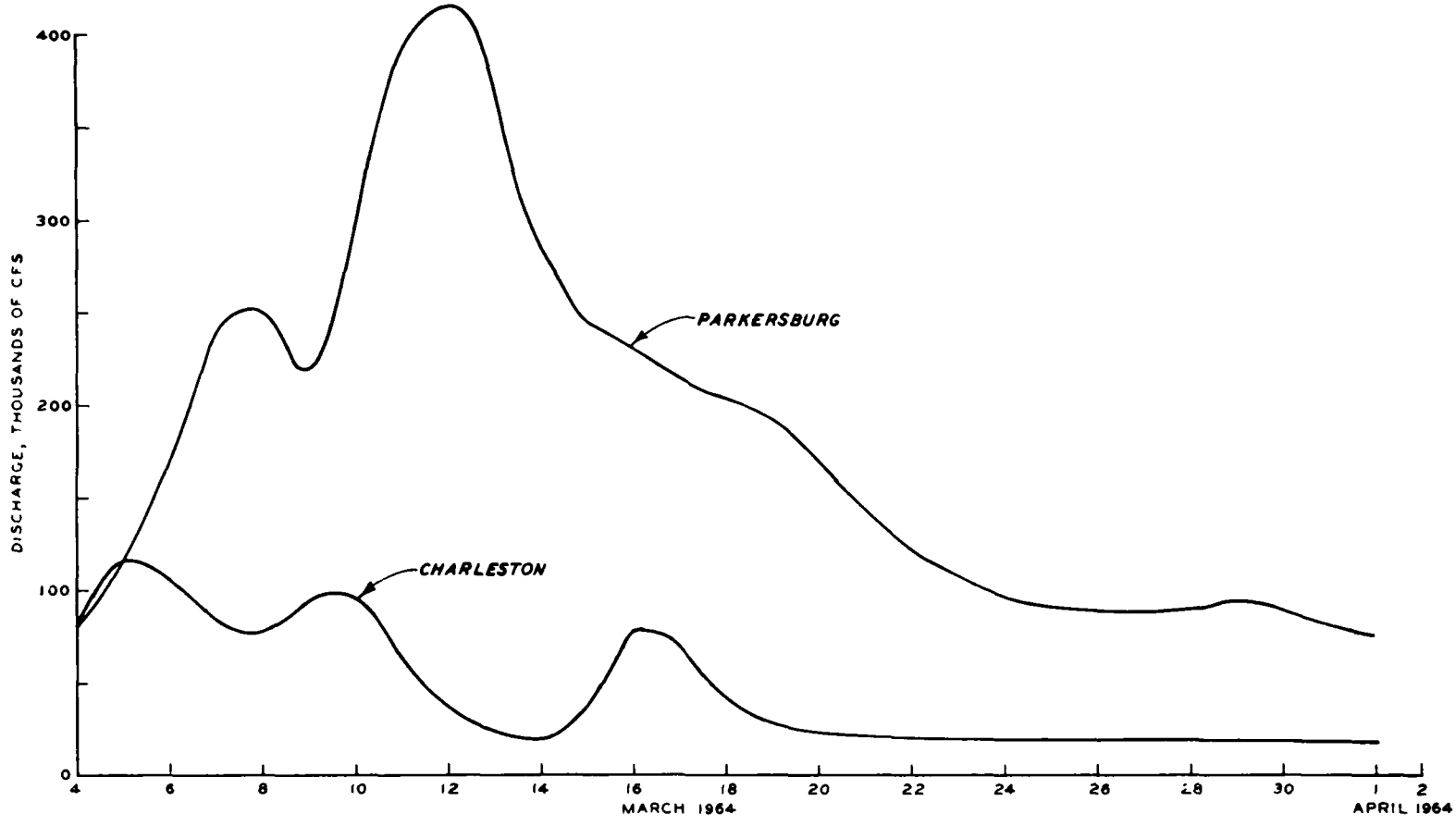

Figure 29. Boundary inflows prescribed in the Parkersburg-Huntington application

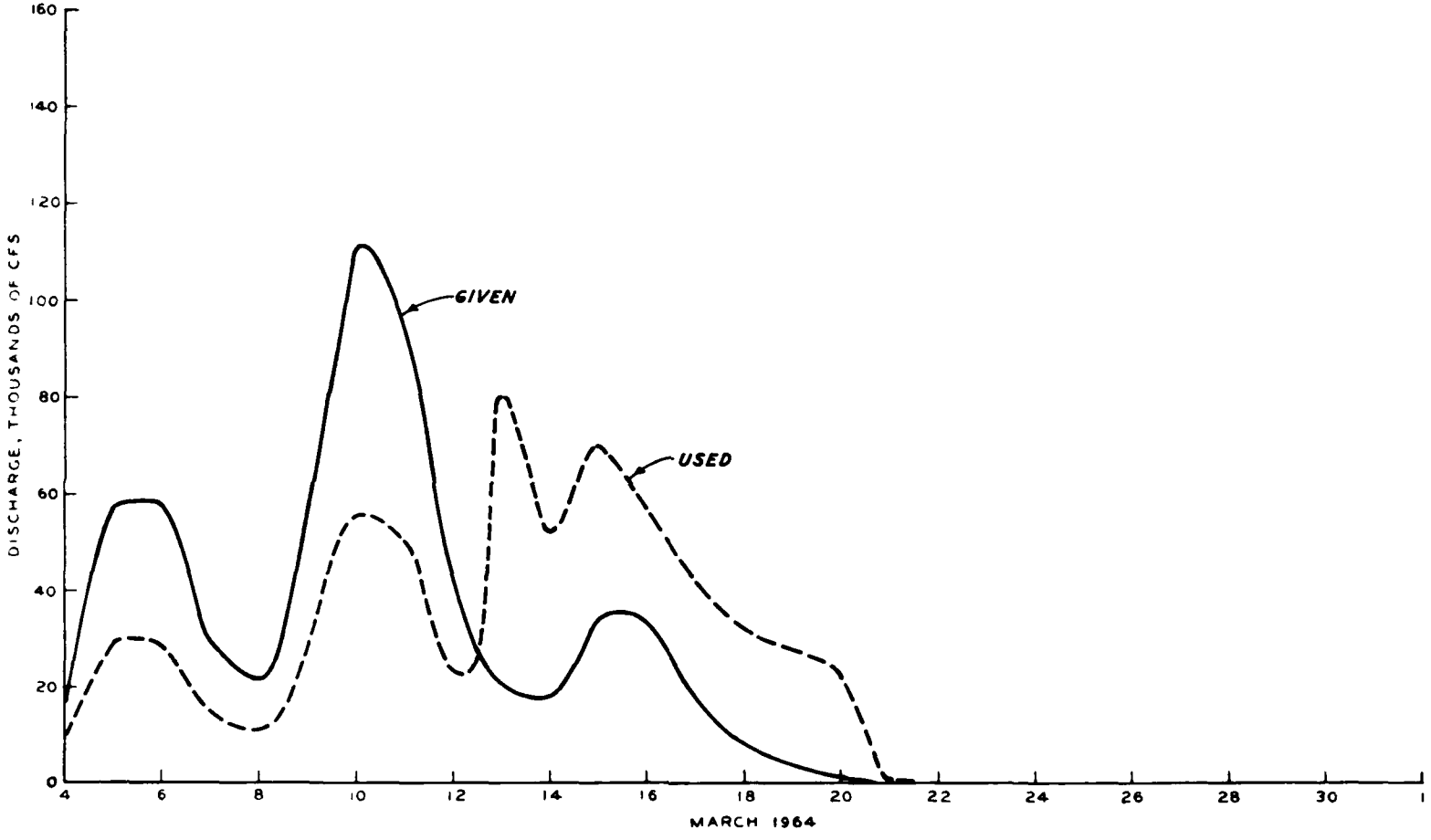

Figure 30. Ungaged lateral inflow from Parkersburg to Huntington

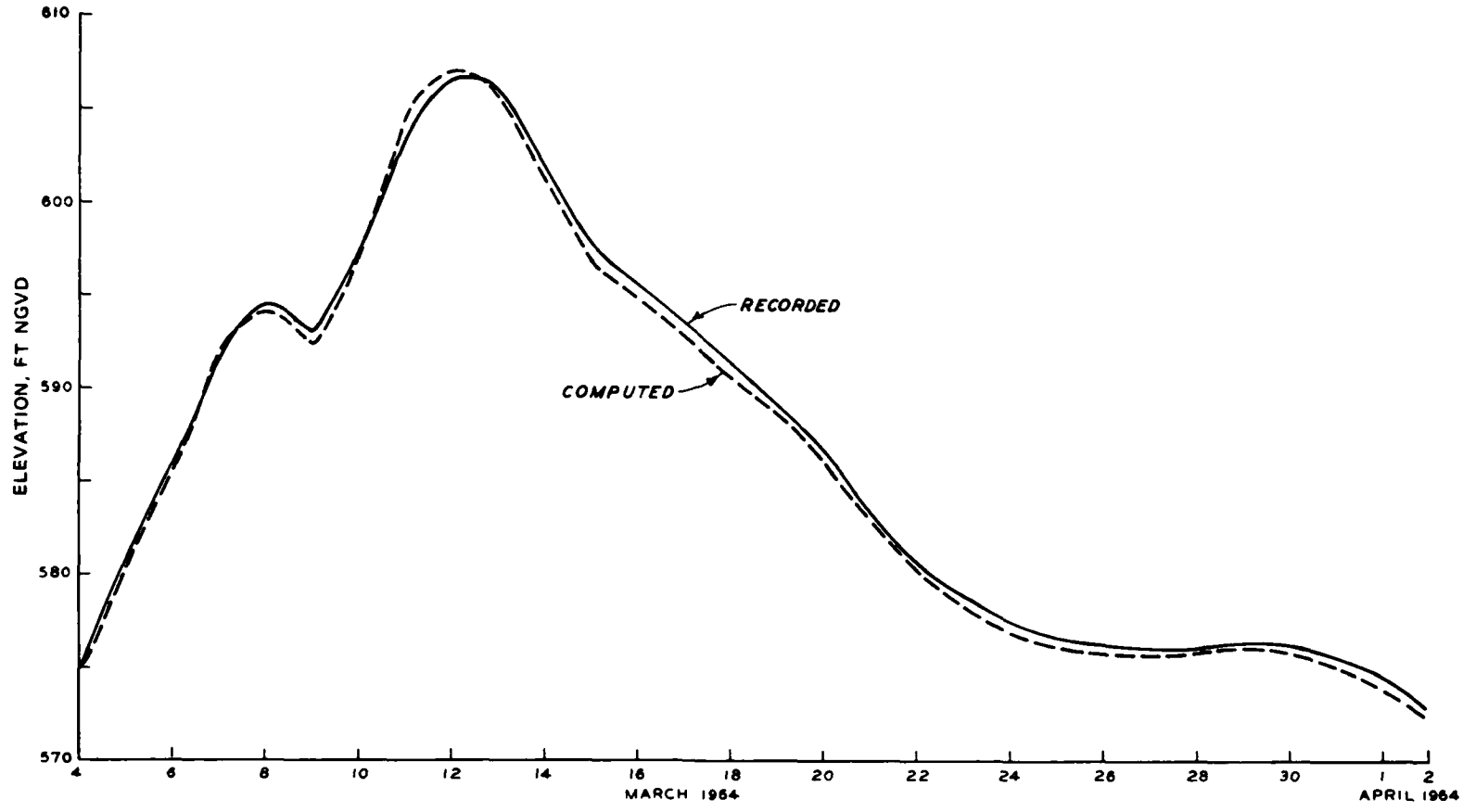

Figure 31. Recorded versus computed elevations at Parkersburg

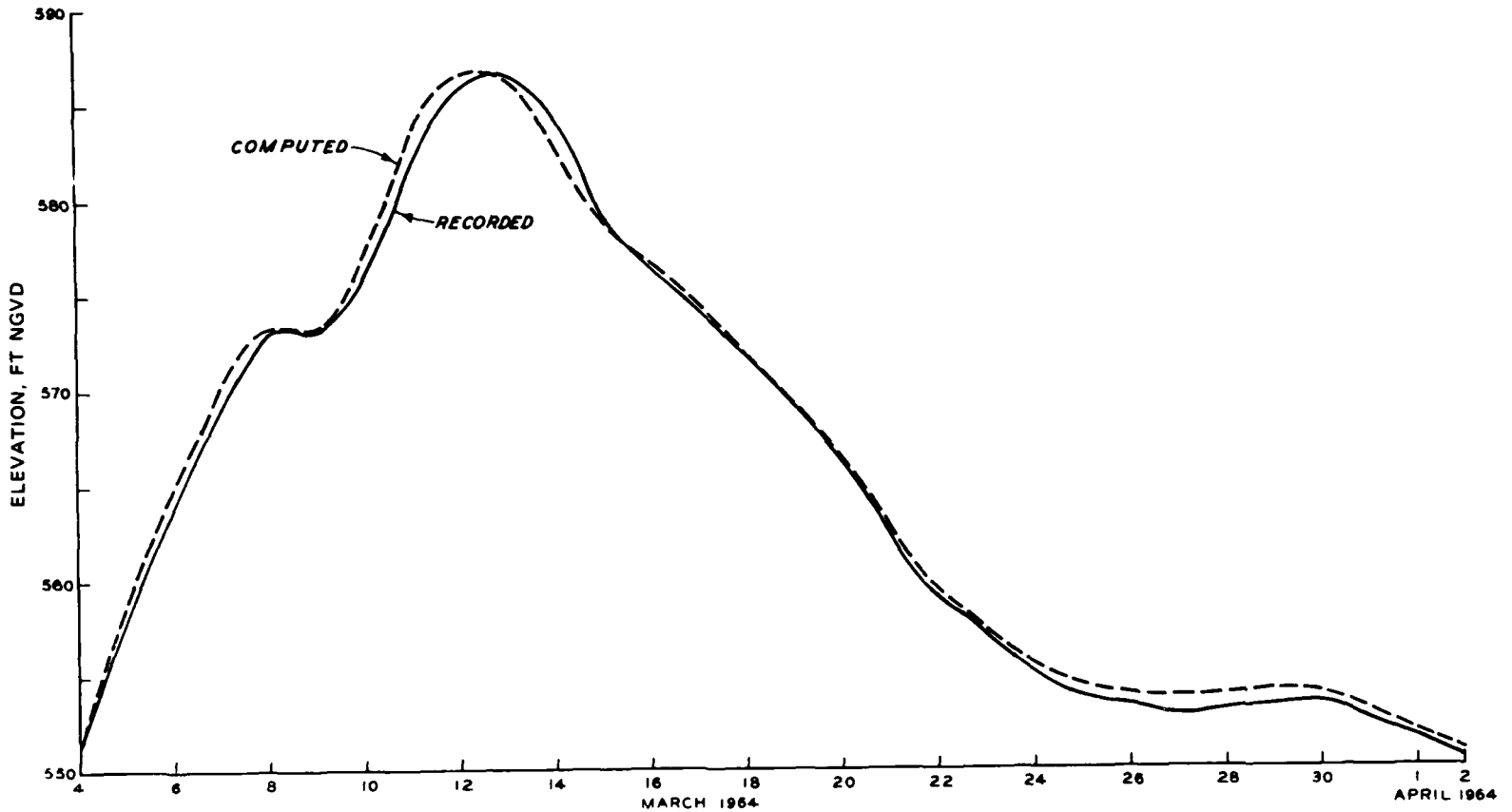

Figure 32. Recorded versus computed elevations at Dam 22, upper gage

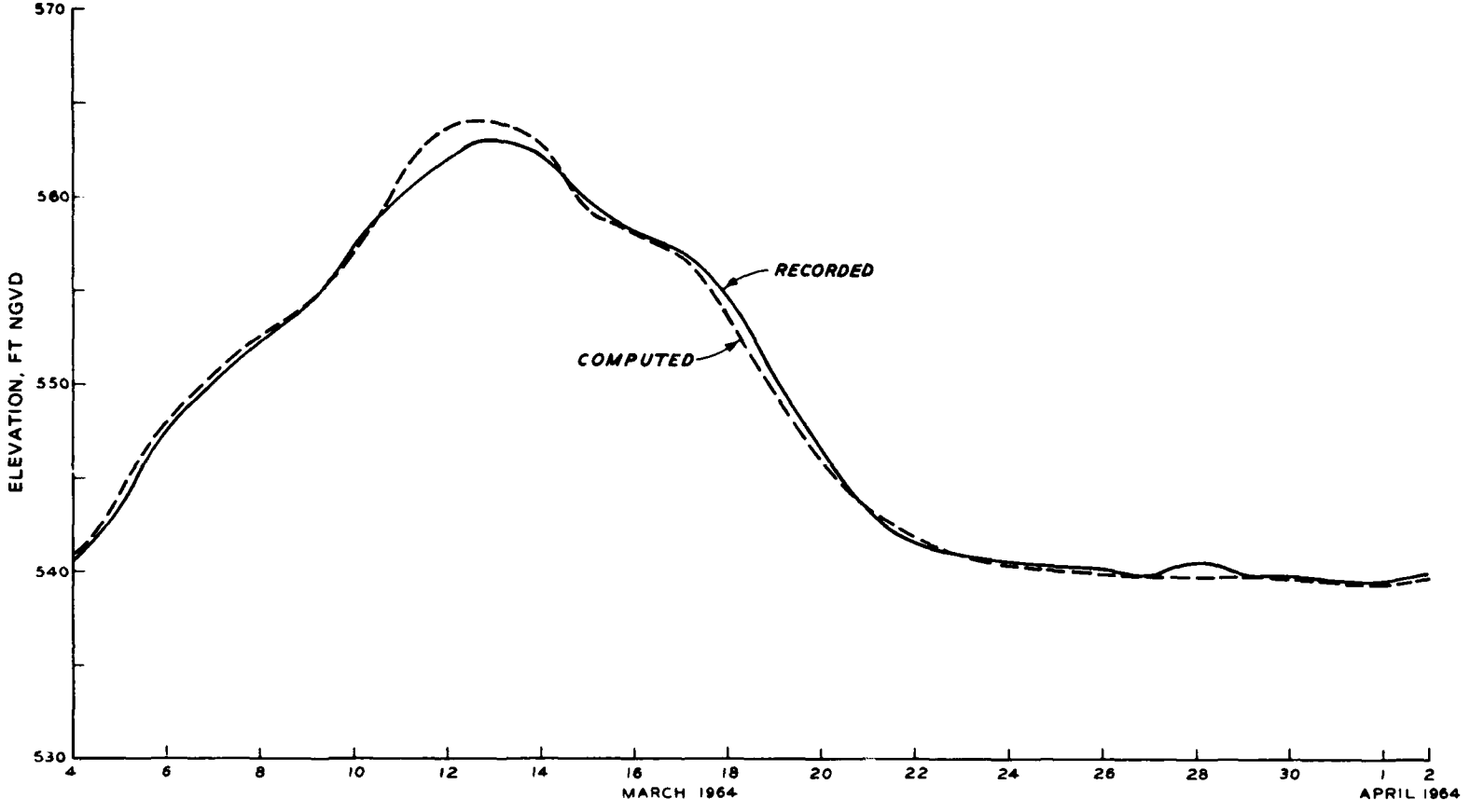

Figure 33. Recorded versus computed elevations at Point Pleasant

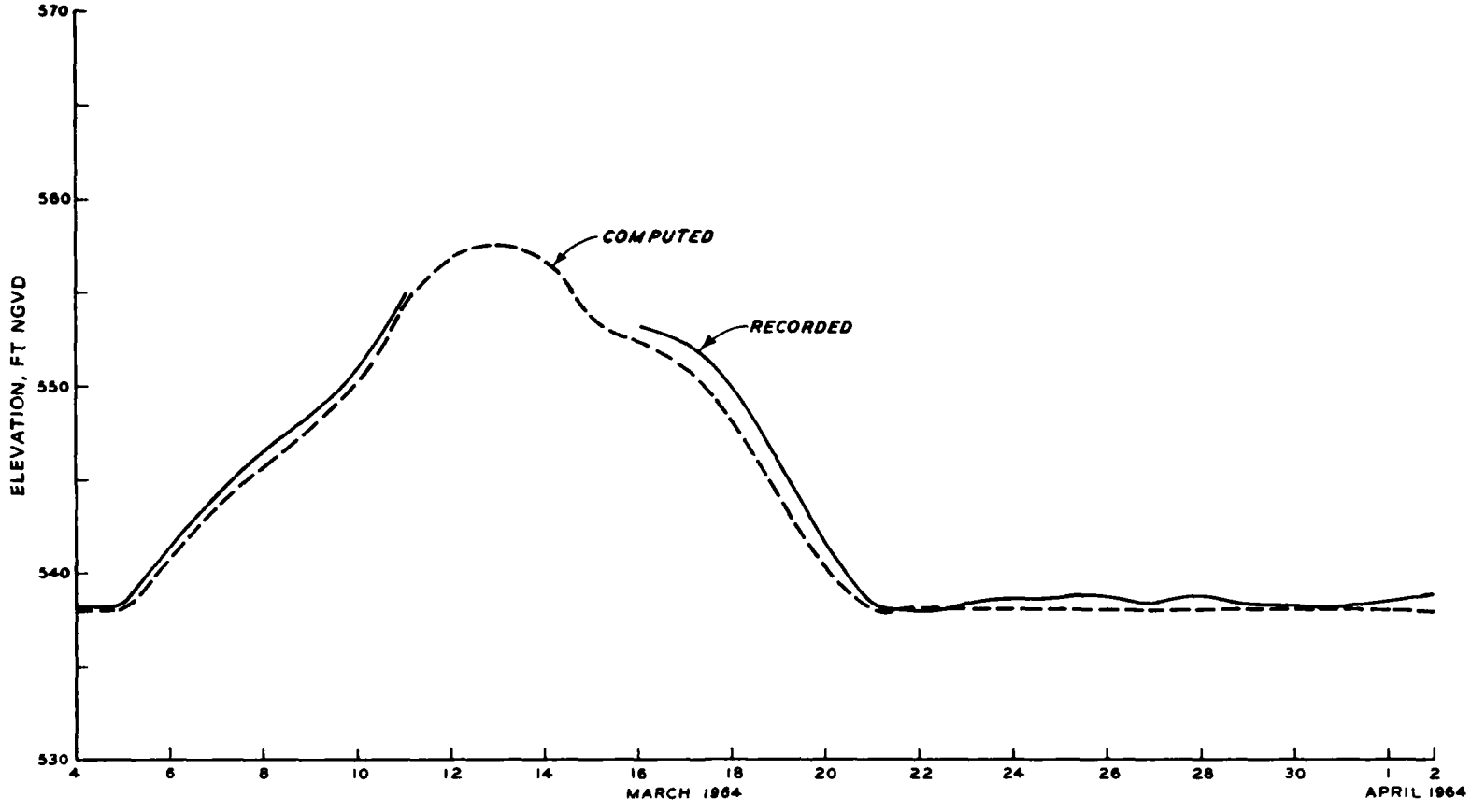

Figure 34. Recorded versus computed elevations at Gallipolis L&D, upper gage

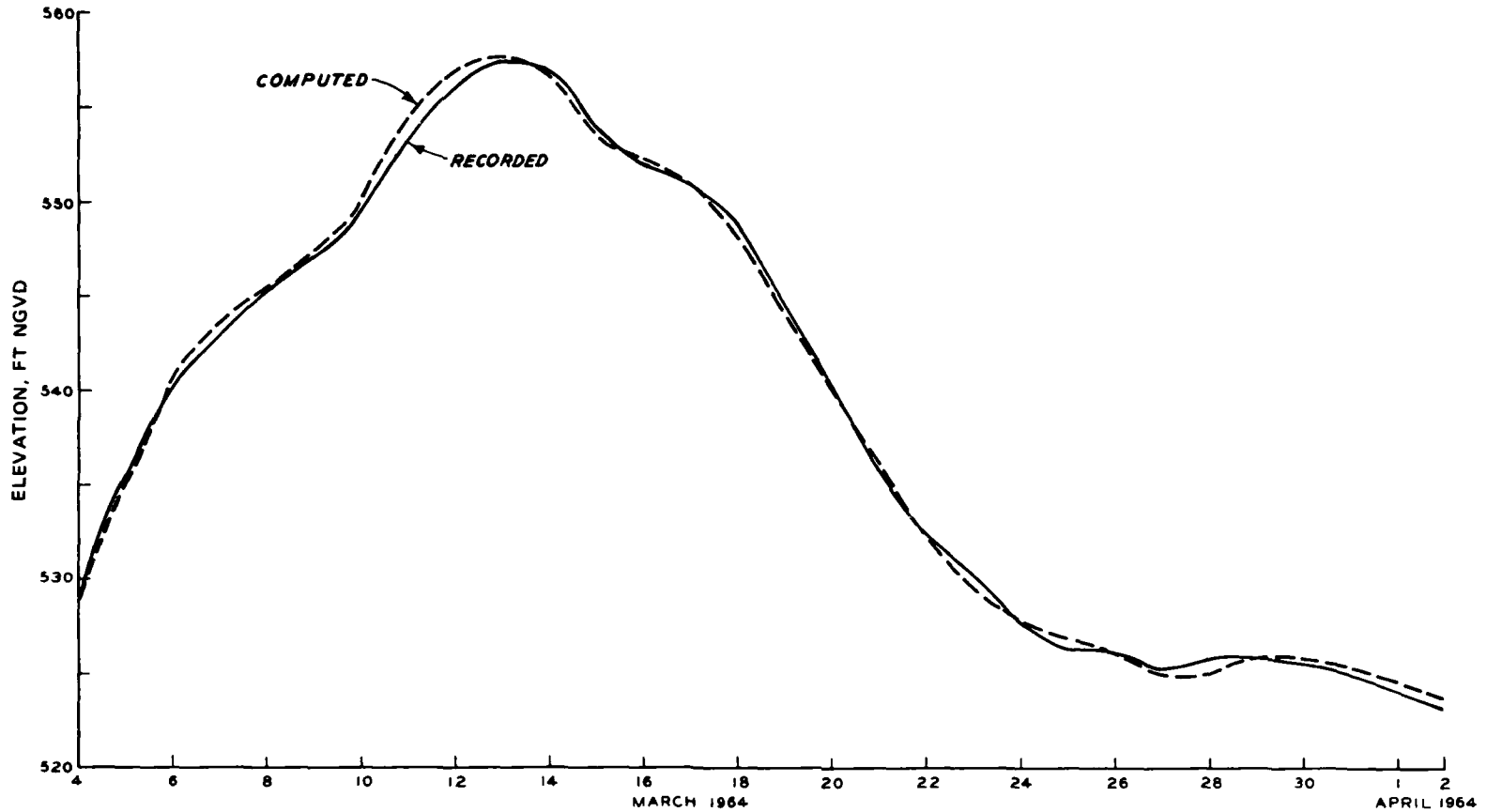

Figure 35. Recorded versus computed elevations at Gallipolis L&D, lower gage

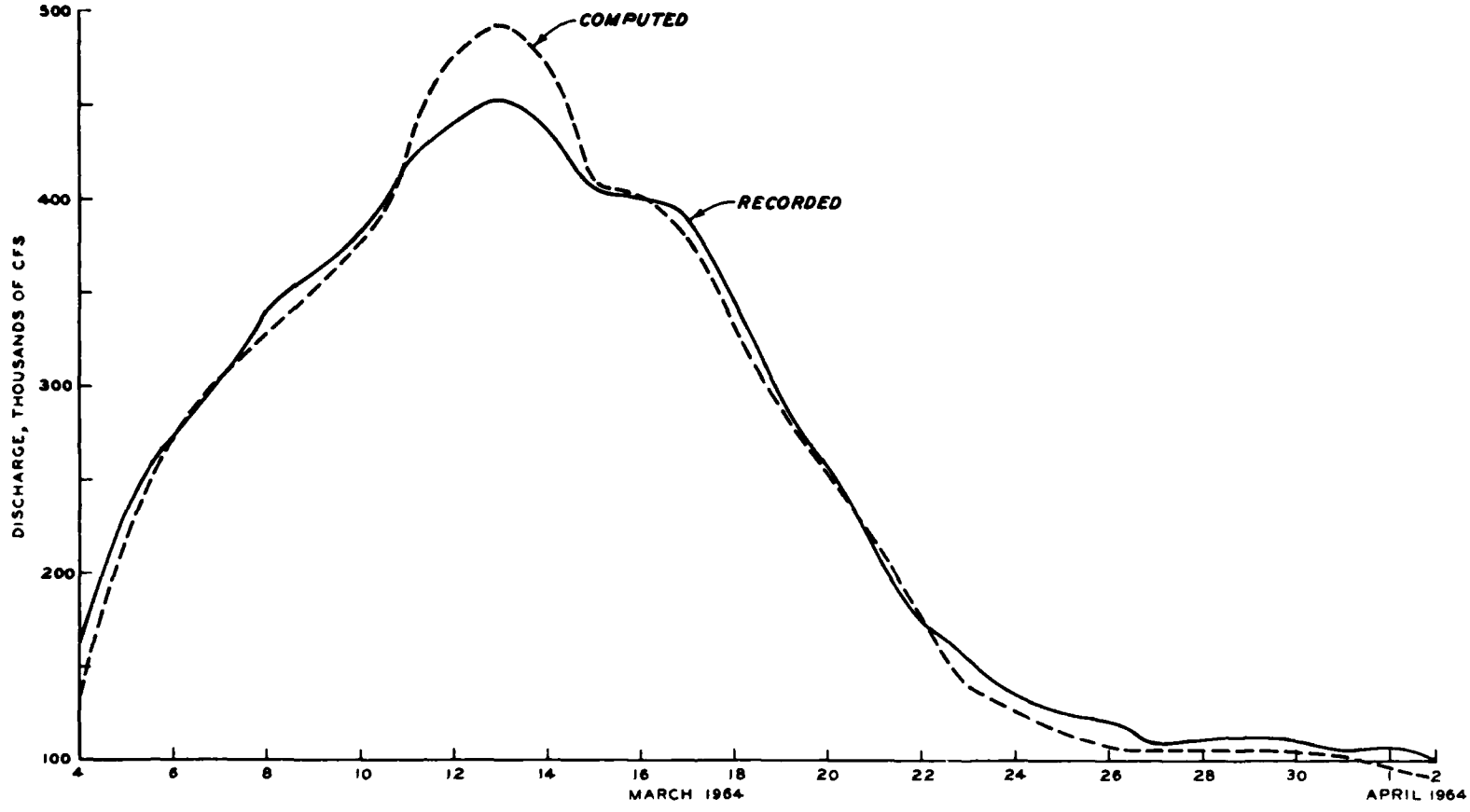

Figure 36. Recorded versus computed discharge at Huntington

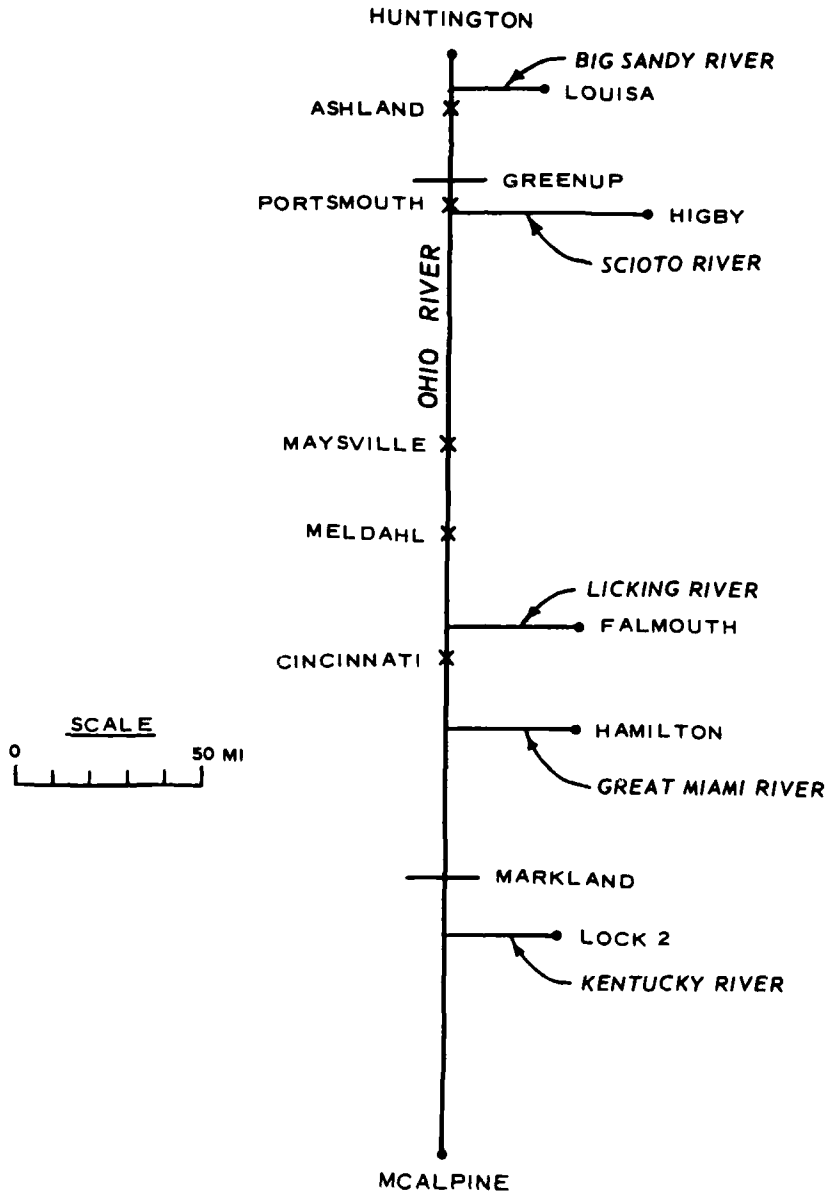

Figure 37. Location map for Huntington-McAlpine reach

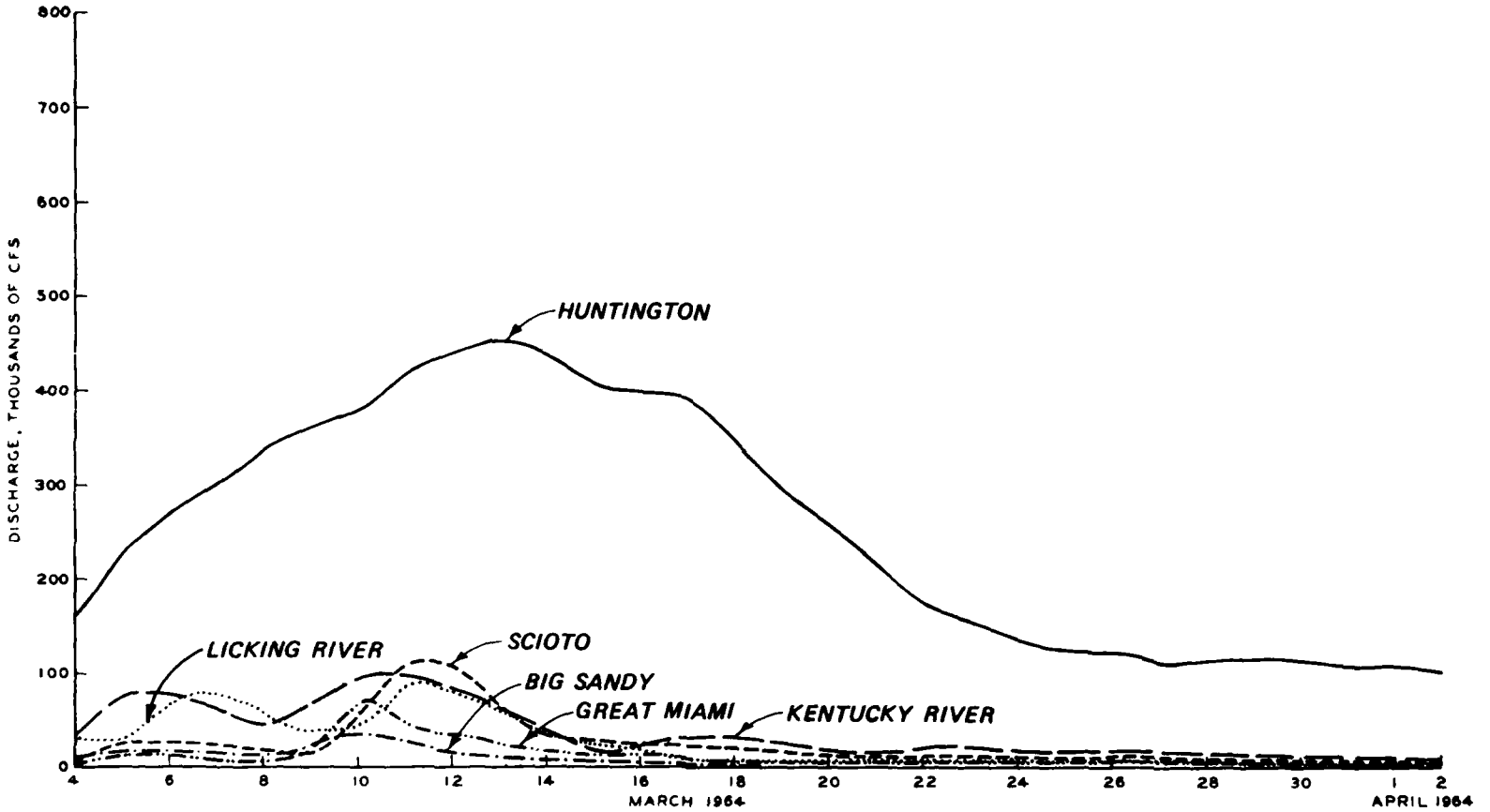

Figure 38. Inflow boundary conditions for Huntington to McAlpine application

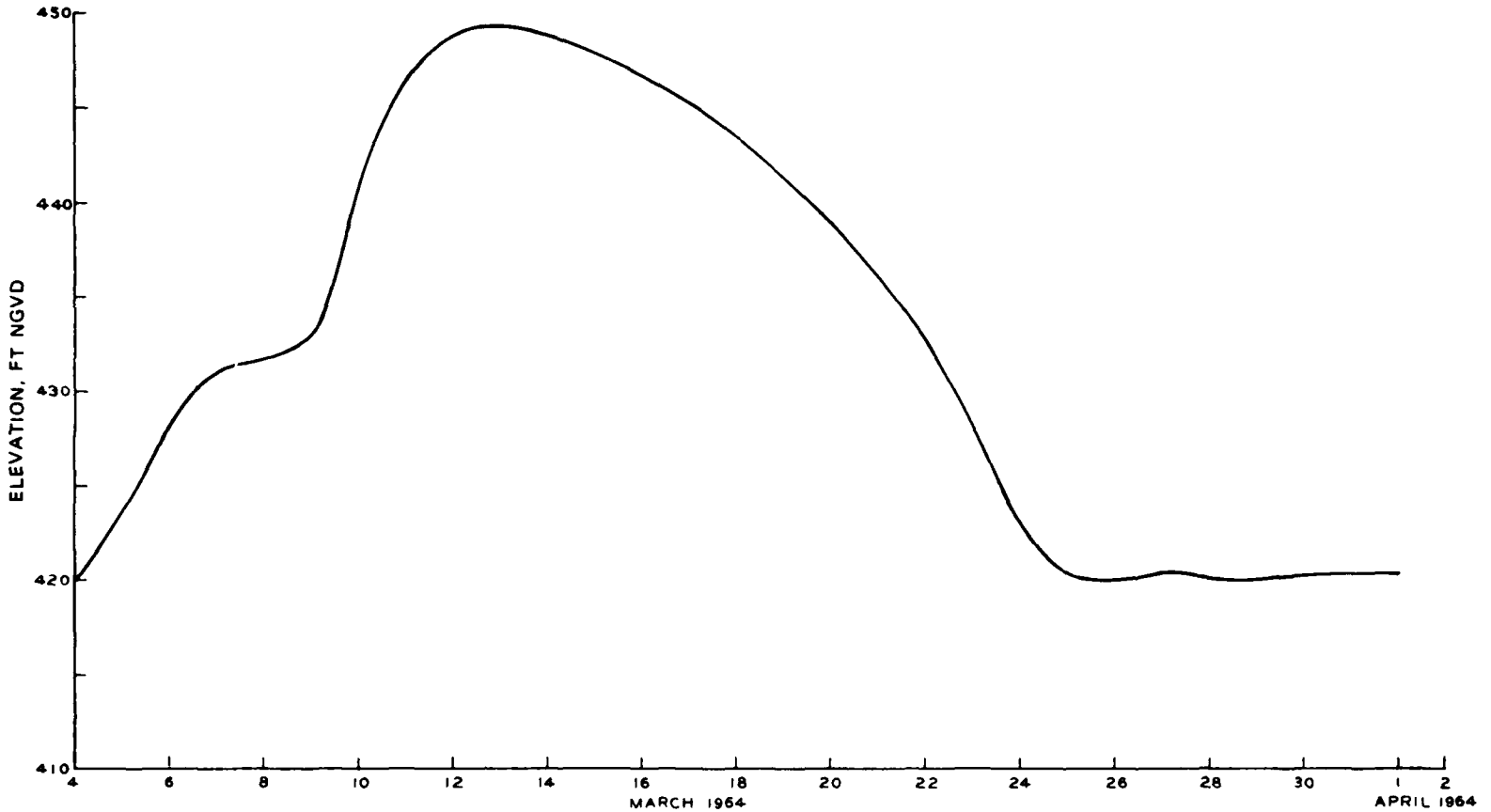

Figure 39. Boundary elevations set at McAlpine L&D

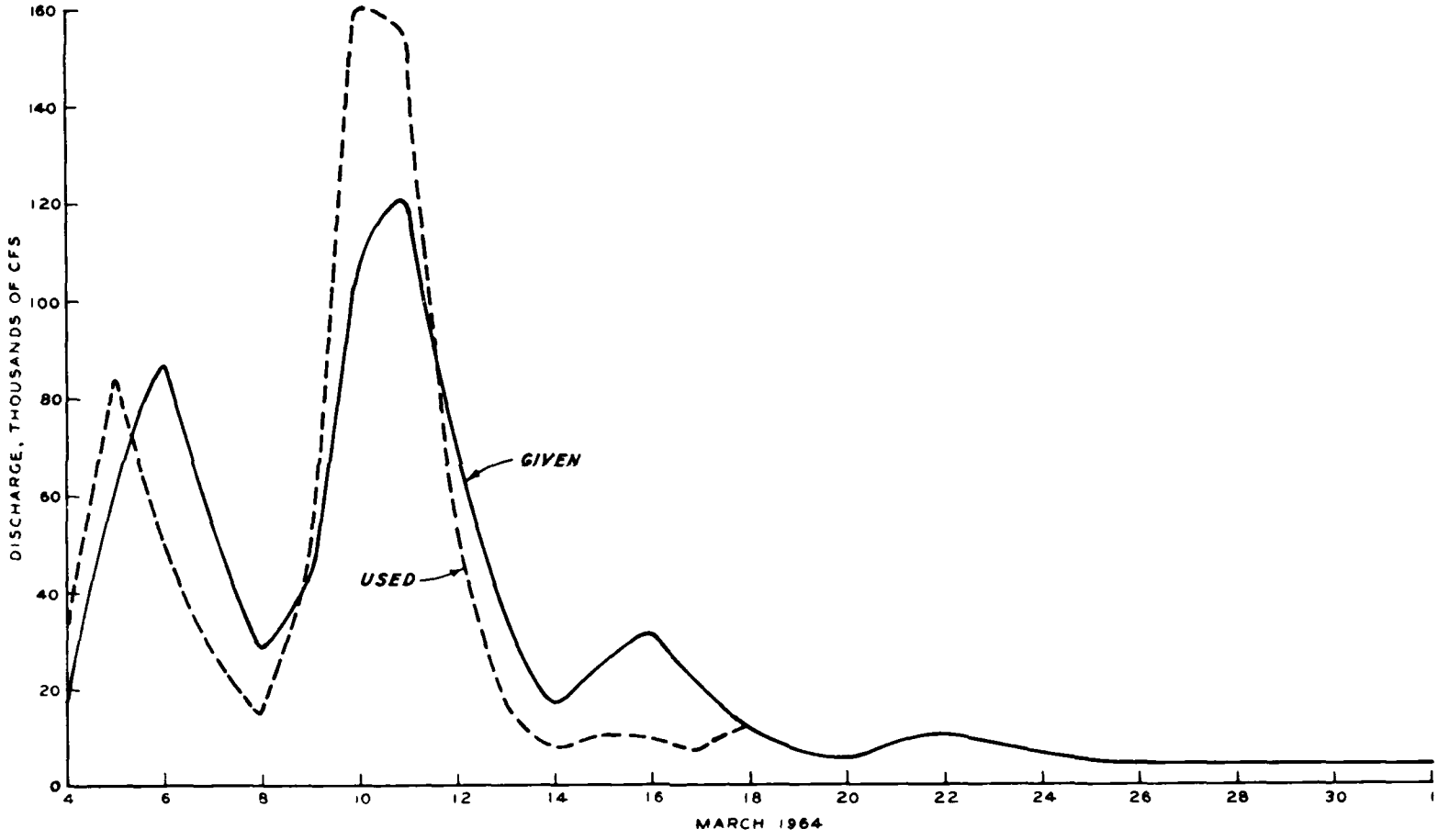

Figure 40. Ungaged lateral inflow in Huntington-Maysville reach

AD-A121 283 DEVELOPMENT OF A NUMERICAL MODELING CAPABILITY FOR THE COMPUTATION OF UNS..(U) ARMY ENGINEER WATERWAYS EXPERIMENT STATION VICKSBURG MS HYDRA.. B H JOHNSON 2/2

UNCLASSIFIED AUG 82 WES-TR-HL-82-20 F/G 8/8 NL

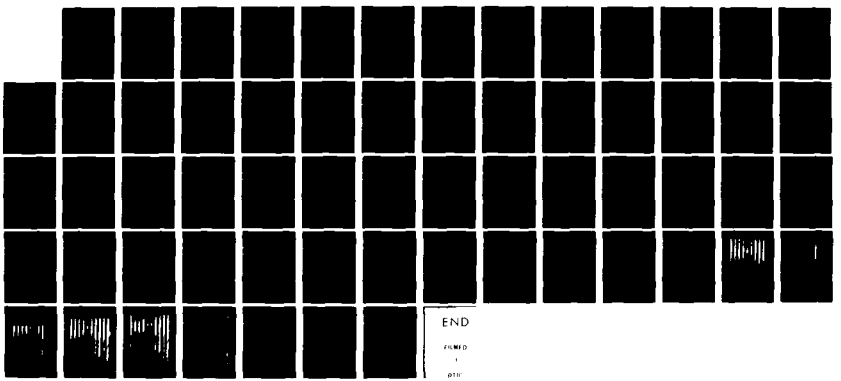

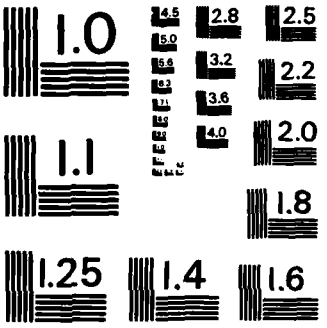

MICROCOPY RESOLUTION TEST CHART
NATIONAL BUREAU OF STANDARDS - 1963 - A

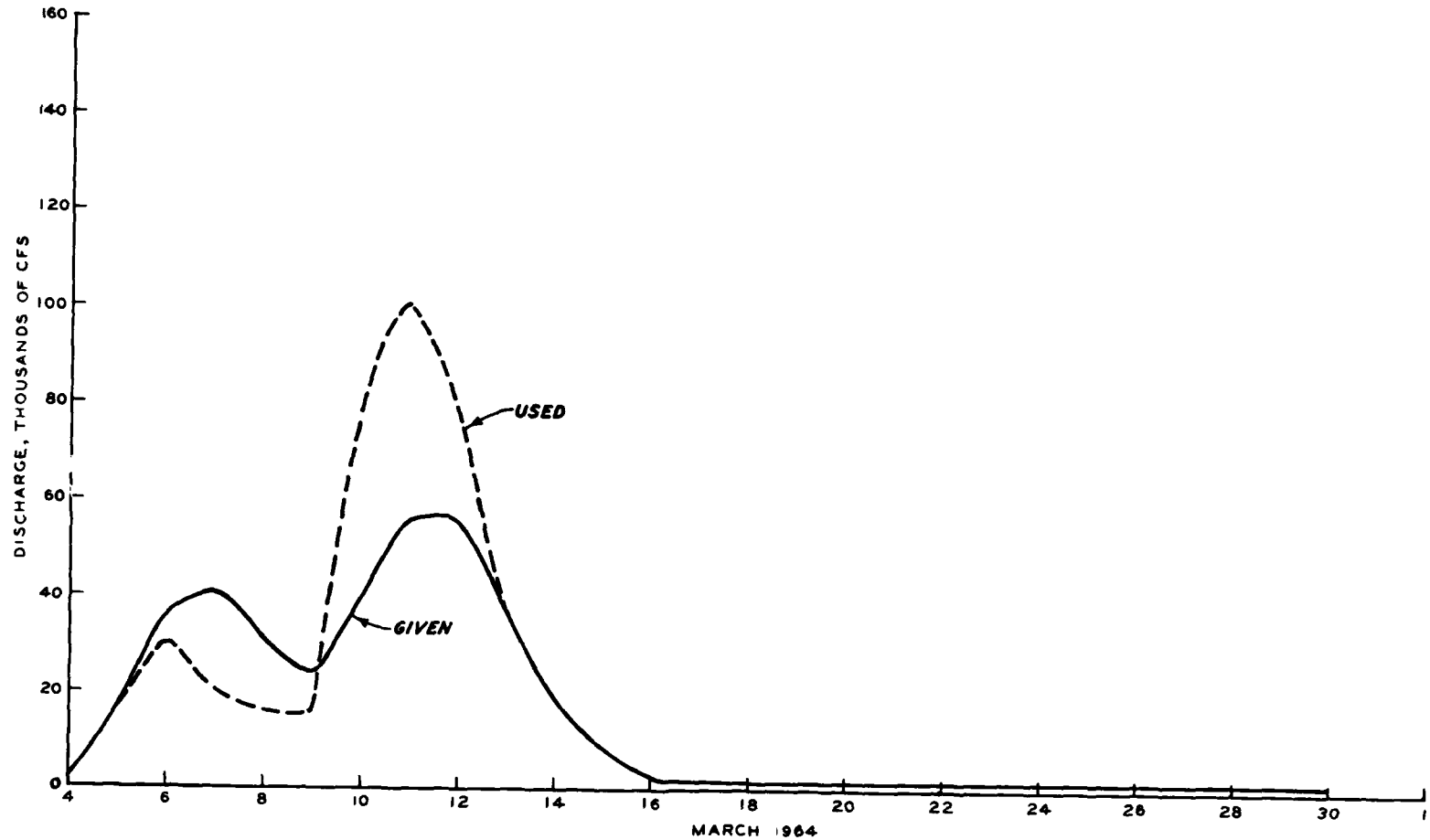

Figure 41. Ungaged lateral inflow in Maysville-Cincinnati reach

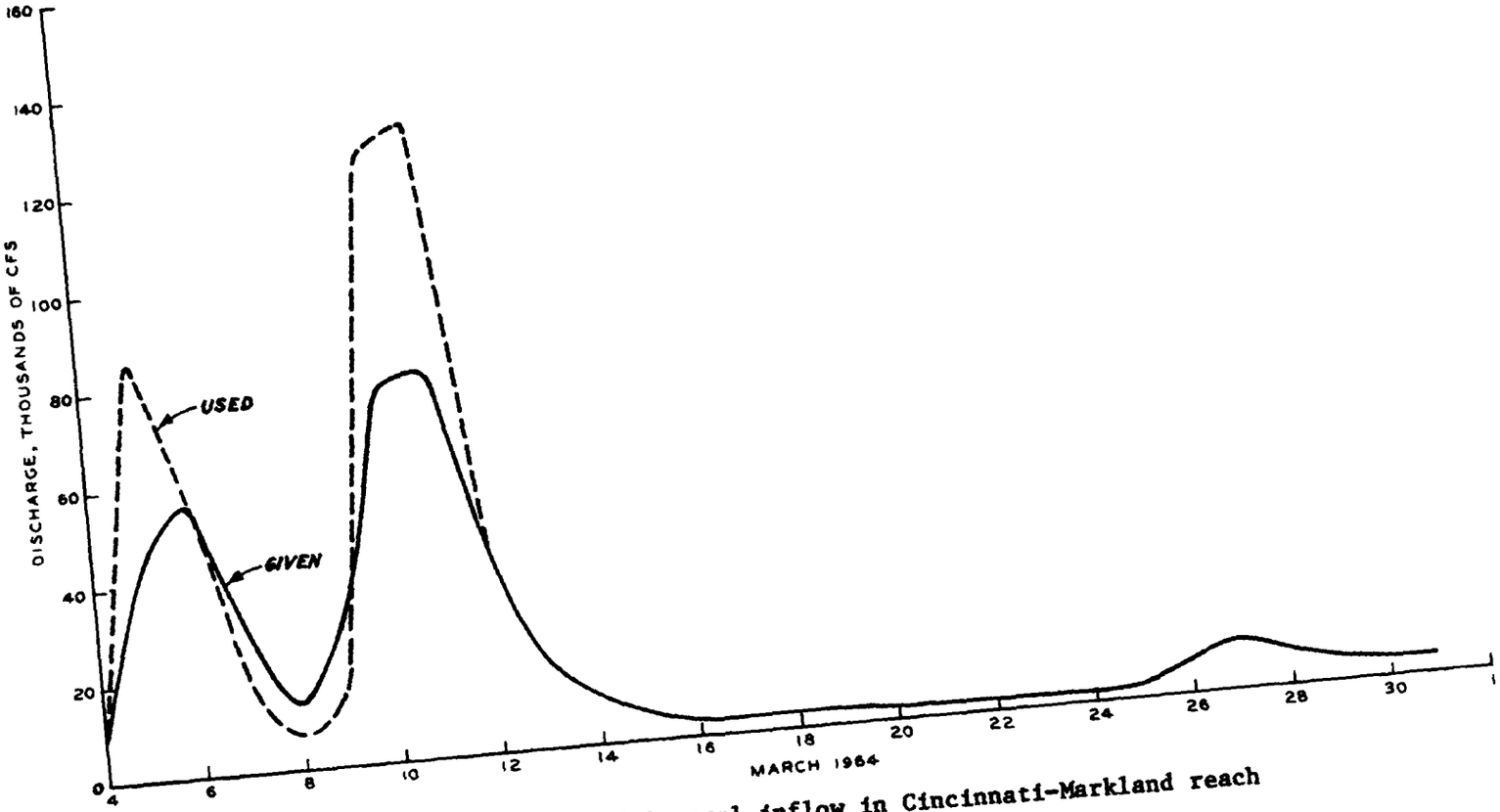

Figure 42. Ungaged lateral inflow in Cincinnati-Markland reach

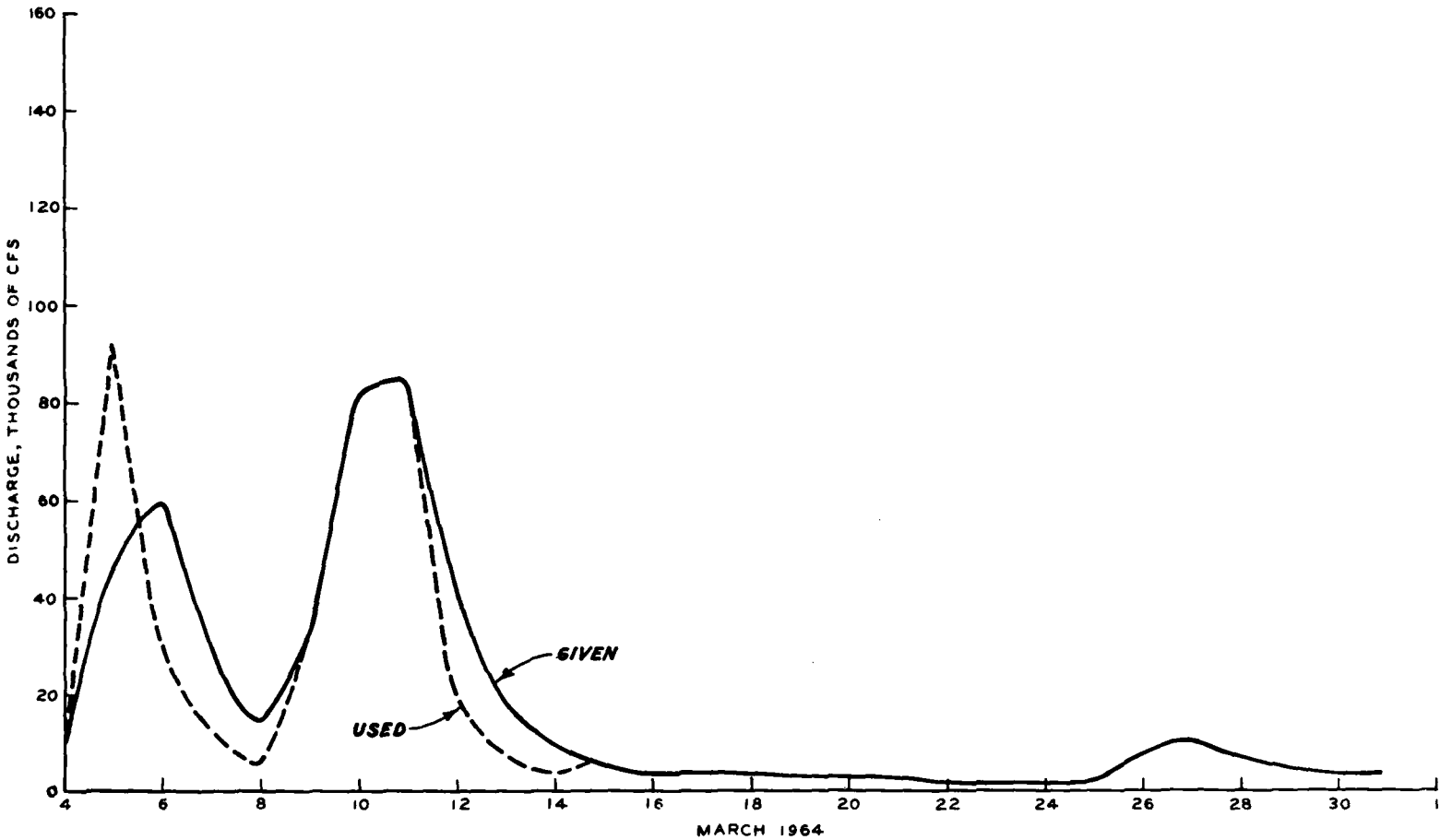

Figure 43. Ungaged lateral inflow in Markland-McAlpine reach

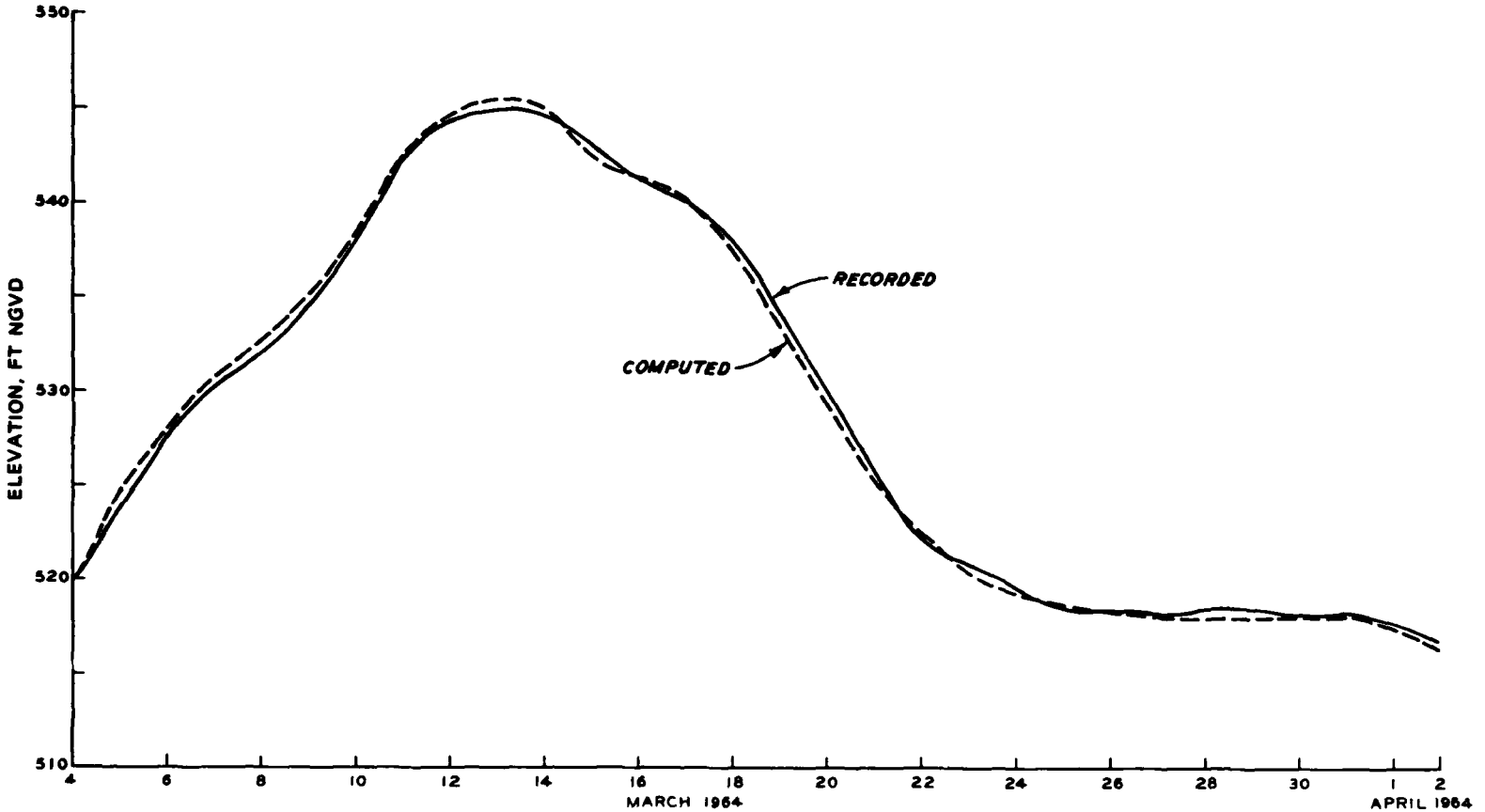

Figure 44. Recorded versus computed elevations at Huntington

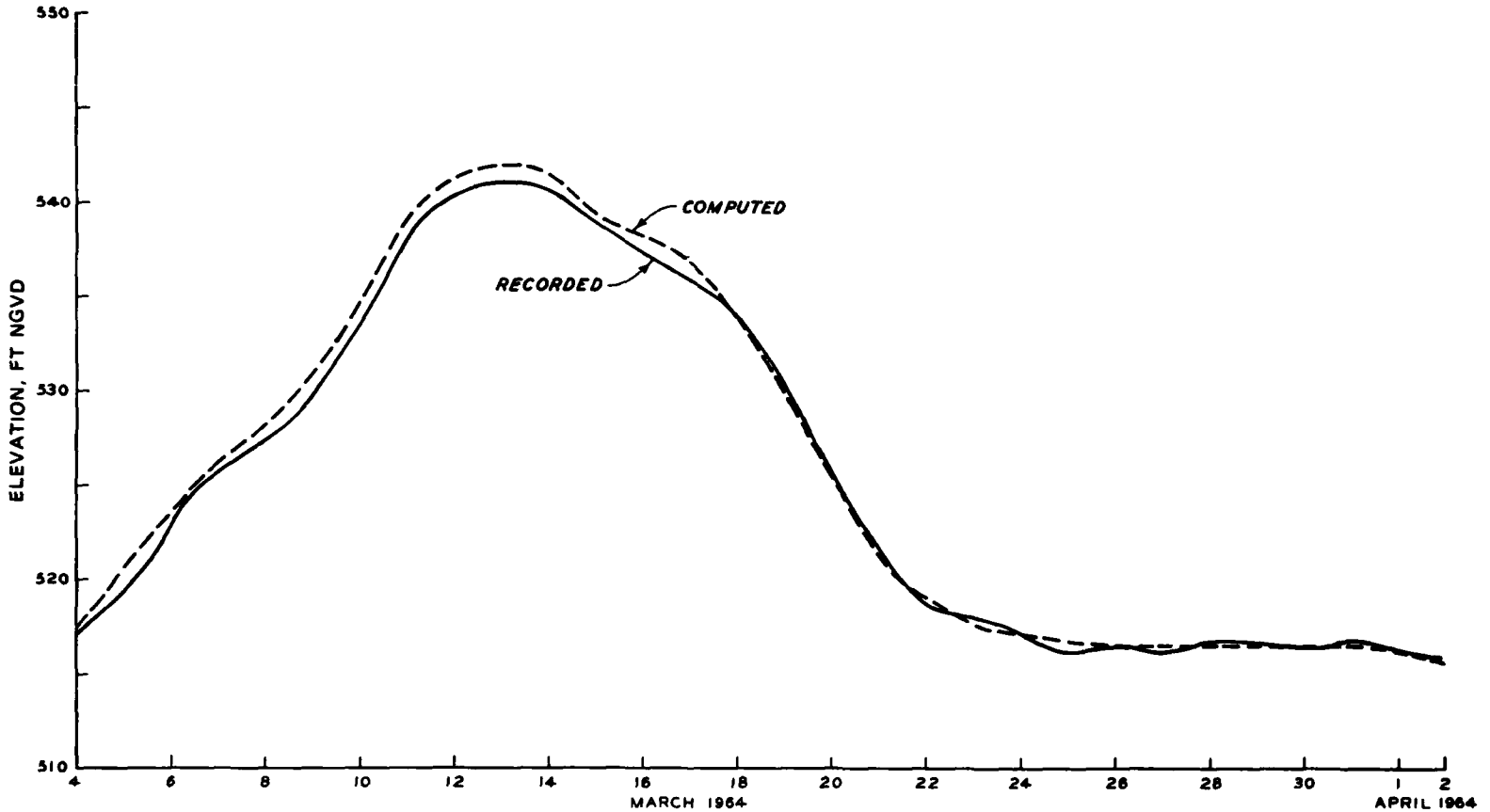

Figure 45. Recorded versus computed elevations at Ashland

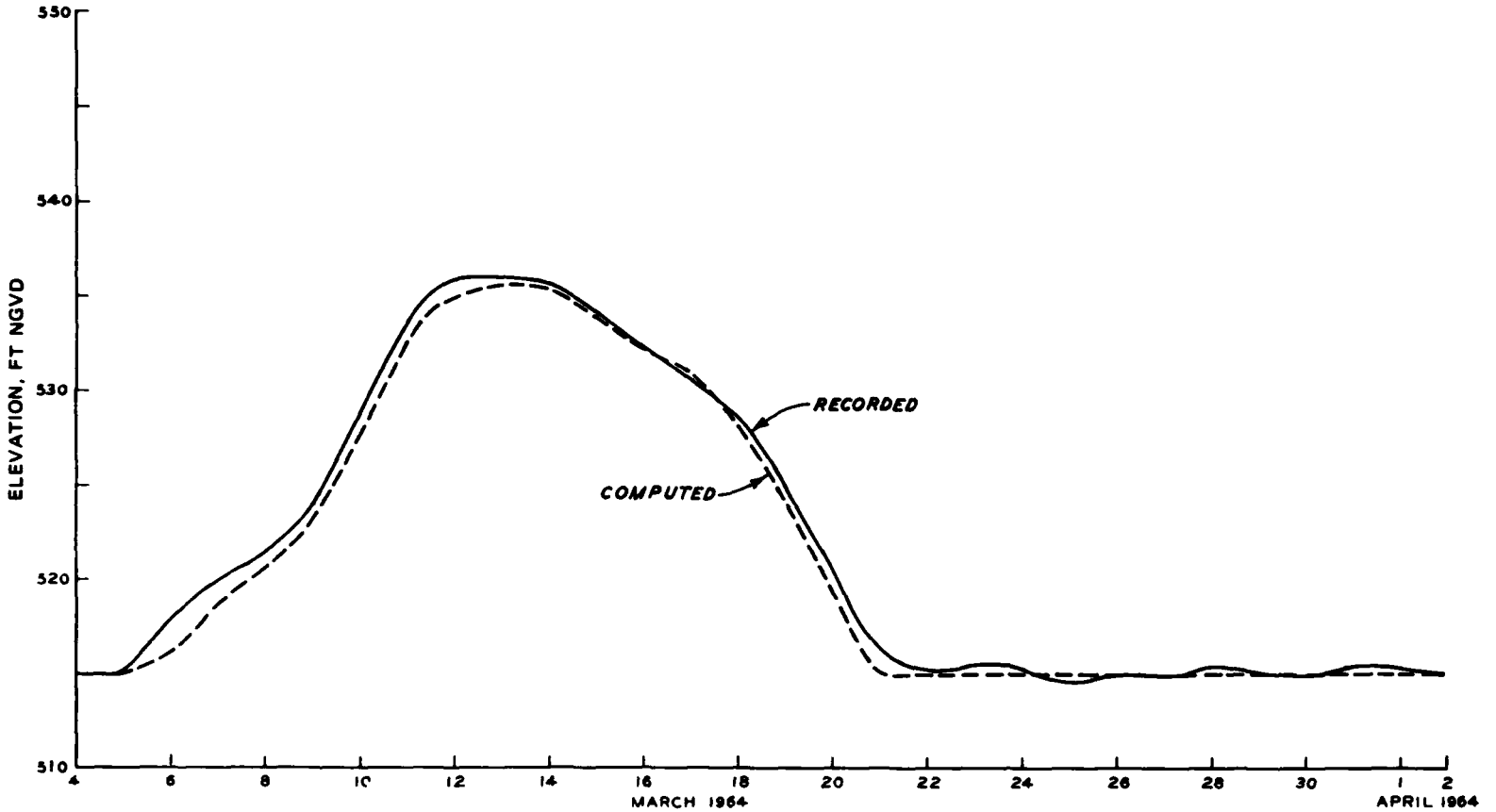

Figure 46. Recorded versus computed elevations at Greenup L&D, upper gage

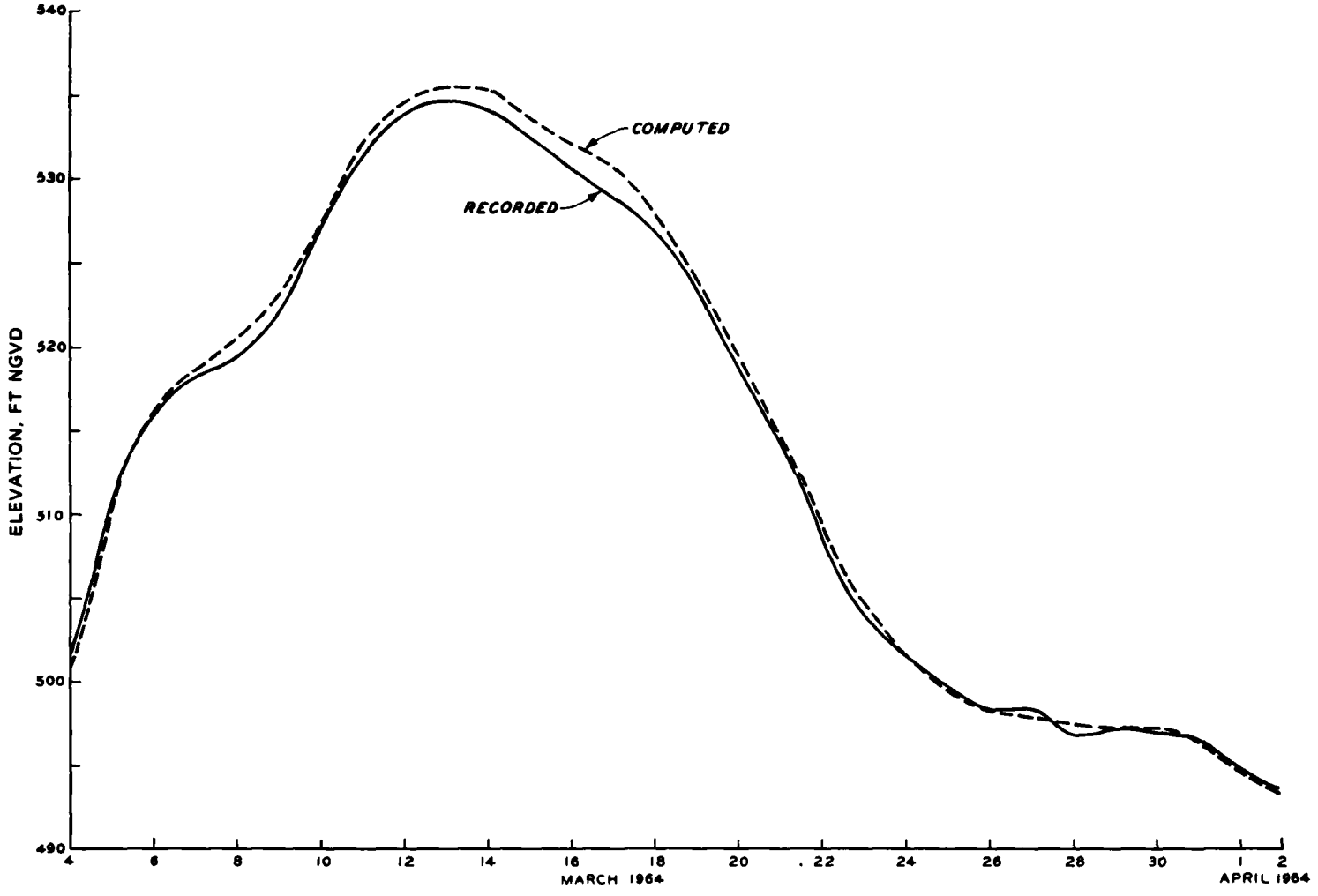

Figure 47. Recorded versus computed elevations at Greenup L&D, lower gage

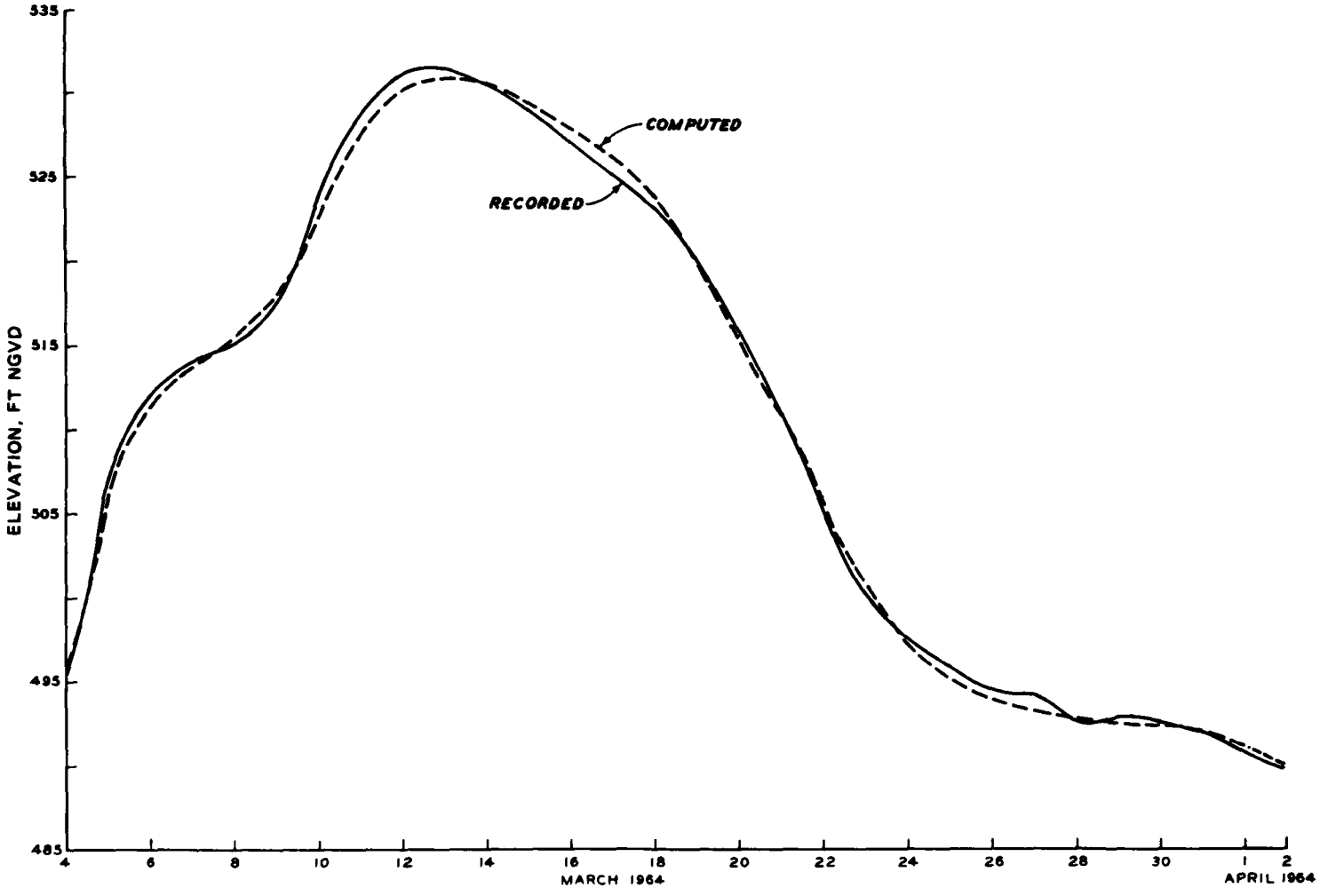

Figure 48. Recorded versus computed elevations at Portsmouth

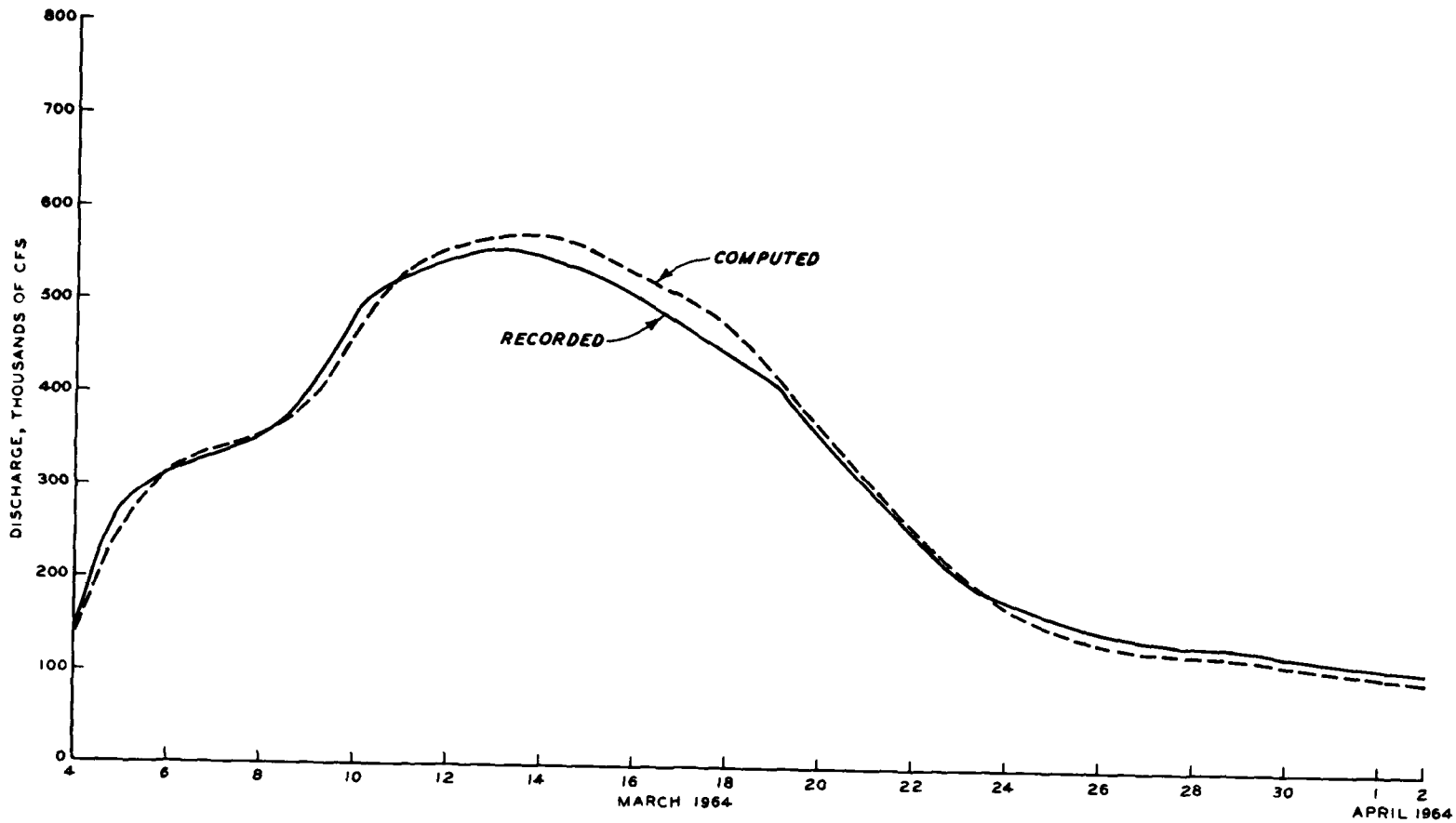

Figure 49. Recorded versus computed discharge at Maysville

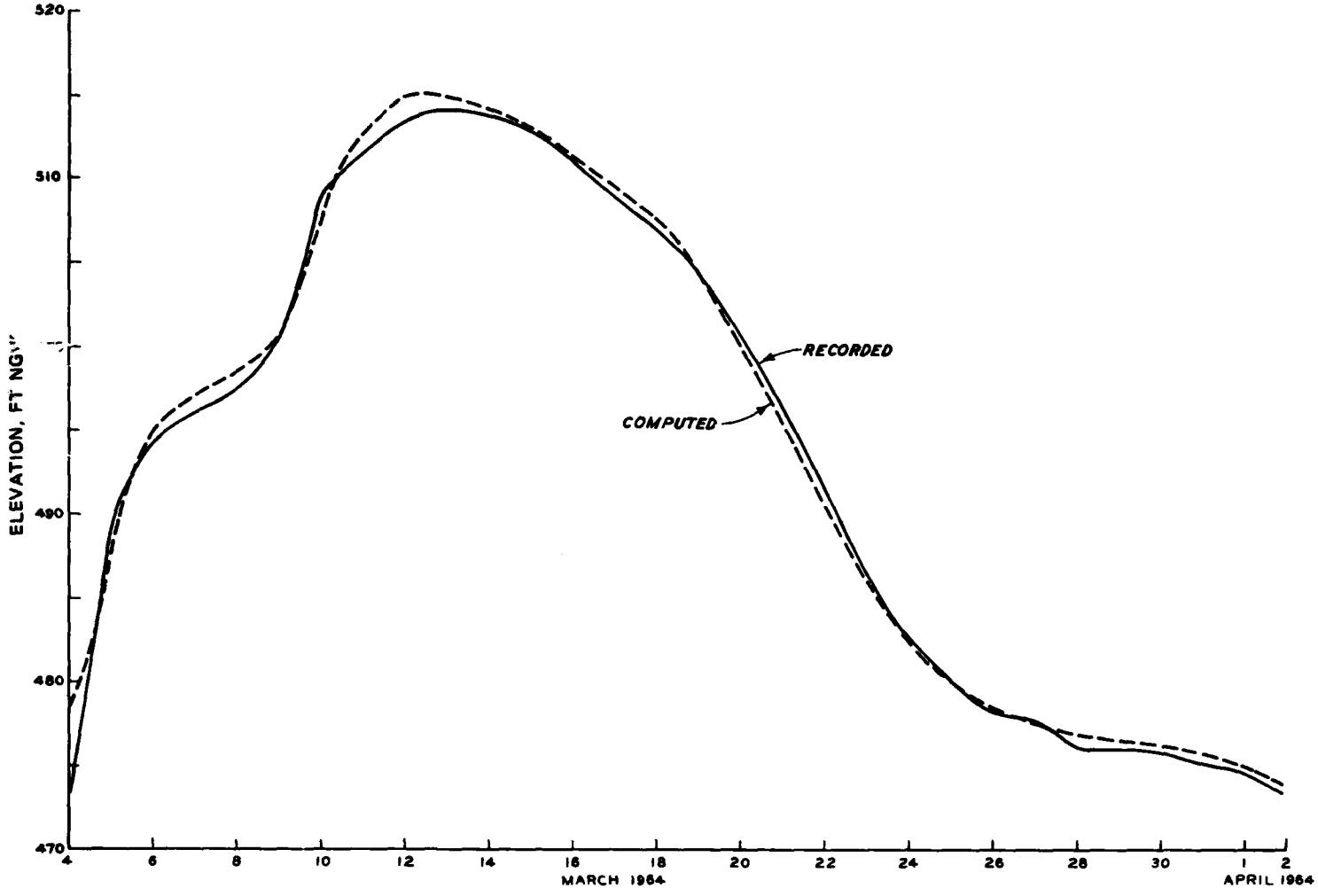

Figure 50. Recorded versus computed elevations at Maysville

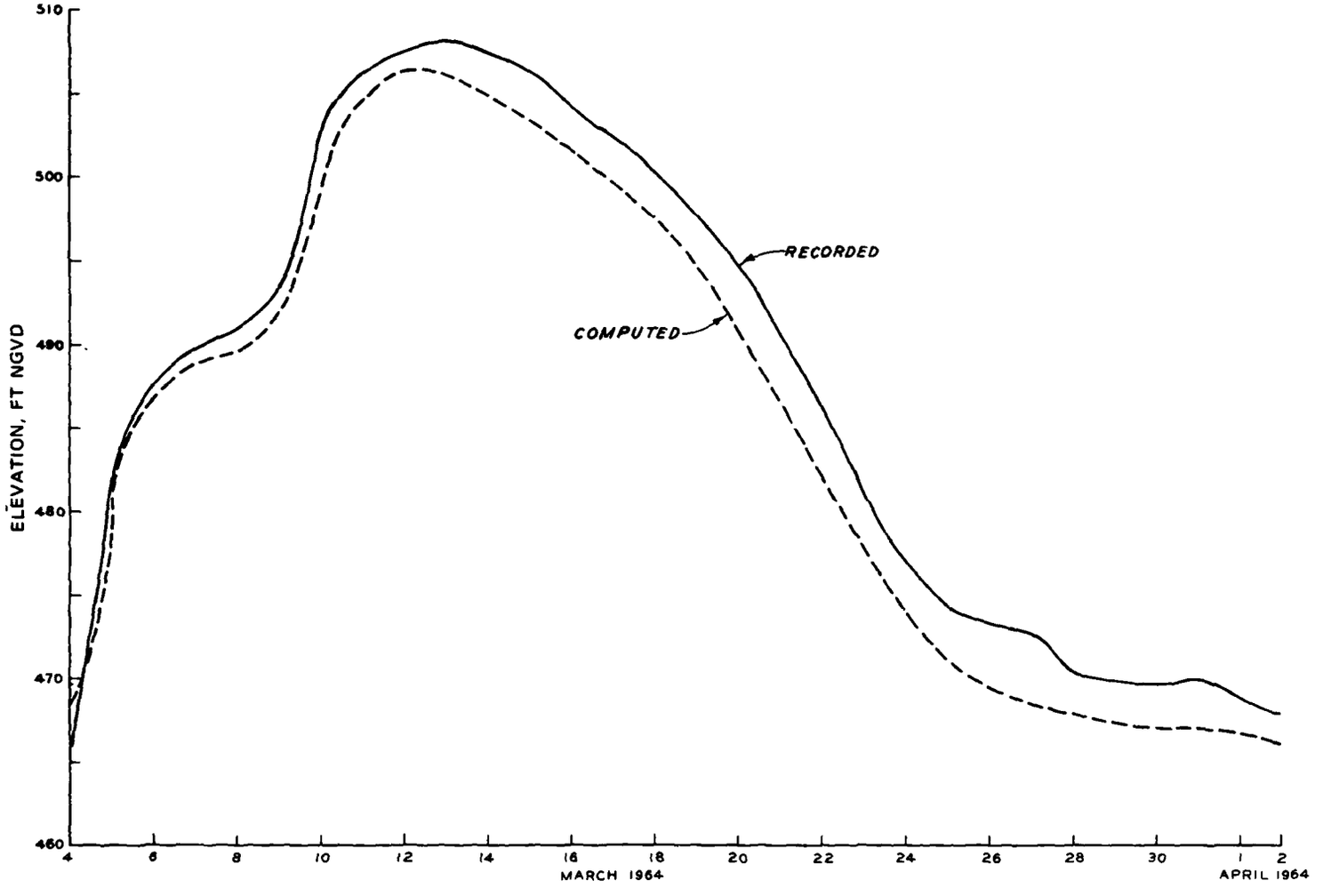

Figure 51. Recorded versus computed elevations at Meldahl L&D, upper gage

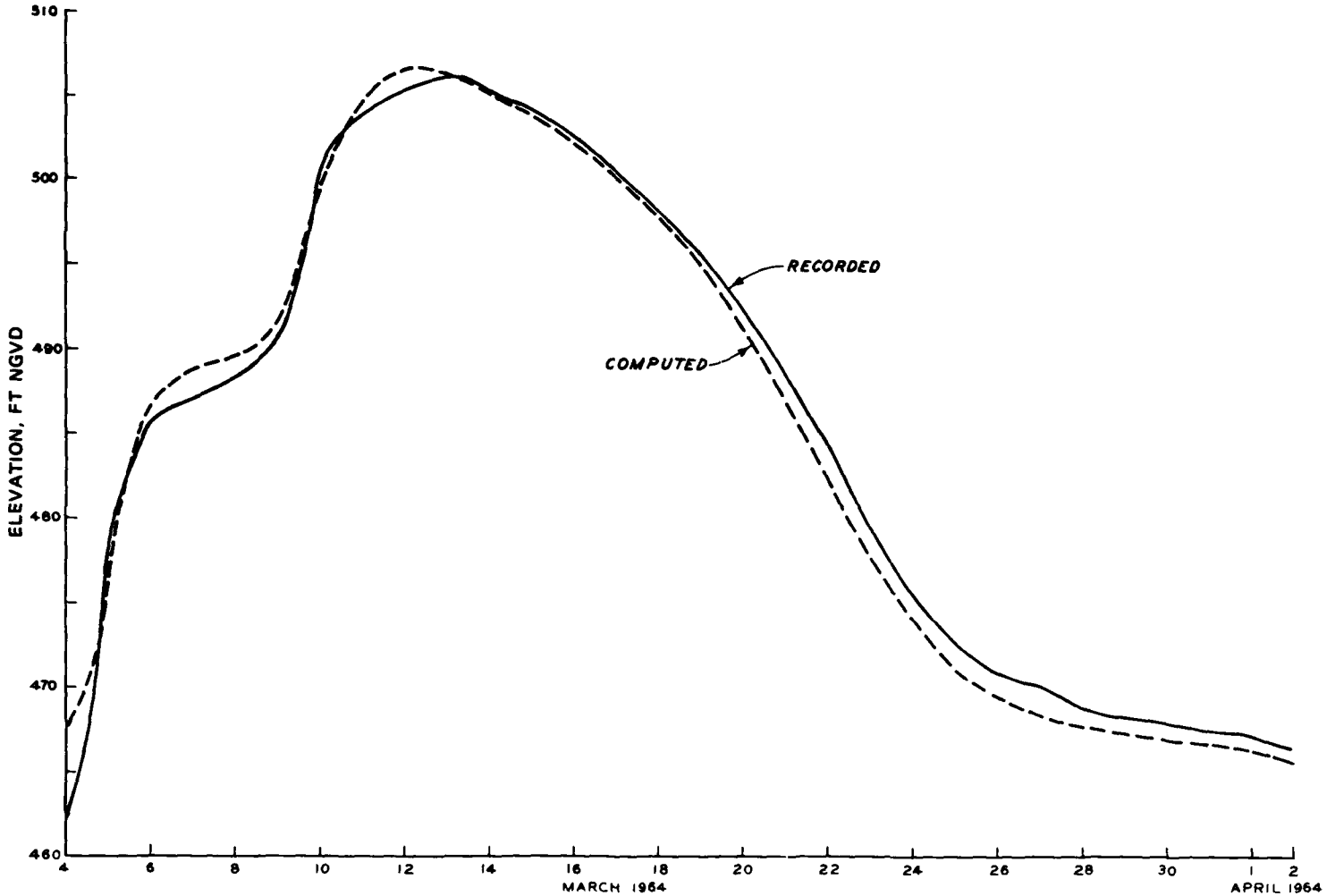

Figure 52. Recorded versus computed elevations at Meldahl L&D, lower gage

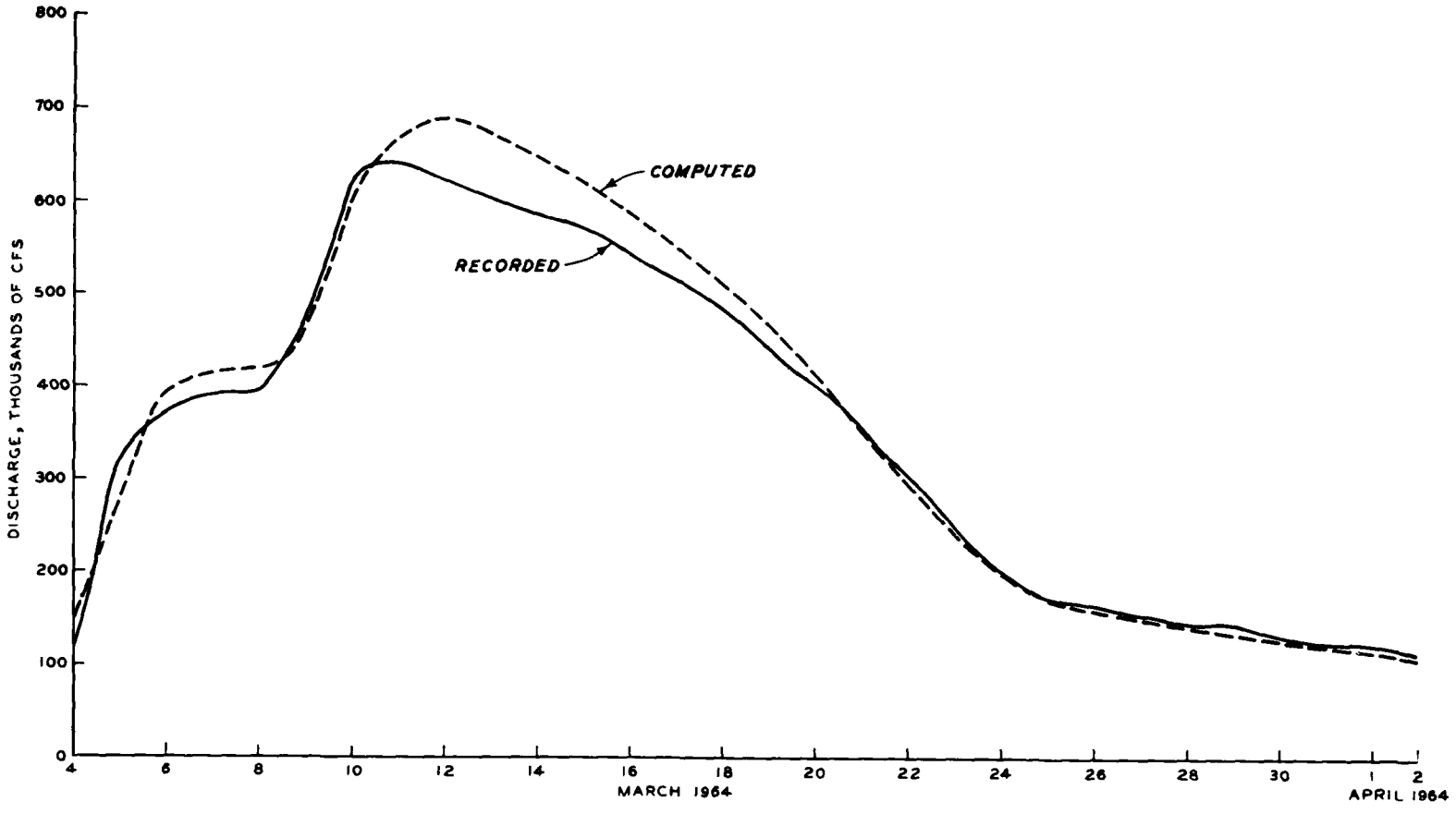

Figure 53. Recorded versus computed discharge at Cincinnati

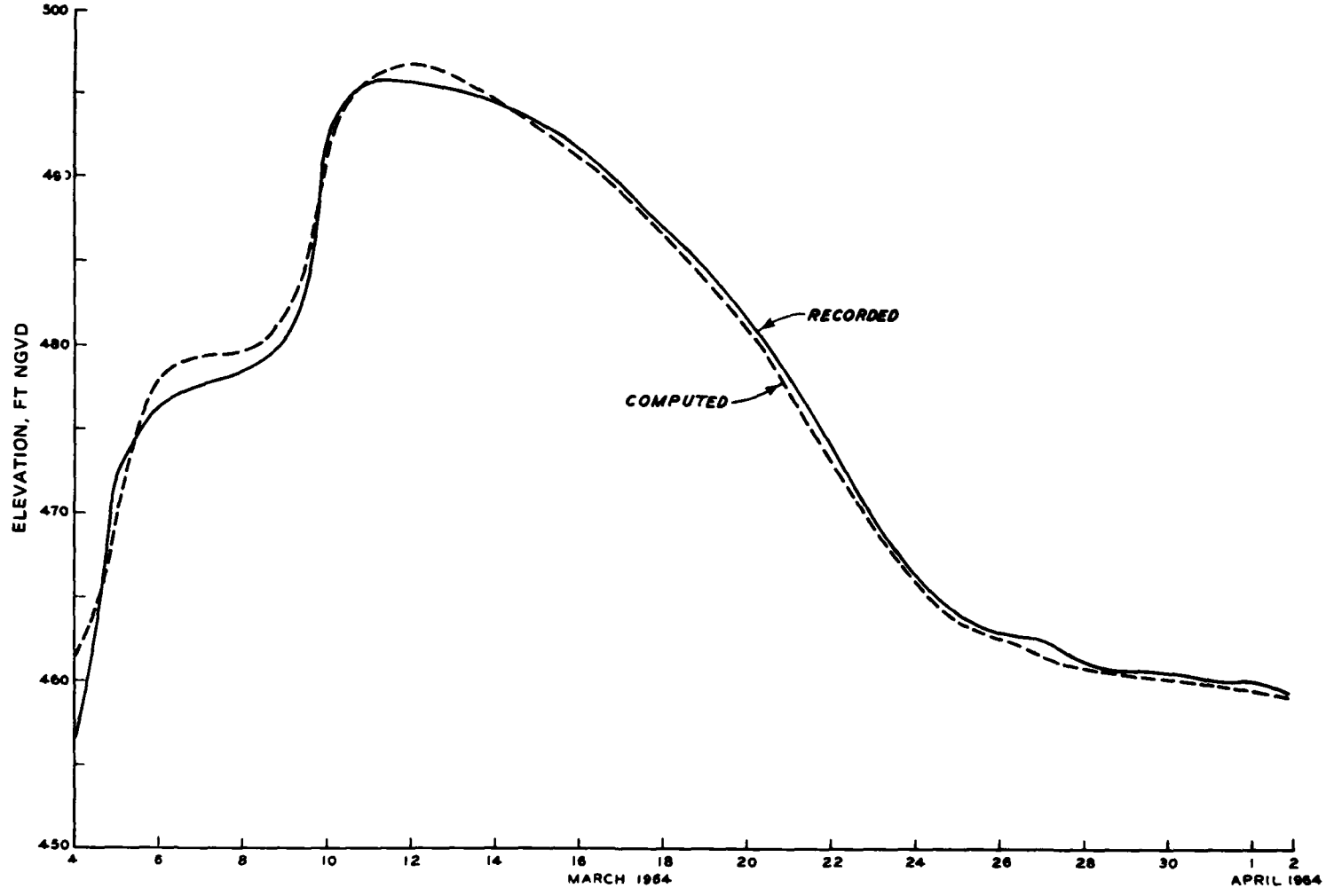

Figure 54. Recorded versus computed elevations at Cincinnati

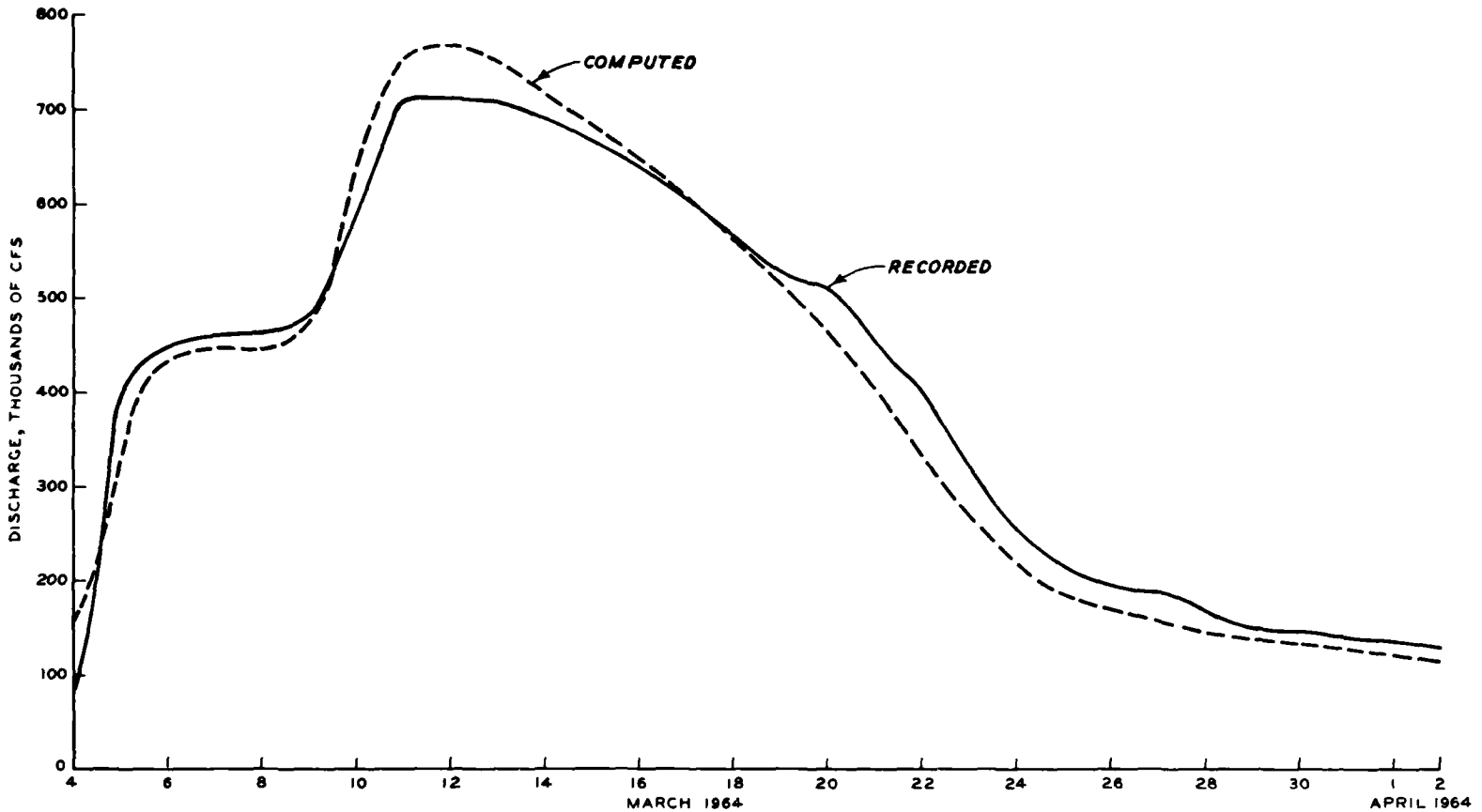

Figure 55. Recorded versus computed discharge at Markland L&D

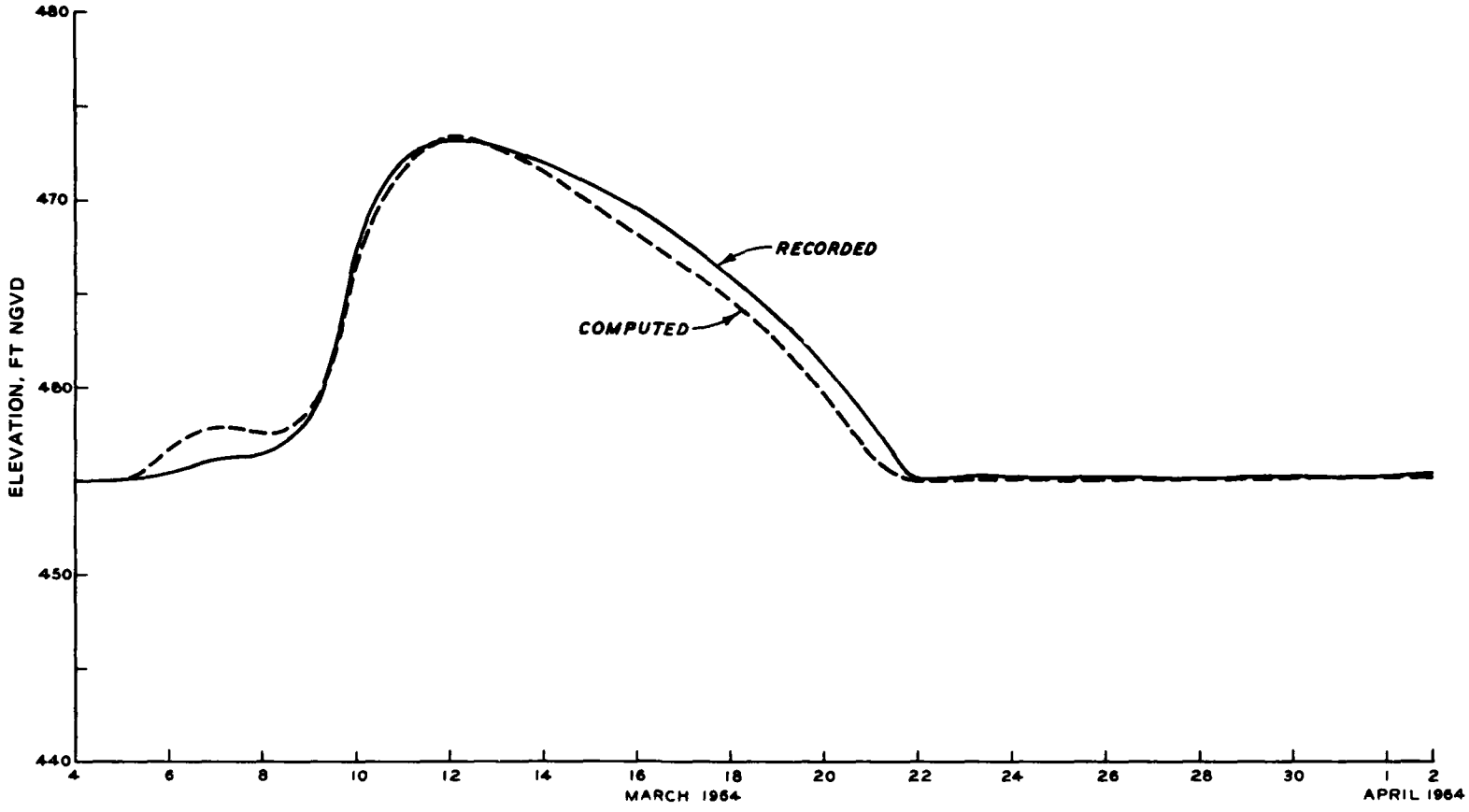

Figure 56. Recorded versus computed elevations at Markland L&D, upper gage

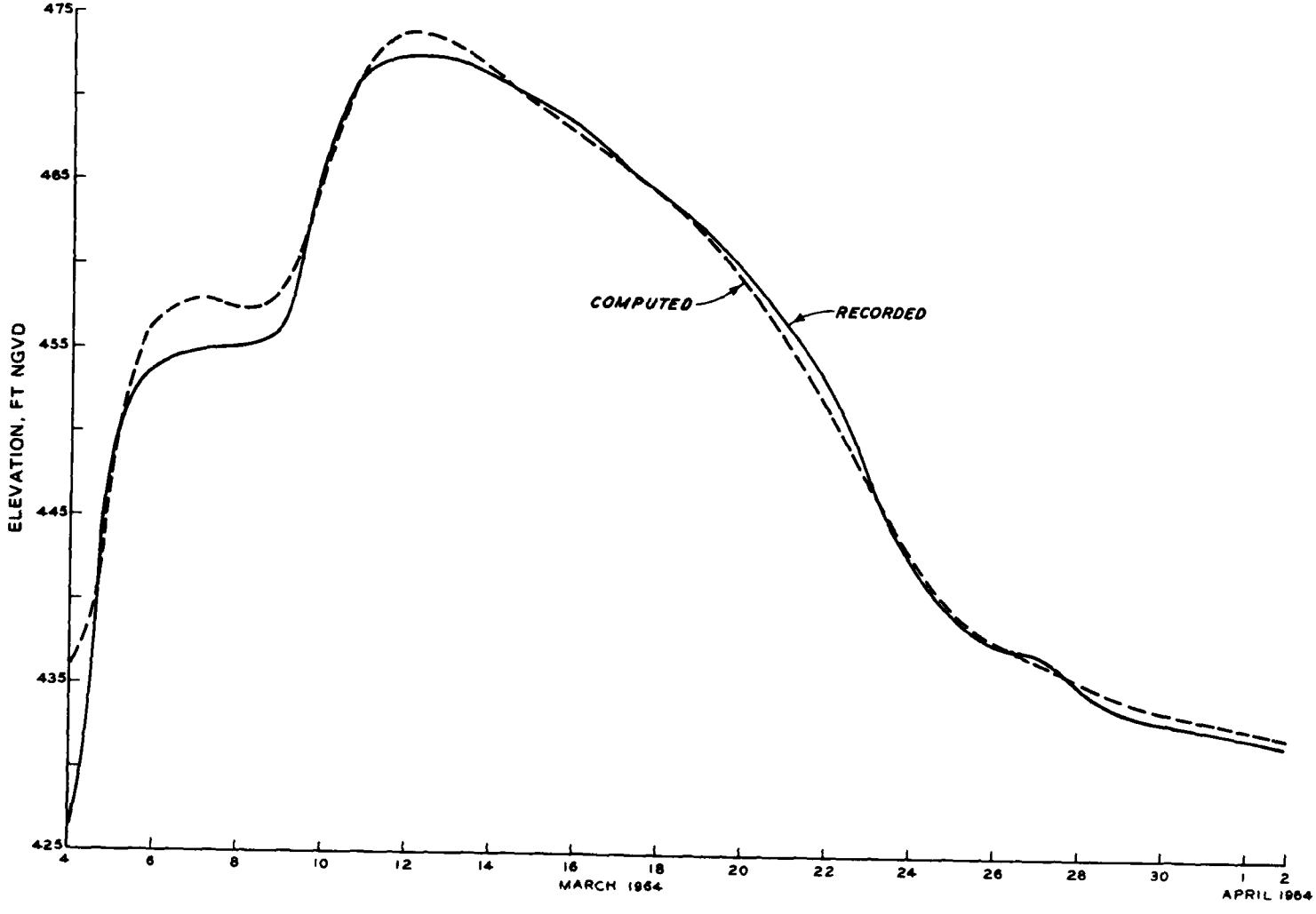

Figure 57. Recorded versus computed elevations at Markland L&D, lower gage

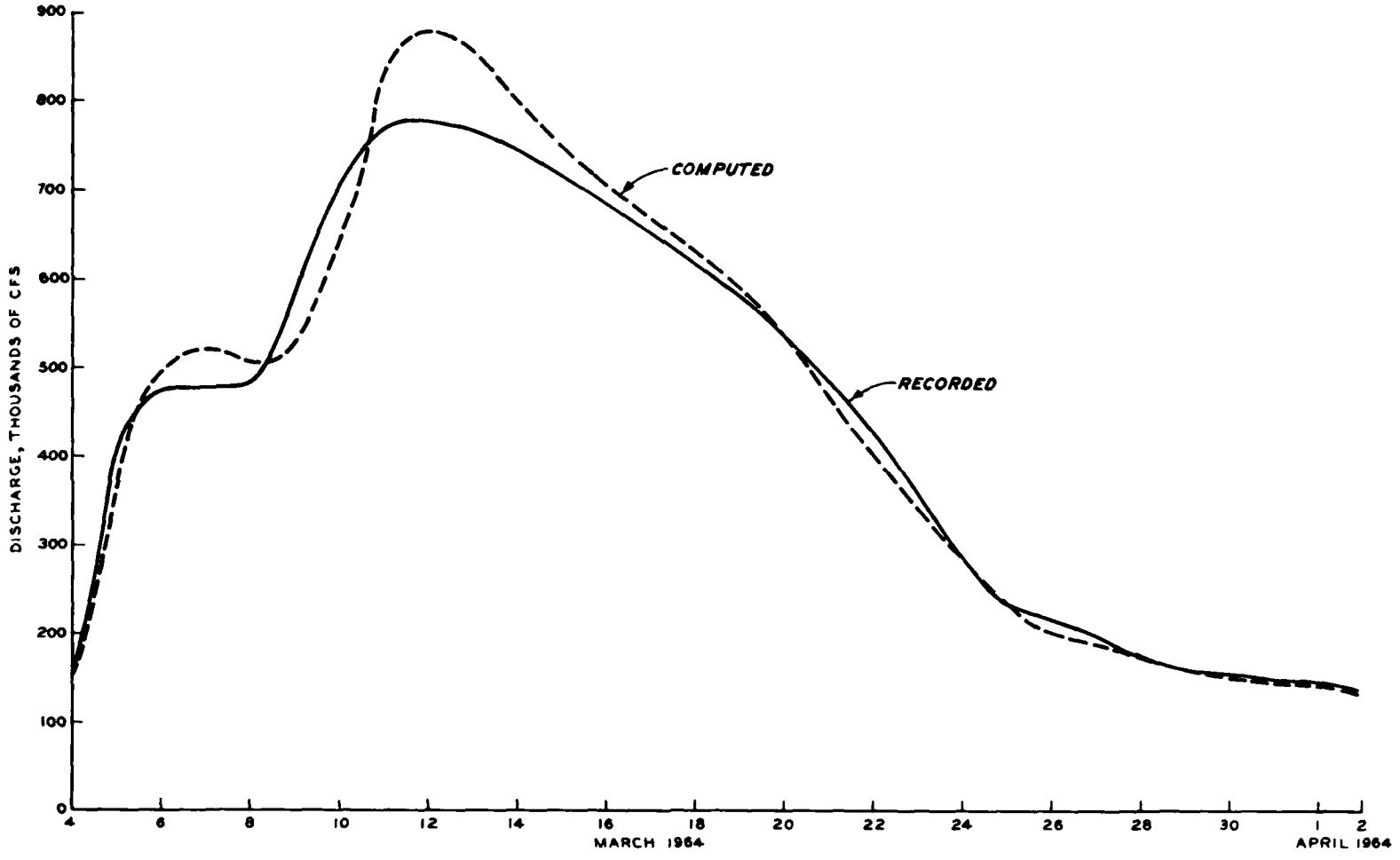

Figure 58. Recorded versus computed discharges at McAlpine L&D

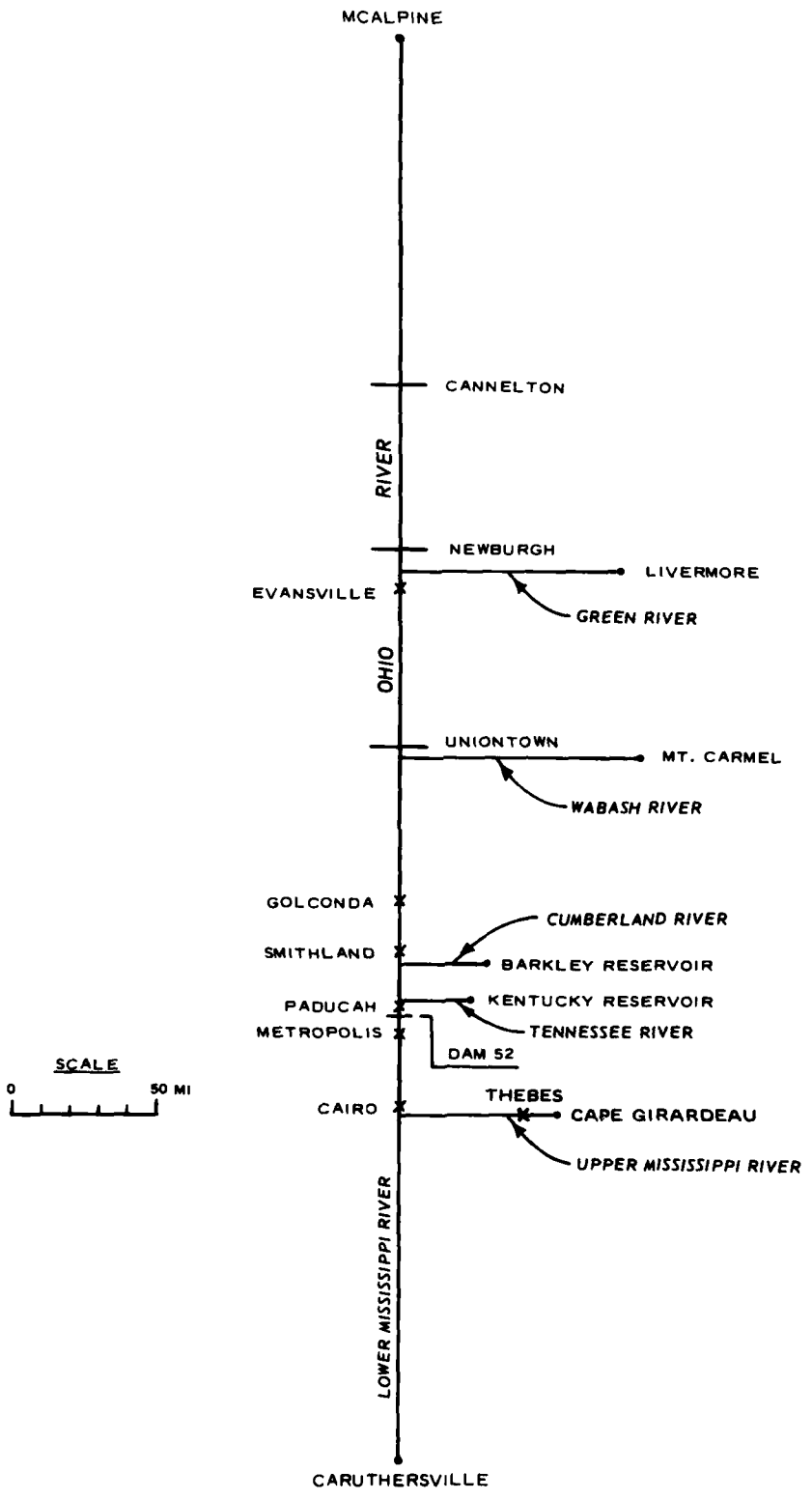

Figure 59. Location map for McAlpine to Caruthersville application

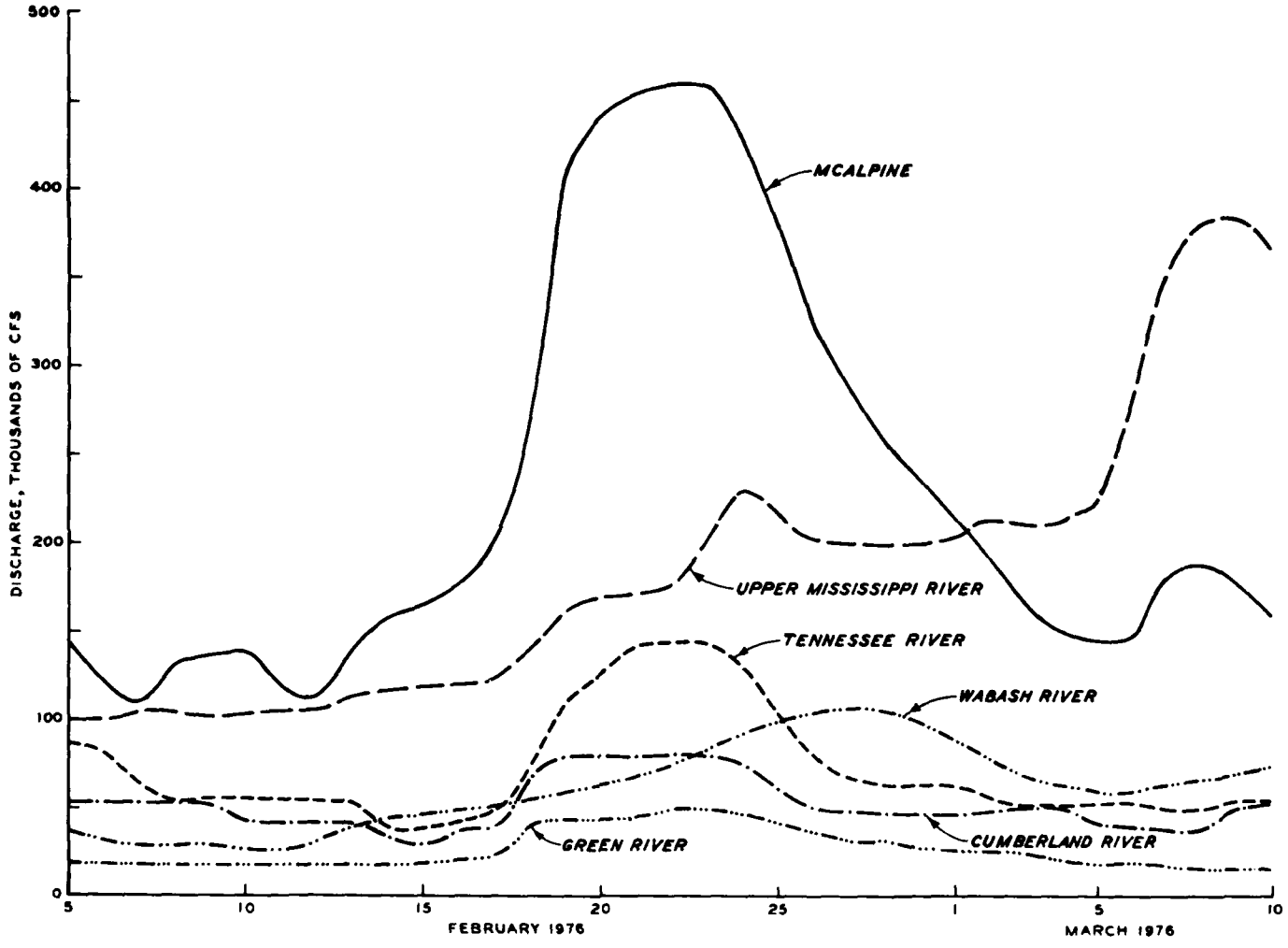

Figure 60. Boundary inflow hydrograph for McAlpine-Caruthersville application

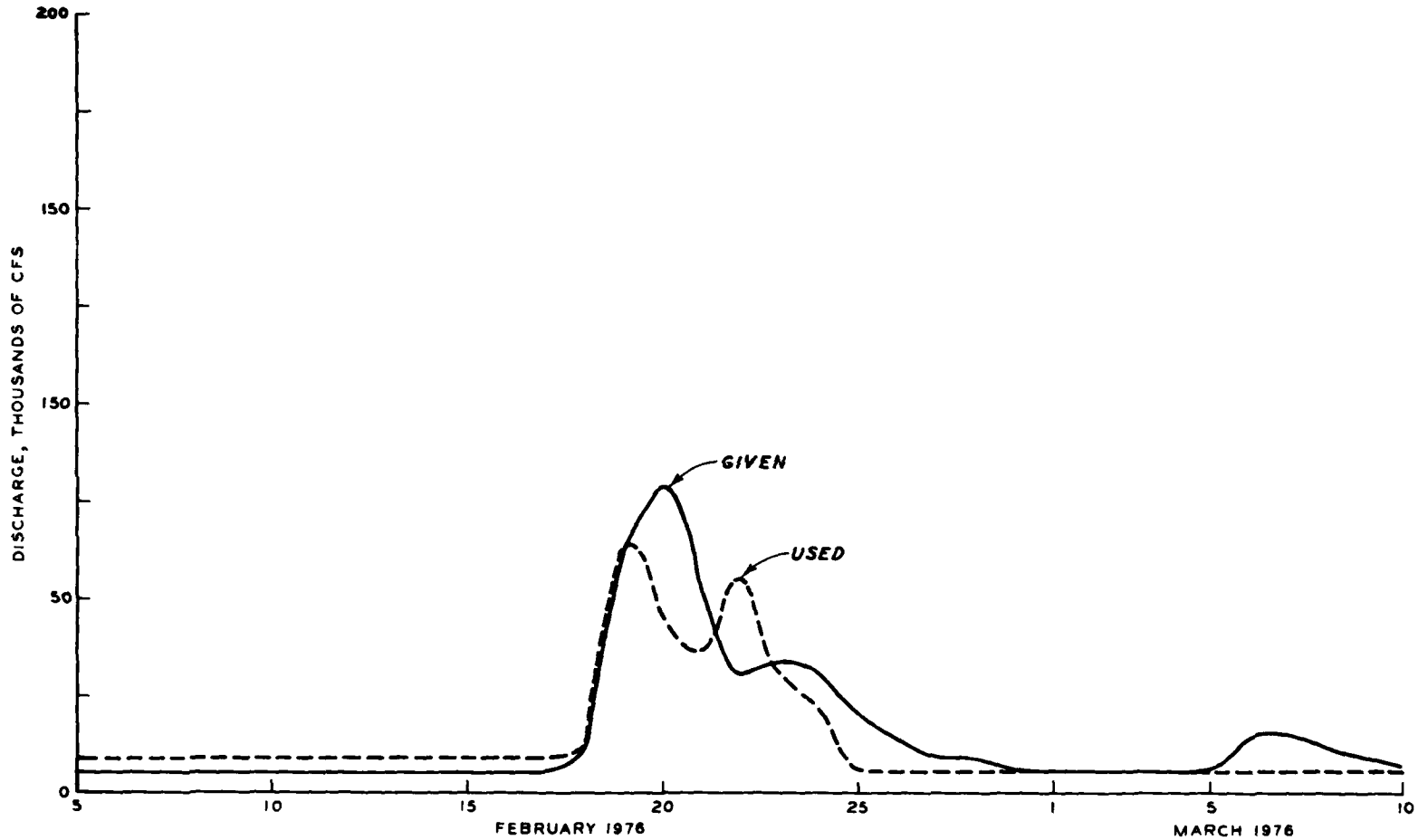

Figure 61. Ungaged lateral inflow in McAlpine-Evansville reach

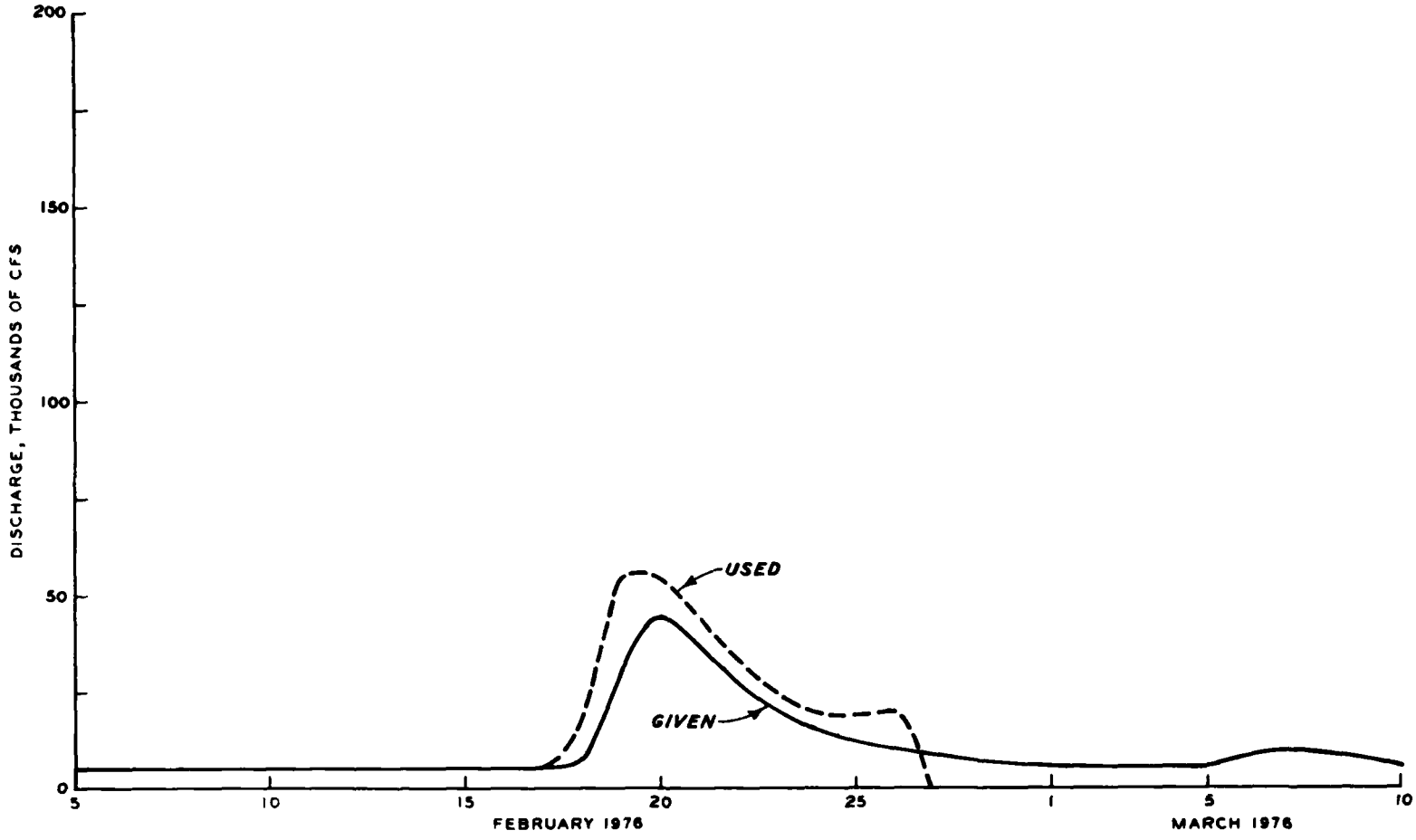

Figure 62. Ungaged lateral inflow in Evansville-Golconda reach

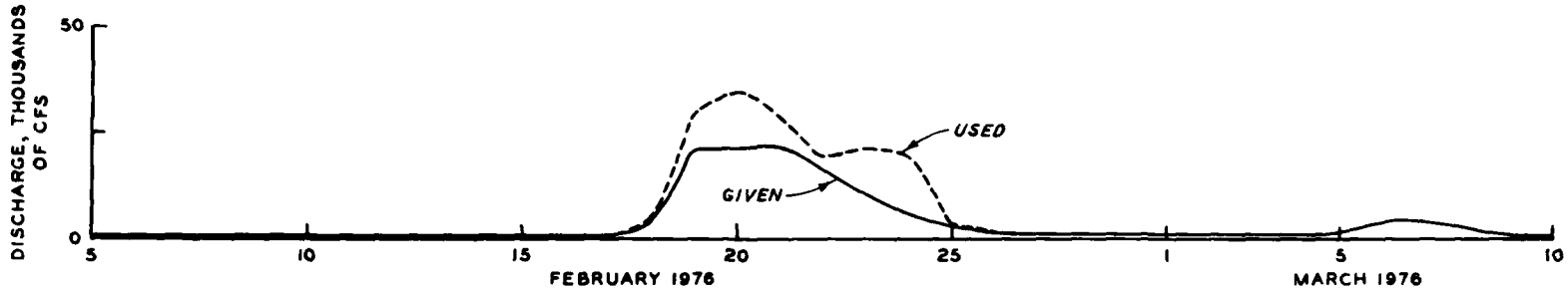

Figure 63. Ungaged lateral inflow in Golconda-Metropolis reach

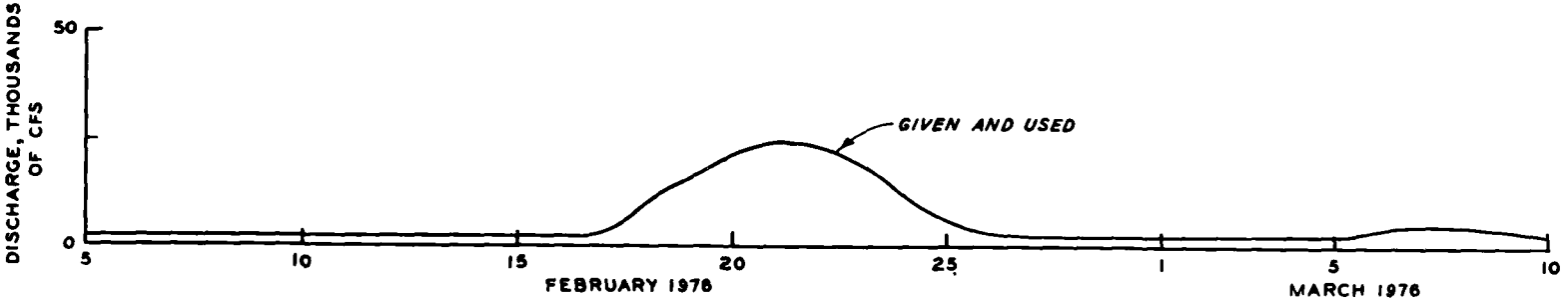

Figure 64. Ungaged lateral inflow in Metropolis-Cairo reach

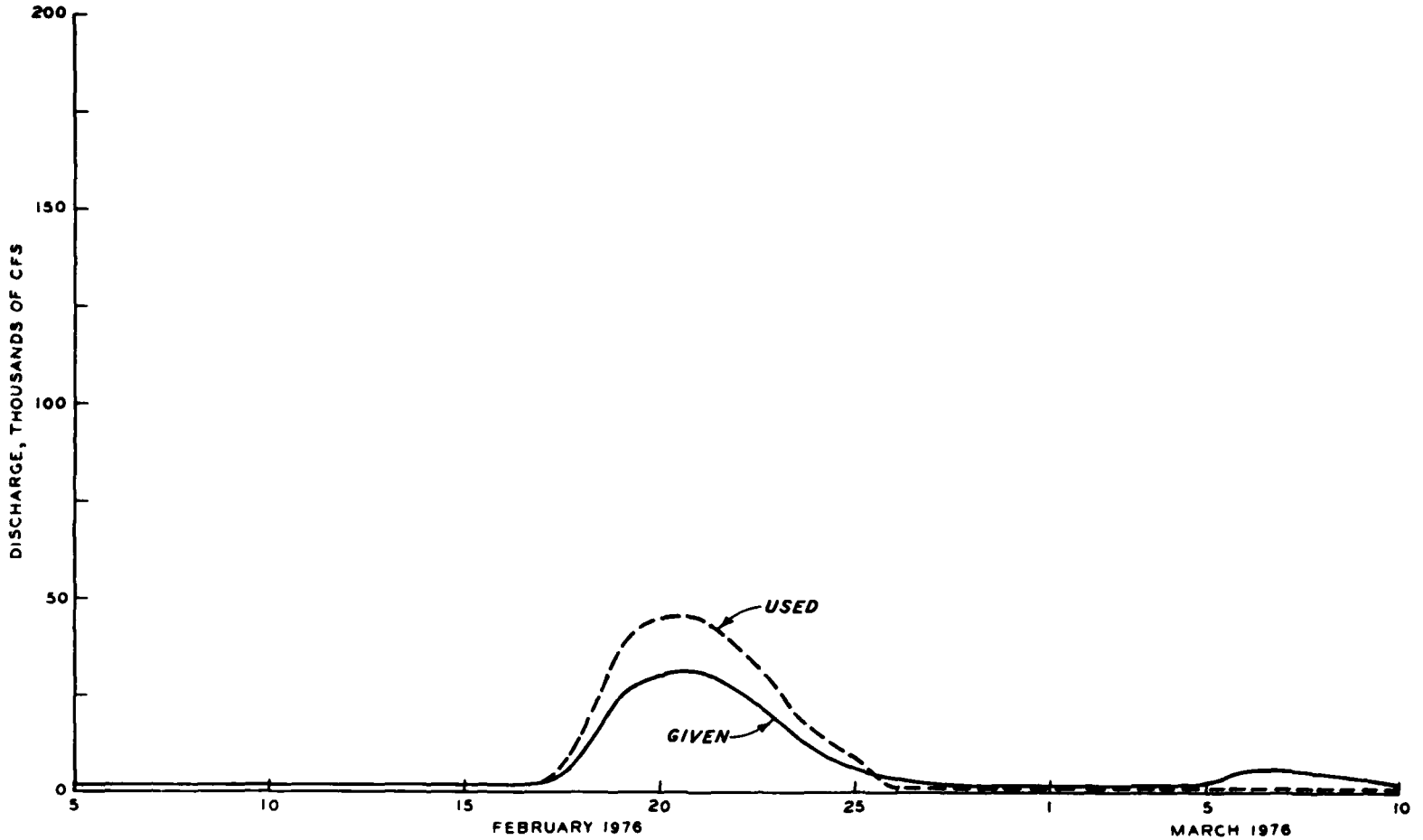

Figure 65. Ungaged lateral inflow in Thebes-Cairo reach

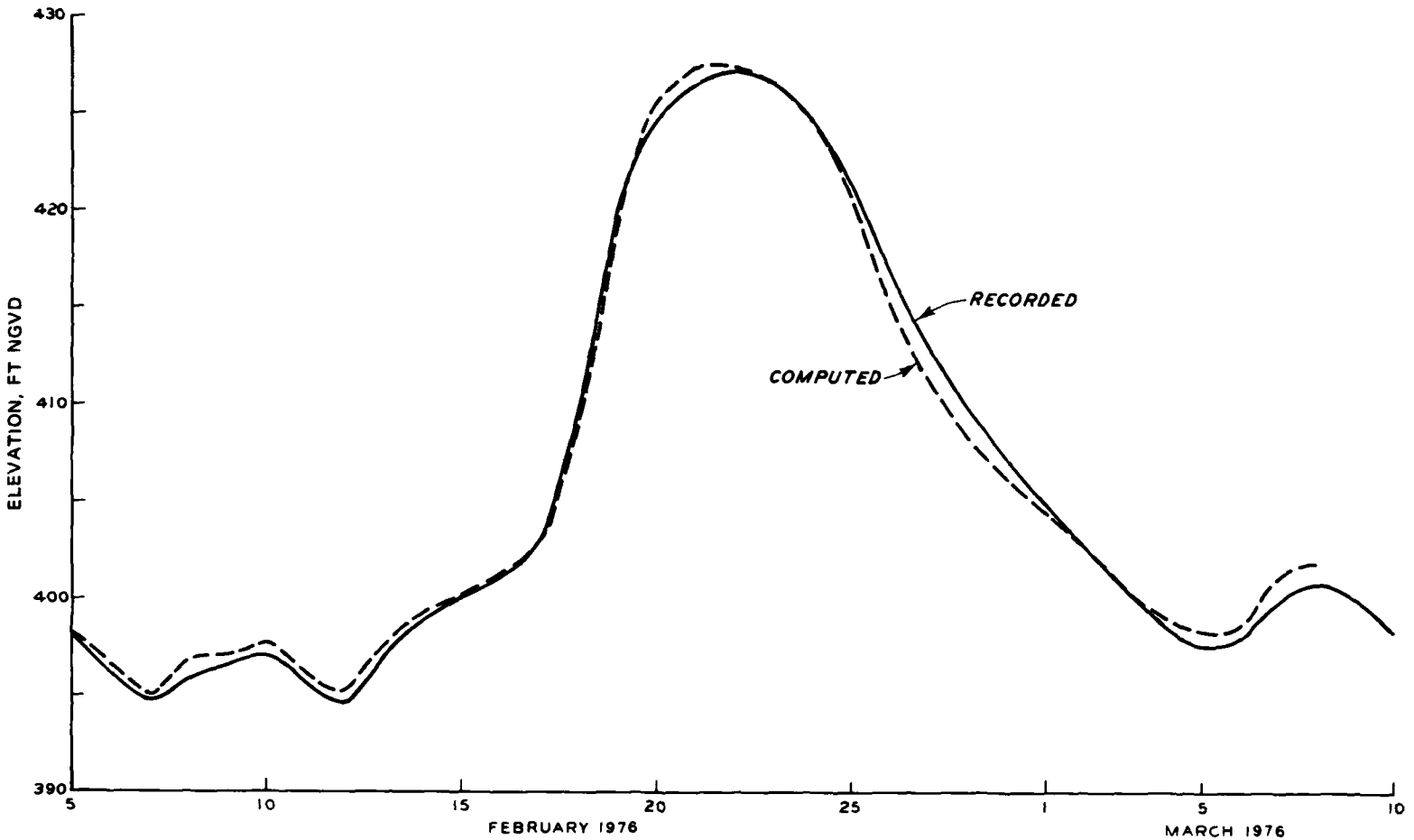

Figure 66. Recorded versus computed elevations at McAlpine L&D

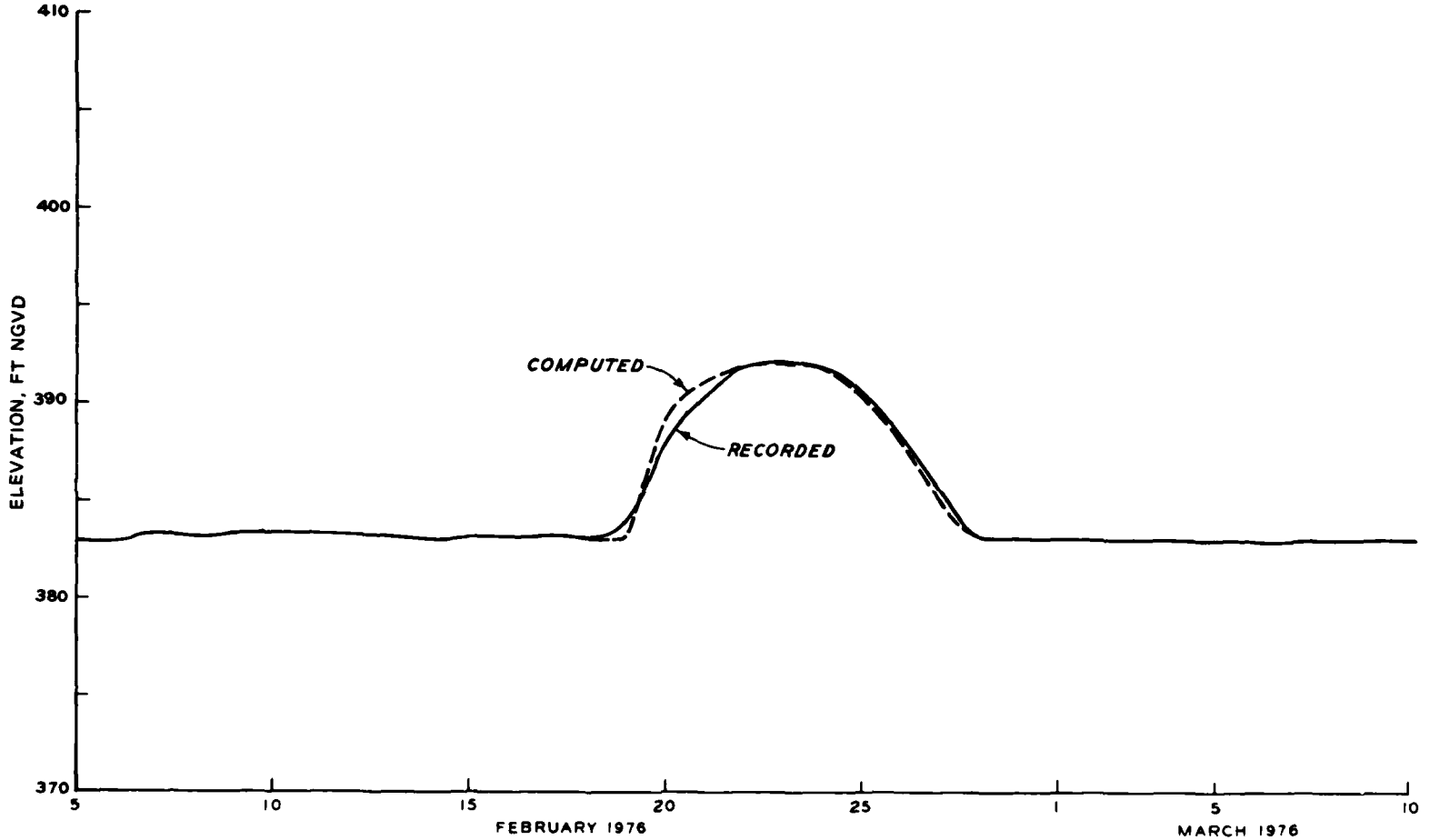

Figure 67. Recorded versus computed elevations at Cannelton L&D, upper gage

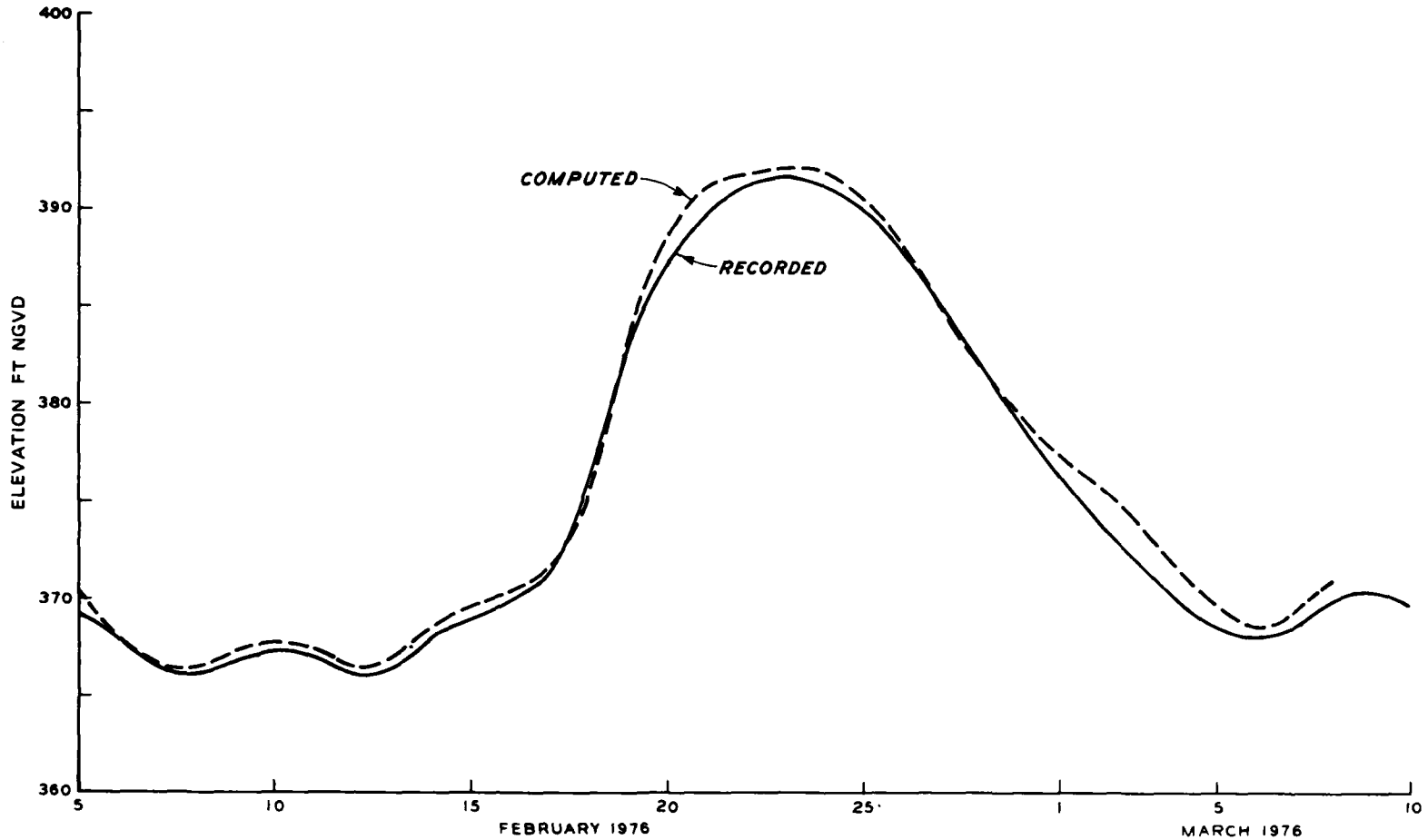

Figure 68. Recorded versus computed elevations at Cannelton L&D, lower gage

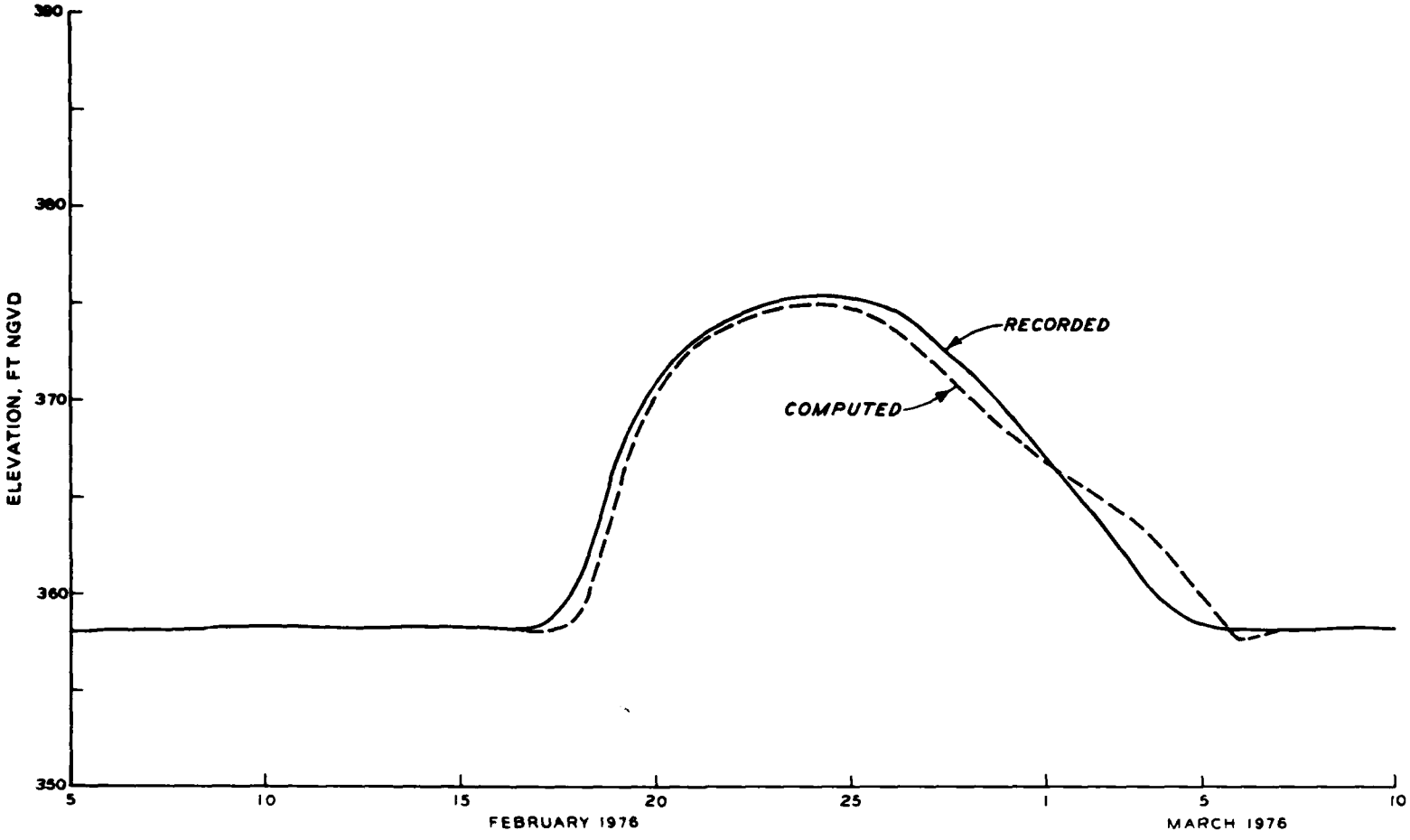

Figure 69. Recorded versus computed elevations at Newburgh L&D, upper gage

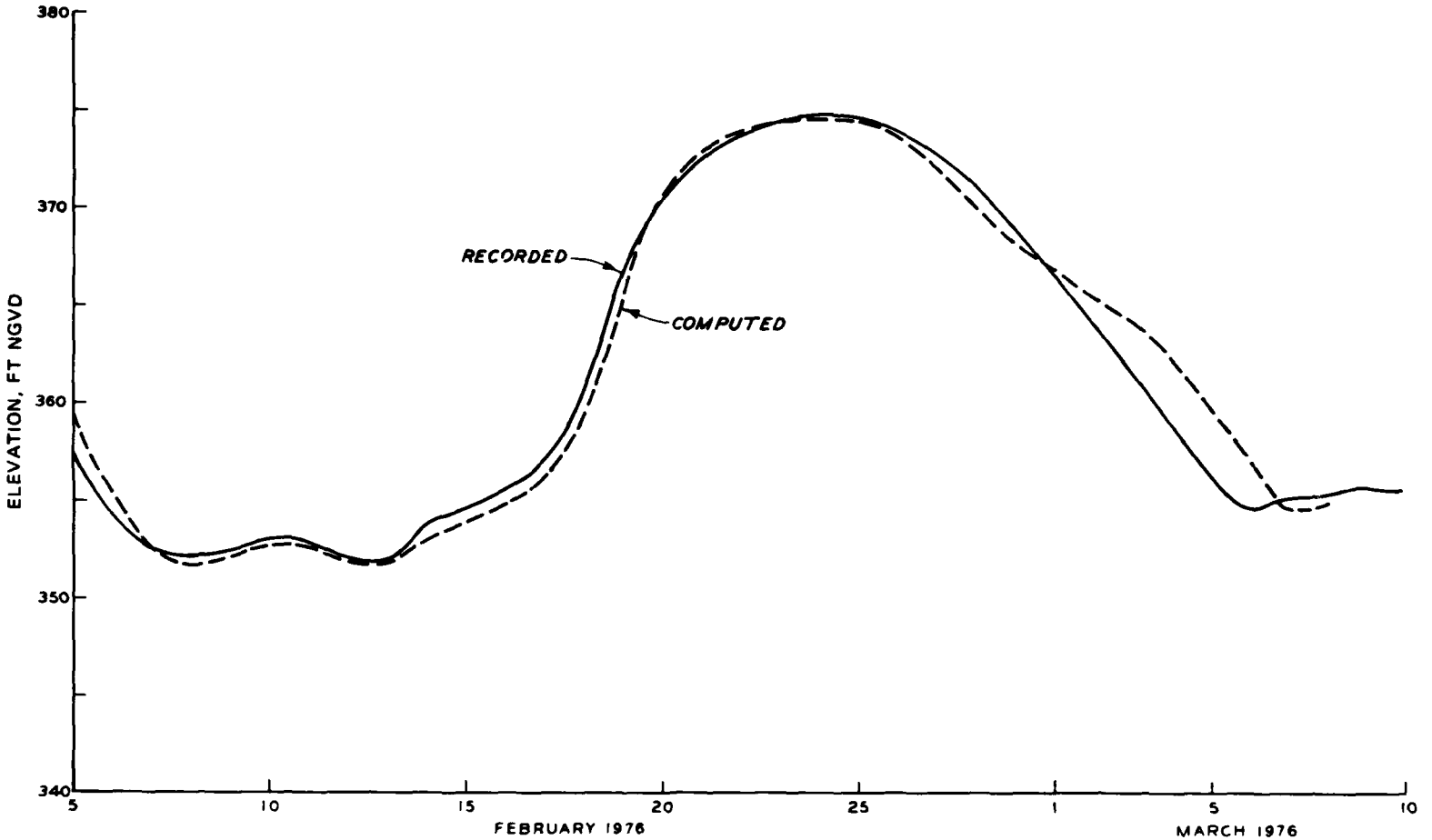

Figure 70. Recorded versus computed elevations at Newburgh L&D, lower gage

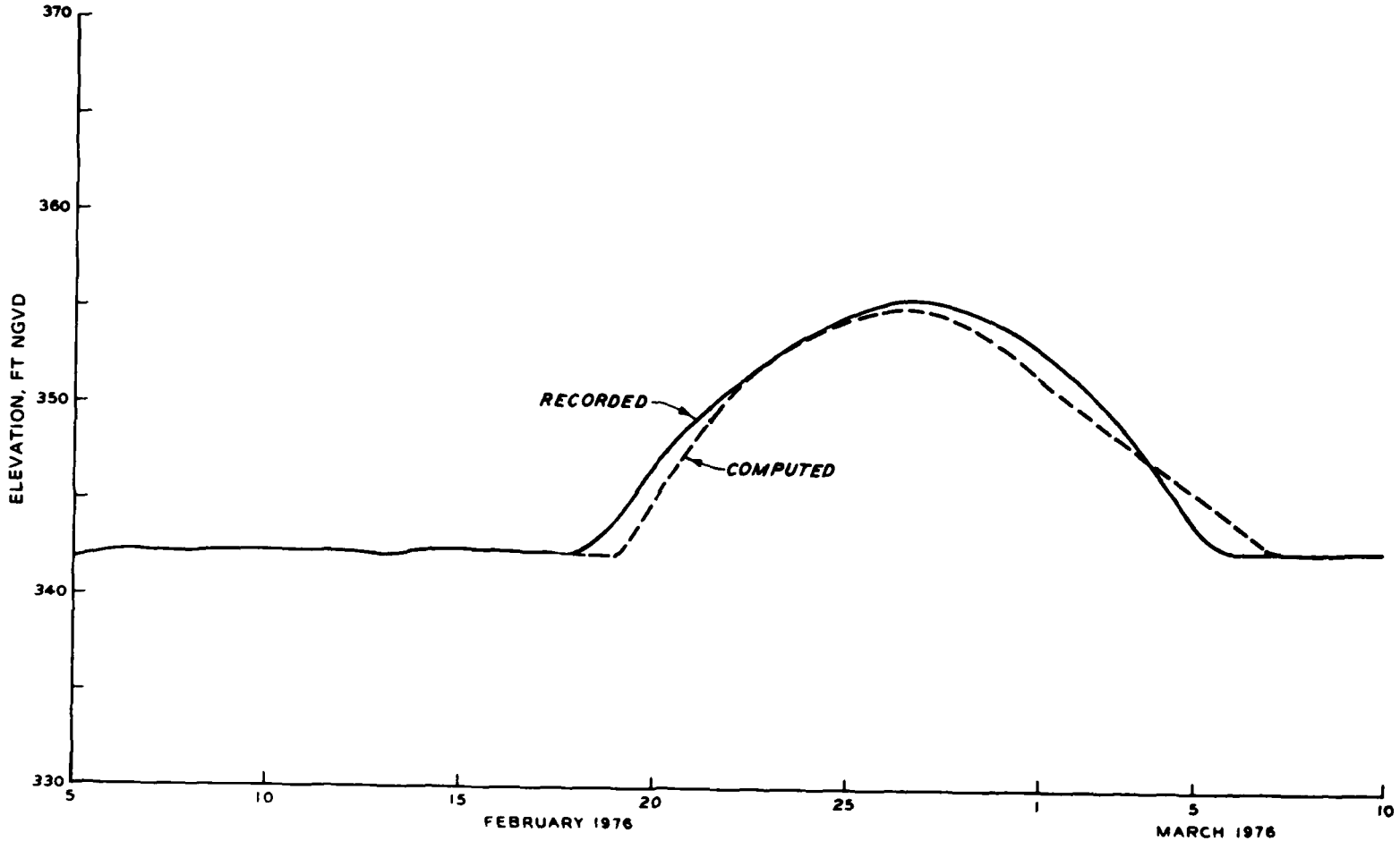

Figure 71. Recorded versus computed elevations at Uniontown L&D, upper gage

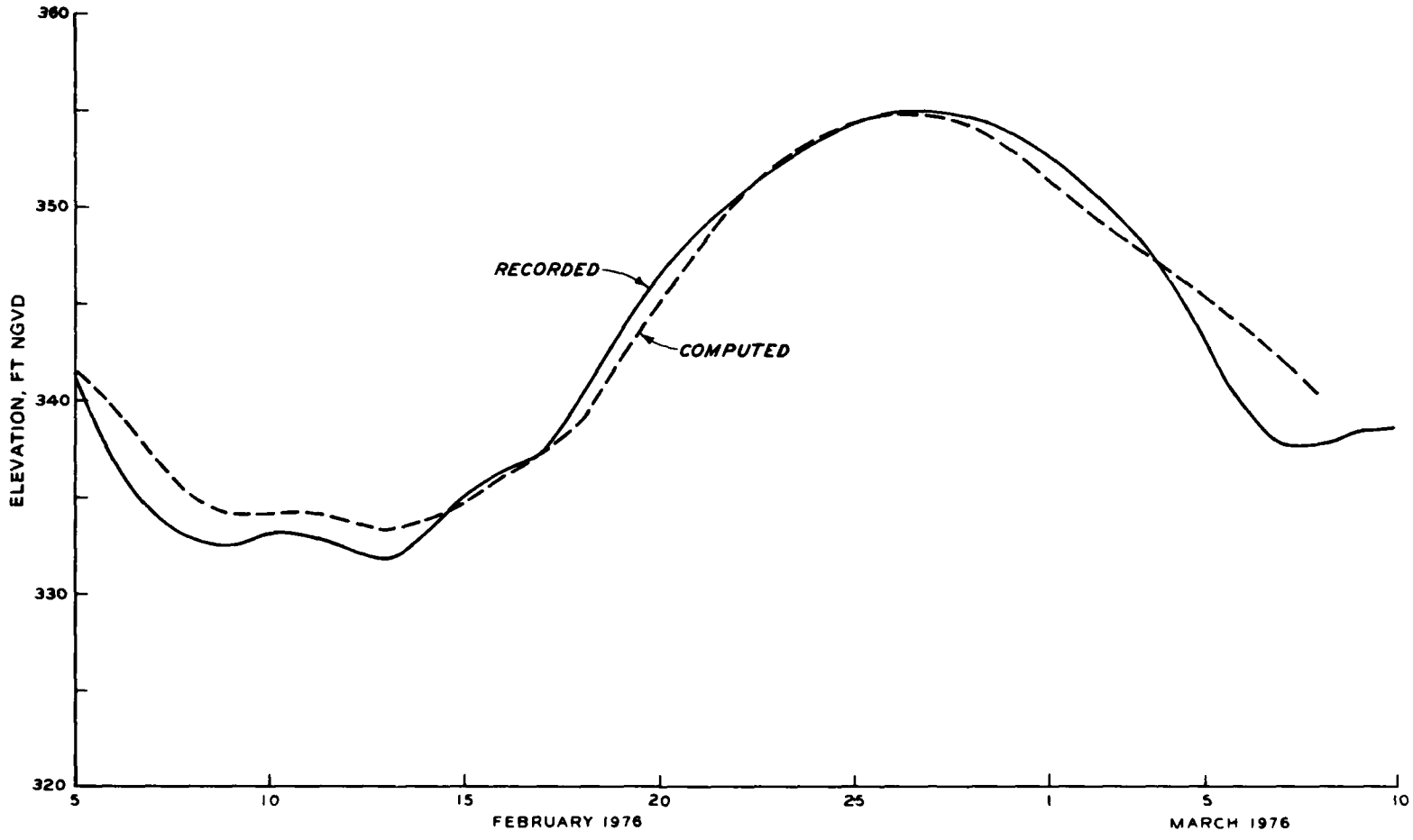

Figure 72. Recorded versus computed elevations at Uniontown L&D, lower gage

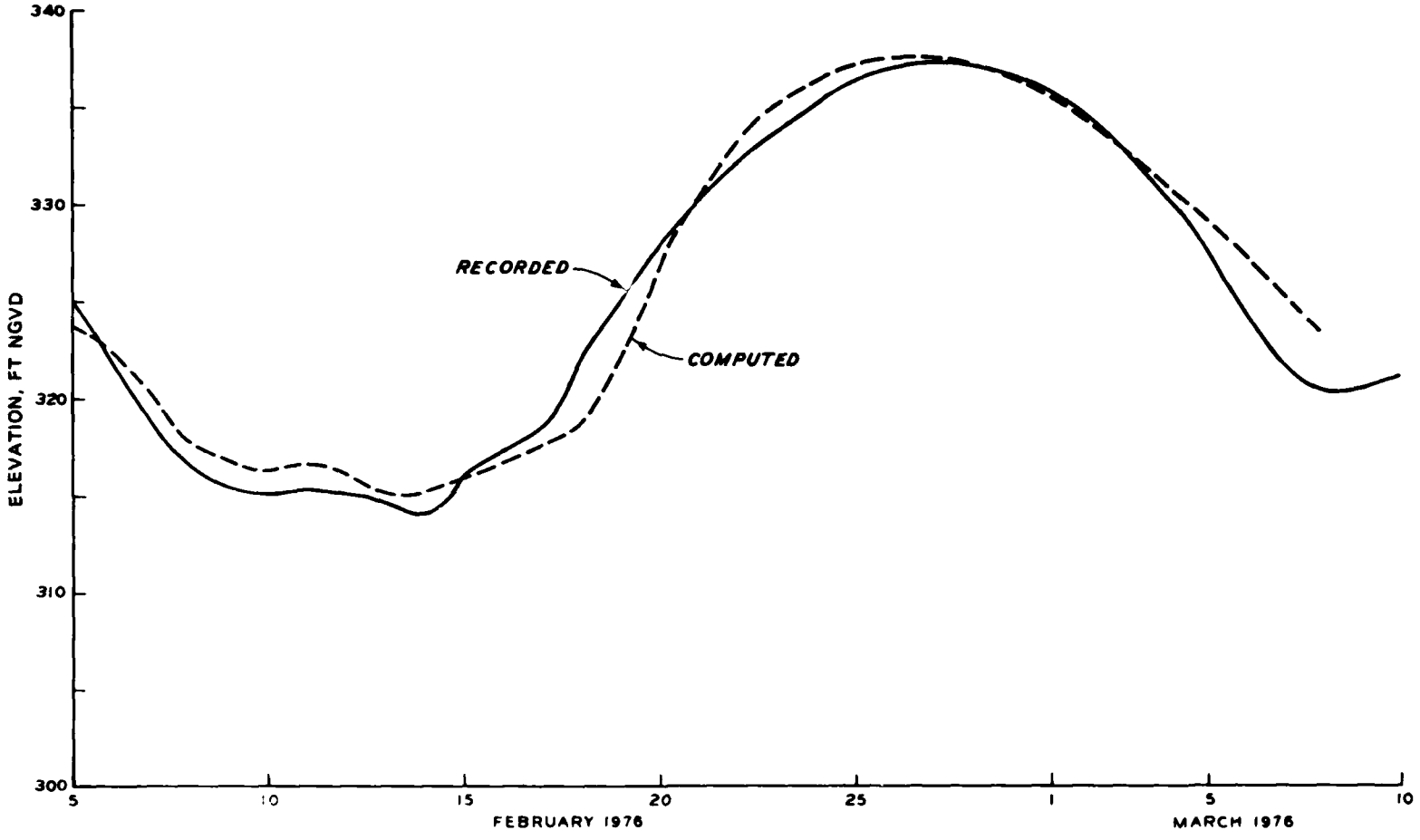

Figure 73. Recorded versus computed elevations at L&D 51

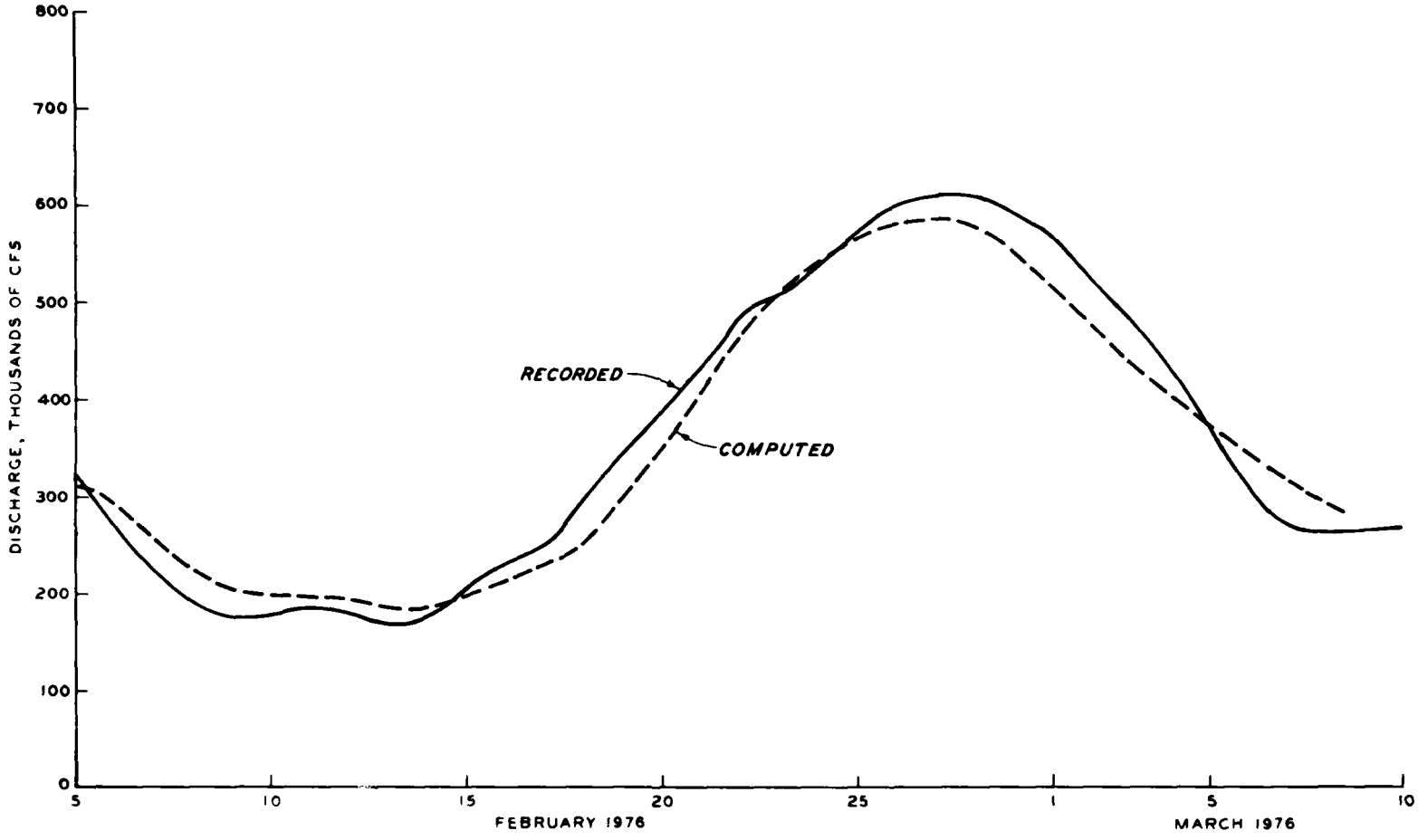

Figure 74. Recorded versus computed discharge L&D 51

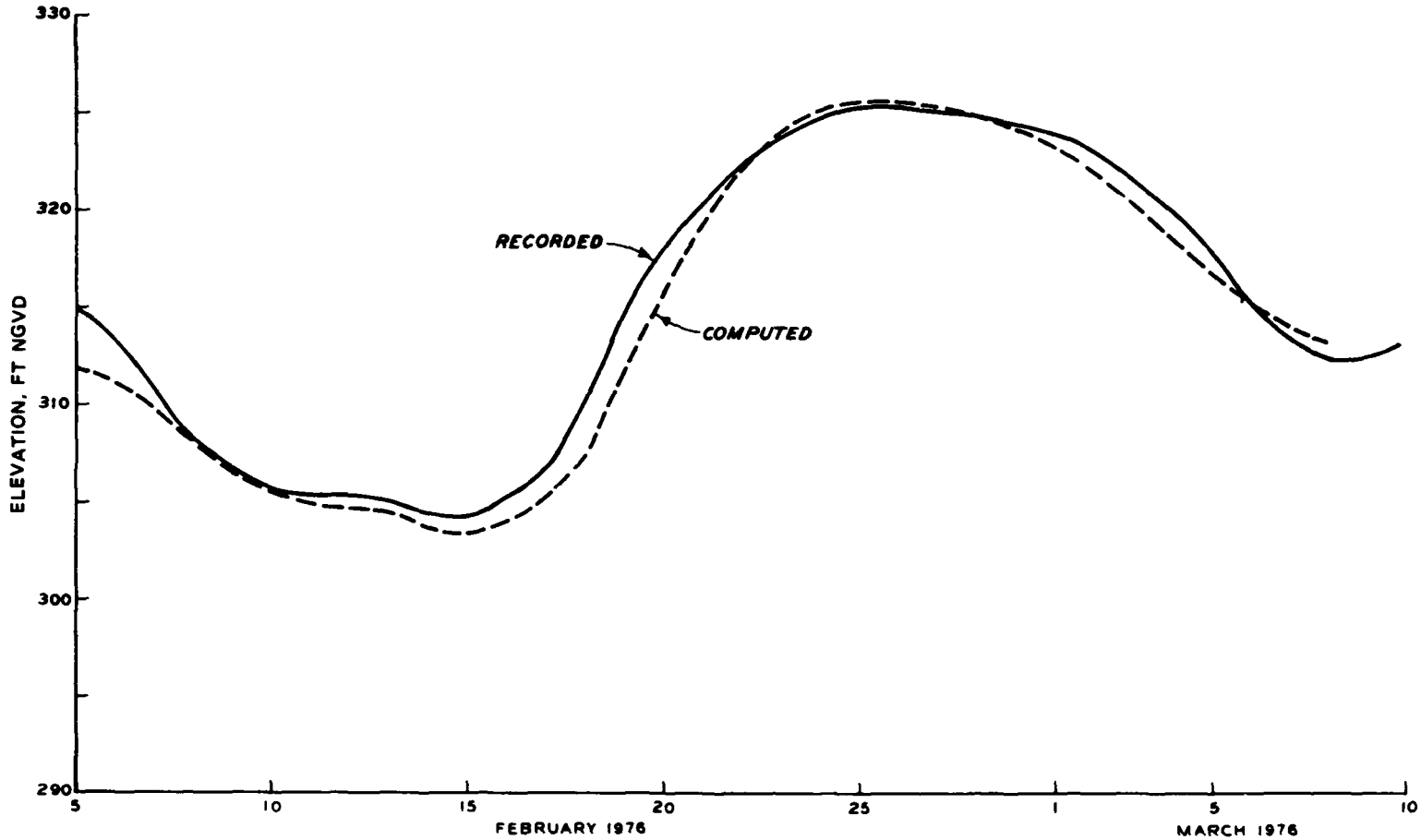

Figure 75. Recorded versus computed elevations at Paducah

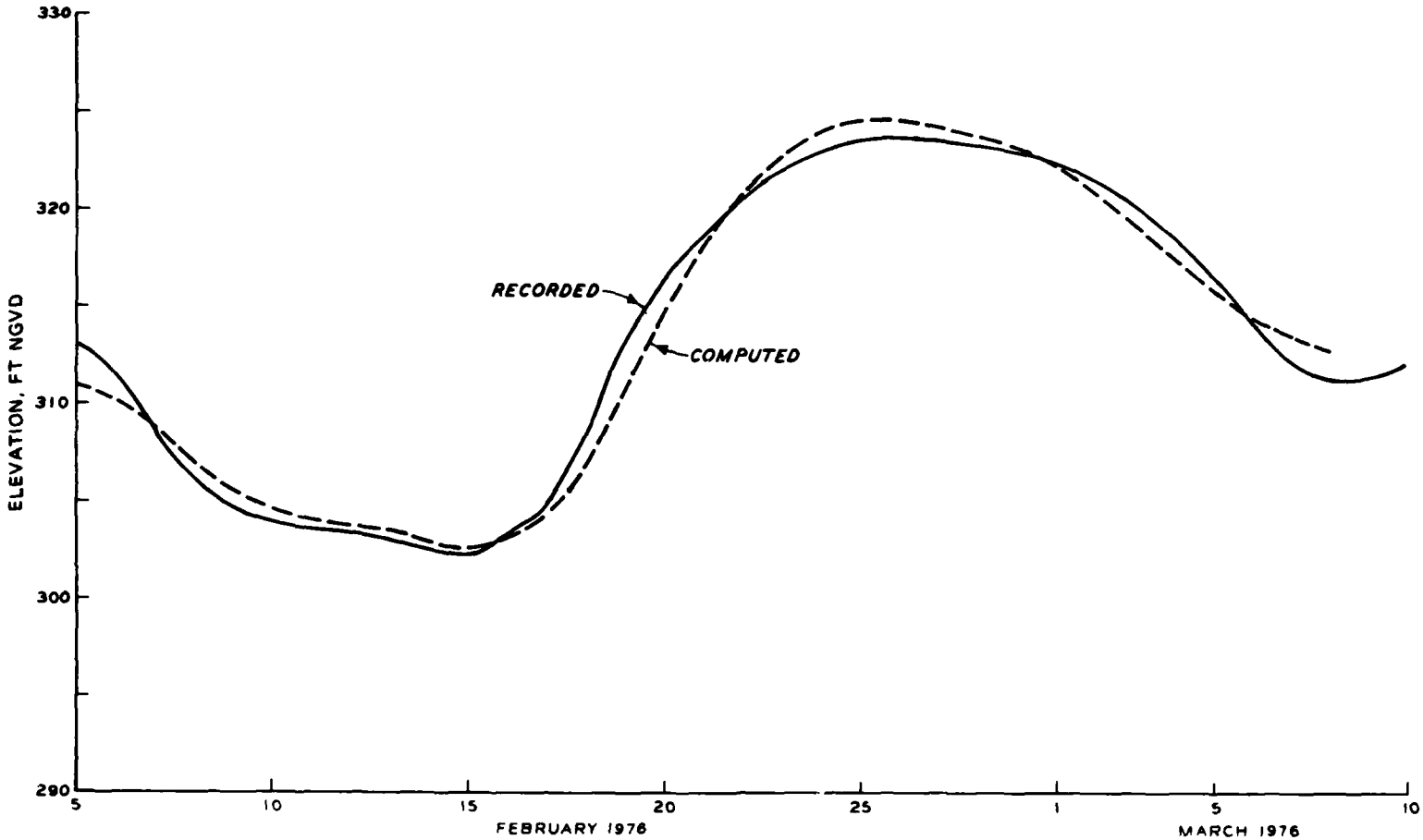

Figure 76. Recorded versus computed elevations at L&D 52

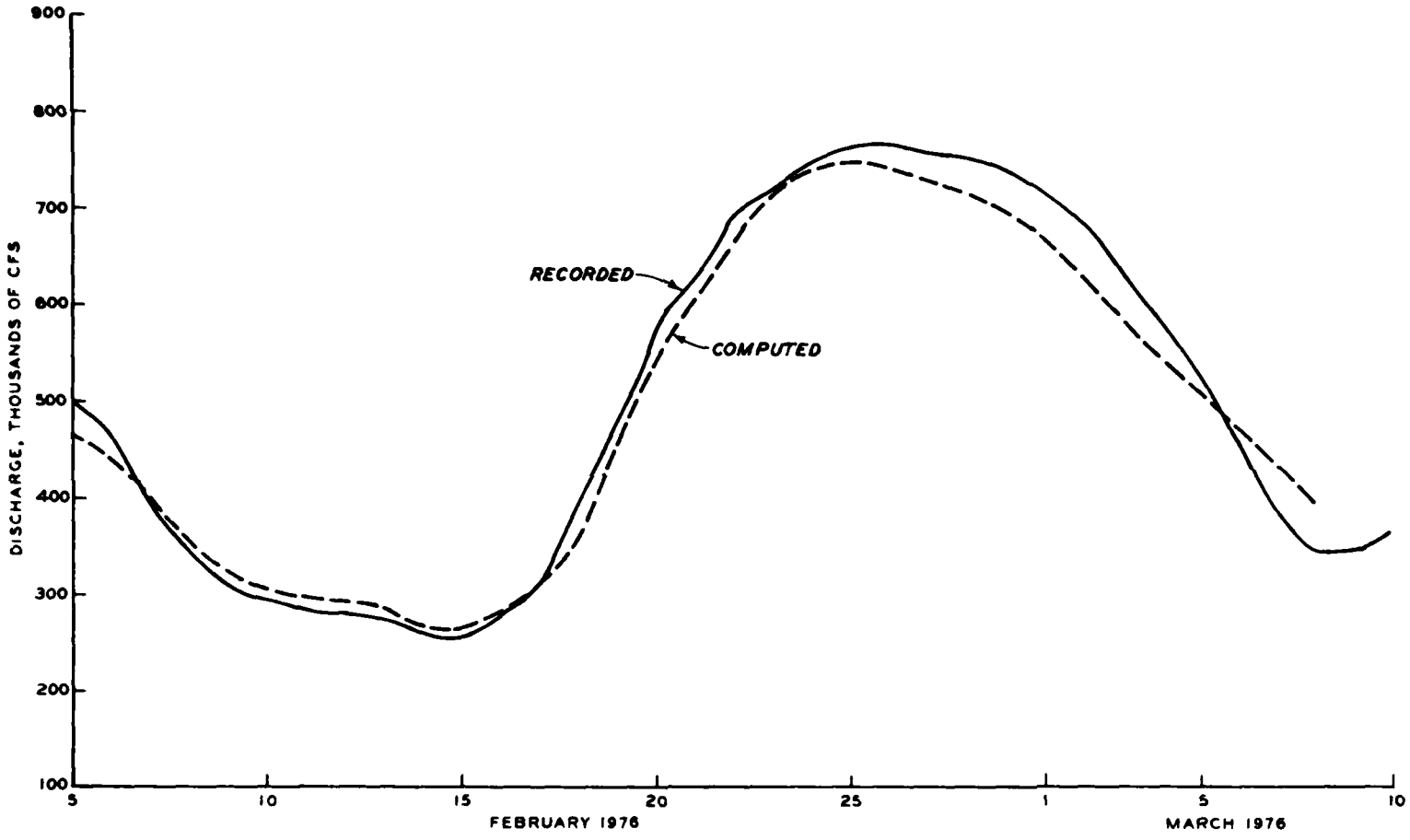

Figure 77. Recorded versus computed discharge at L&D 52

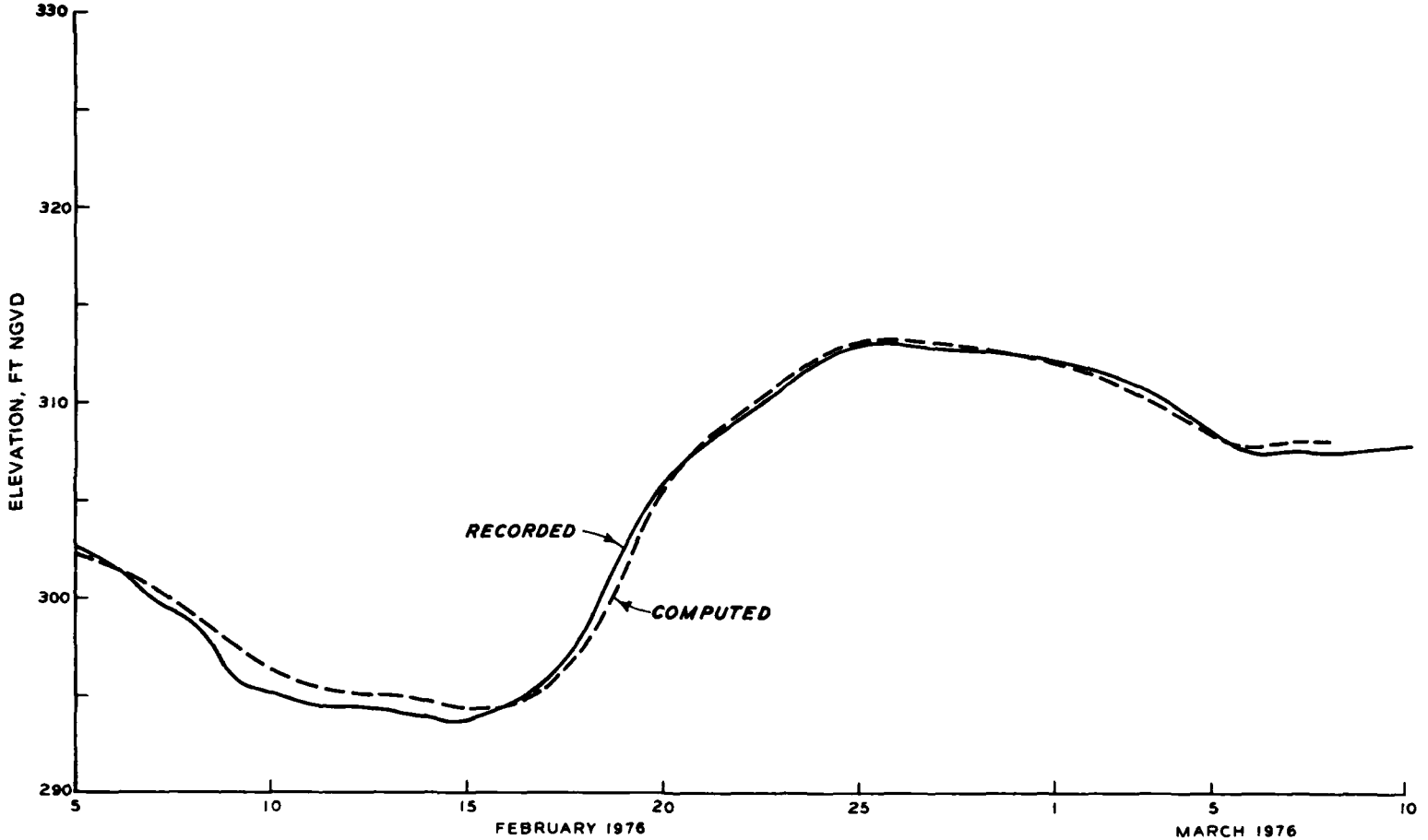

Figure 78. Recorded versus computed elevations at Cairo

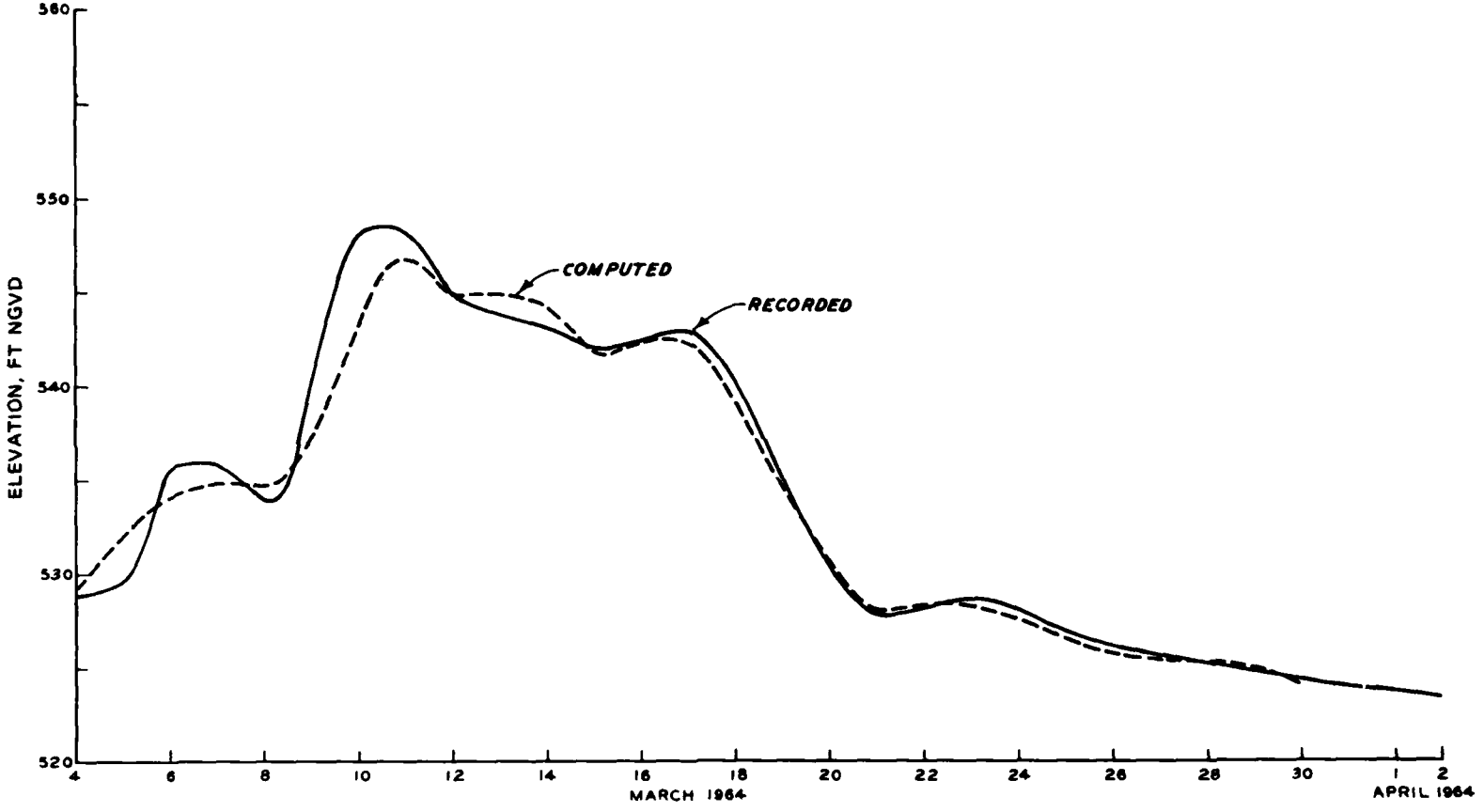

Figure 79. Recorded versus computed elevations at Louisa (Big Sandy River)

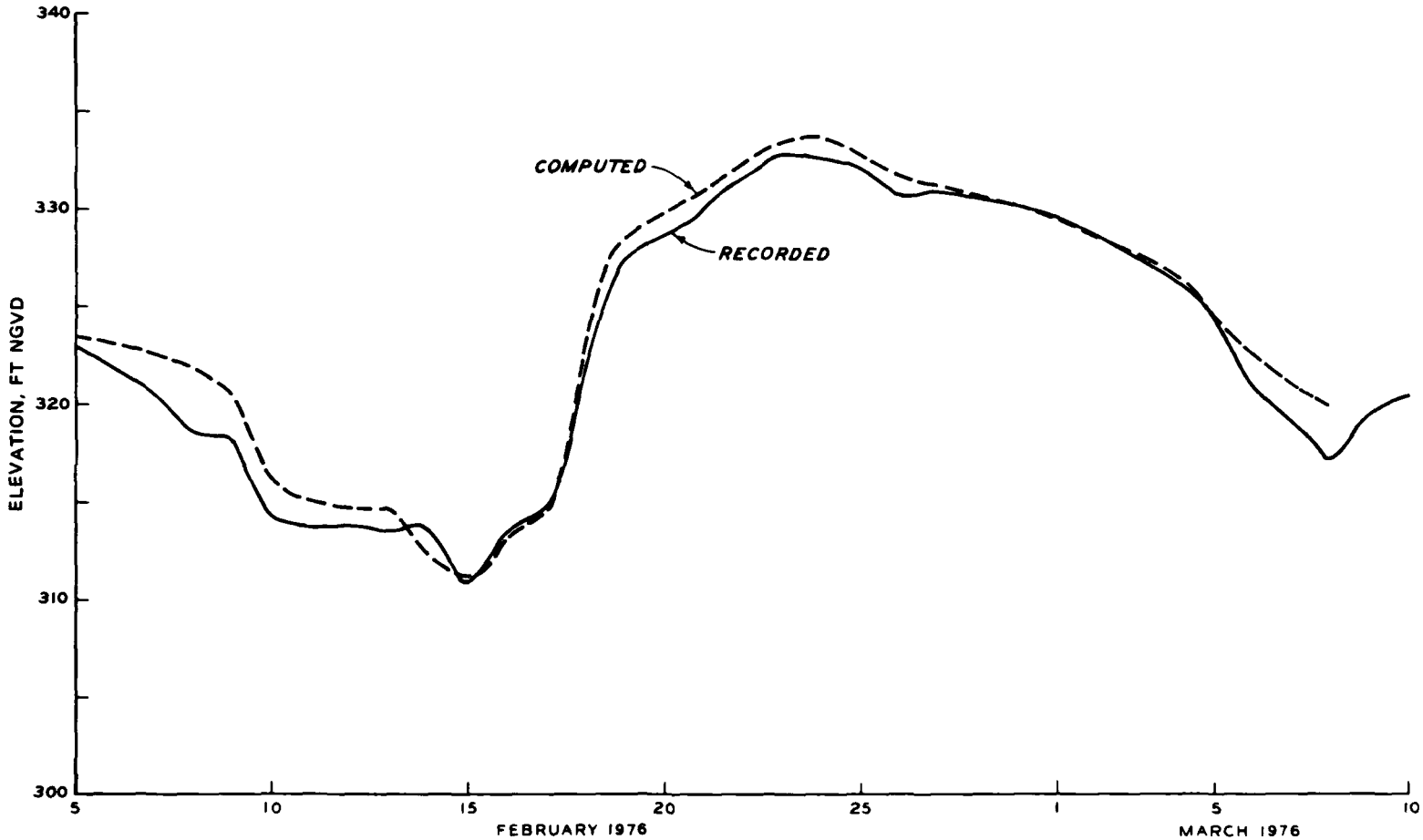

Figure 80. Recorded versus computed elevations at Barkley L&D (Cumberland River)

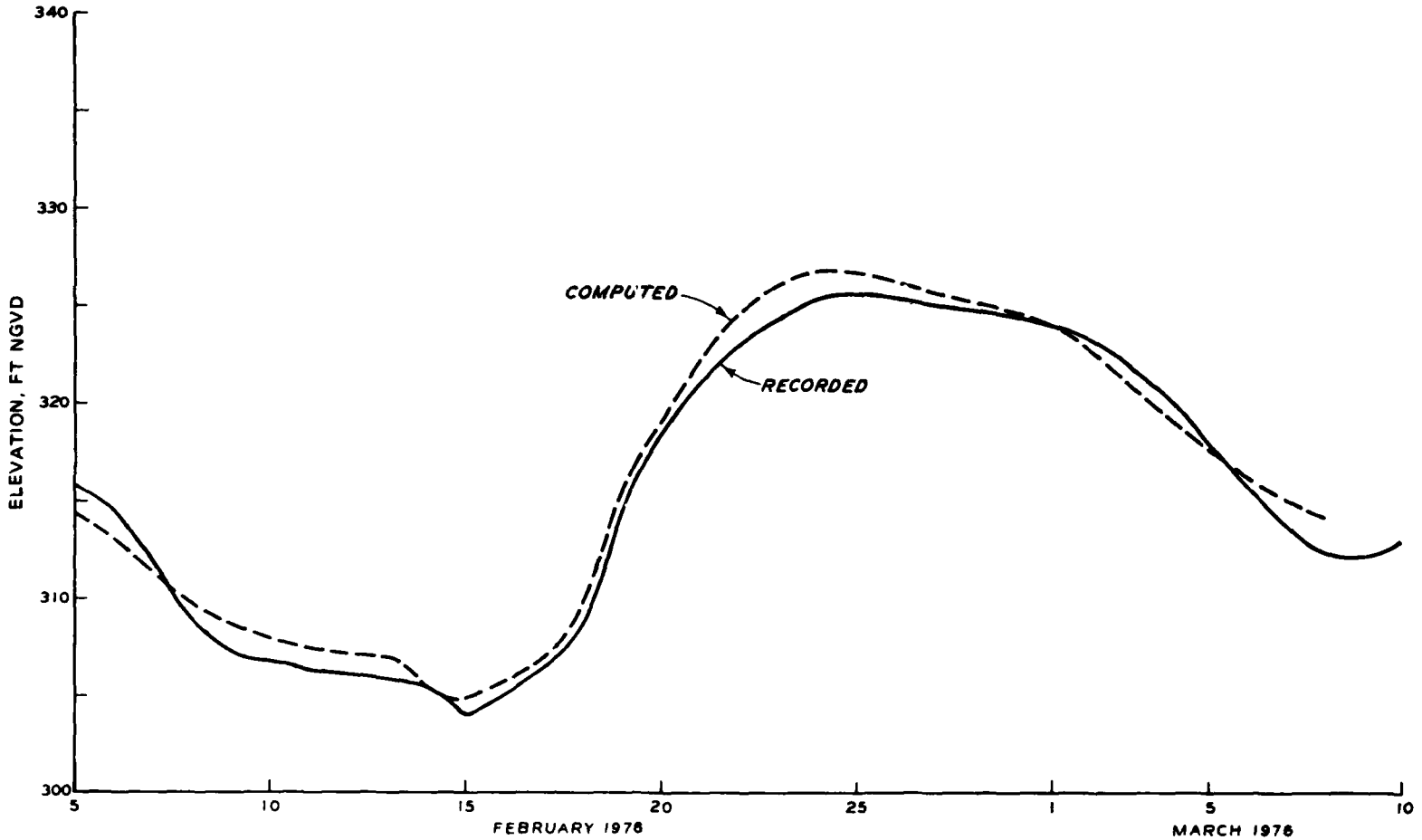

Figure 81. Recorded versus computed elevations at Kentucky L&D (Tennessee River)

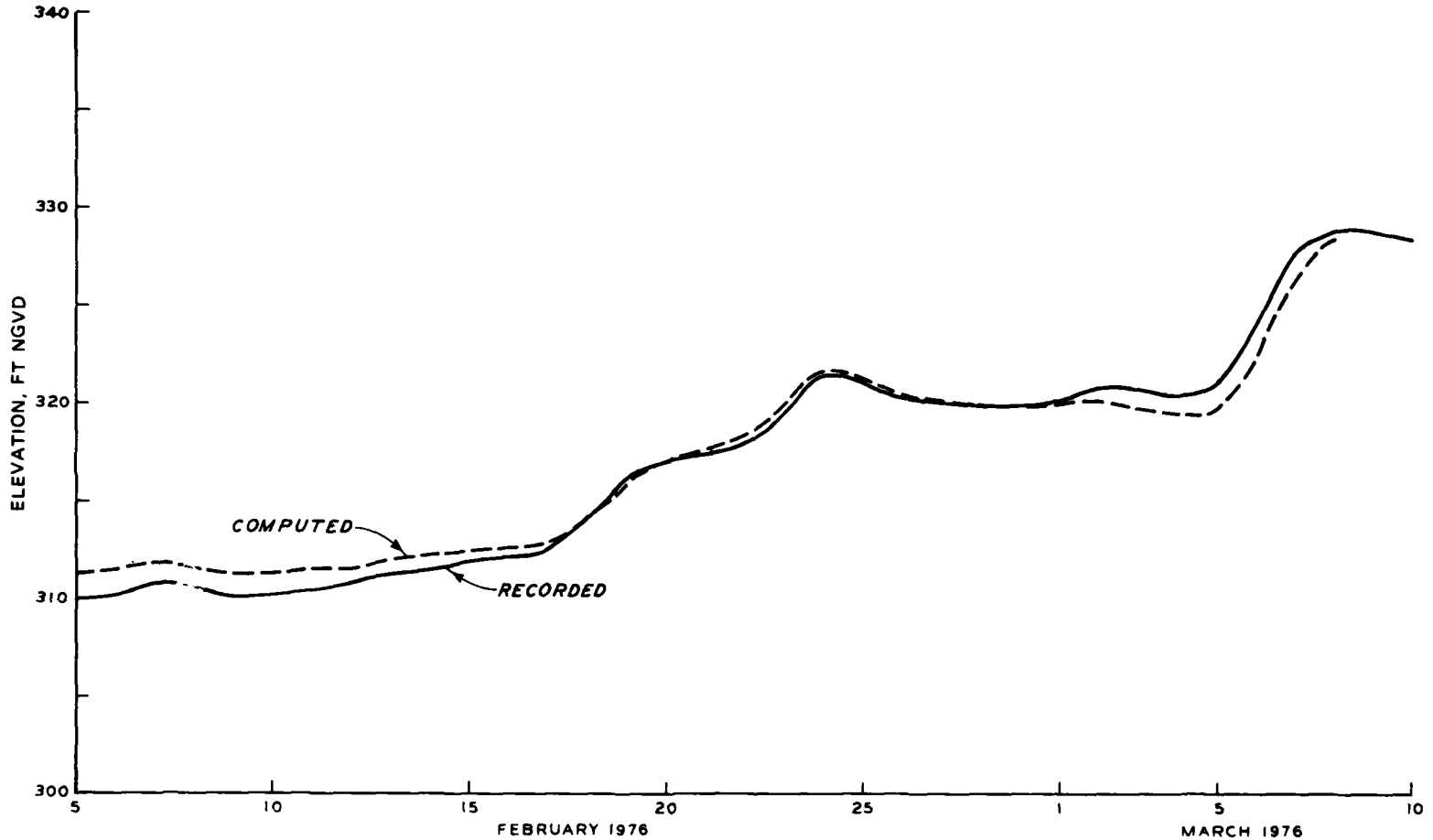

Figure 82. Recorded versus computed elevations at Thebes (upper Mississippi River)

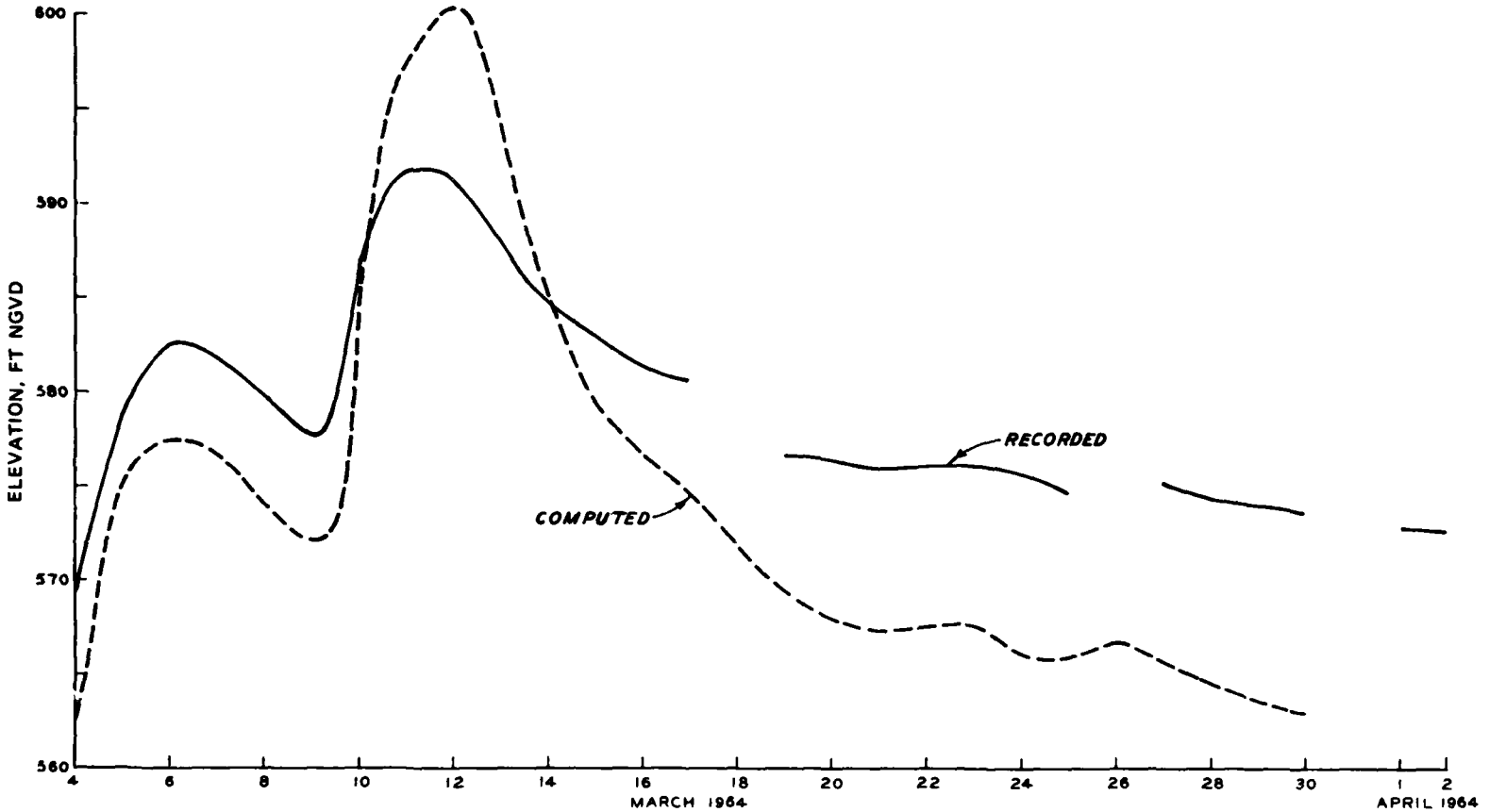

Figure 83. Recorded versus computed elevations at Higby (Scioto River)

APPENDIX A: LIST OF FLOWSED INPUT CARDS

1. TITLE(I) (10A8)

2. IGEOM, ILUG, IPUNCH, IBACK (4I5)

   IGEOM = 0 - Geometry tables printed
   IGEOM = 1 - Tables not printed
   ILUG = Unit from which geometry tables will be read
   IPUNCH = 1 - Restart cards will be punched
   IPUNCH = 0 - No restart cards
   IBACK = 0 - Less printed output

3. NC, NBRS, NJUNC, NDAMS, NXMAIN, ISTAGE, IFPLN, TOTALT, TSTEP (7I5, 10X, 2F10.0)

   NC = Total number of net points minus one
   NBRS = Total number of branches
   NJUNC = Total number of junctions (≥ 1)
   NDAMS = Total number of dams
   NXMAIN = Last net point on main river
   ISTAGE = Number of entries in channel geometry tables
   IFPLN = Number of entries in floodplain tables
   TOTALT = Number of days of computations
   TSTEP = Time-step in seconds

4. MNTH, KDAY, KYEAR, TIME, NOXS (3I5, 5X, F10.0, I5)

   MNTH = Starting month
   KDAY = Starting day
   KYEAR = Starting year
   TIME = Starting time on a 24-hr clock
   NOXS = Number of stations at which plots are desired

5. NSTAT, IPRINT, INTVG, INTVD, INTVP (5I5)

NSTAT = Number of net points at which output is desired
IPRINT = 0 - Limited output
IPRINT = 1 - Detailed output
INTVG = Major print interval
INTVD = Print interval for particular days (see next card)
INTVP = Interval for placing points in plot file
(If INTVD = INTVG, insert blank card for card 6)

6. STDP, ISDDP, ISMDP, ISYDP, ETDP, IEDDP, IEMDP, IEYDP (F10.0, 3I5, 5X, F10.0, 3I5)

STDP = Starting time on 24-hr clock for small print interval
ISDDP = Starting day for small print interval
ISMDP = Starting month for small print interval
ISYDP = Starting year for small print interval
ETDP = Ending time on 24-hr clock for small print interval
IEDDP = Ending day for small print interval
IEMDP = Ending month for small print interval
IEYDP = Ending year for small print interval

7. (NPRINT(I), I=1, NSTAT) (16I5)

NPRINT = Net point numbers at which output is requested

8. IPLT, ISCL, IYCN, IOP1 (4I5)

IPLT = 0 - No plots
IPLT = 1 - Elevation plots
IPLT = 2 - Discharge plots
IPLT = 3 - Elevation, discharge plots
IPLT = 4 - Velocity plots
IPLT = 5 - Elevation, velocity plots

IPLT = 6 - Discharge, velocity plots

IPLT = 7 - Elevation, discharge, velocity plots

ISCL = Number of minutes/inch on x-axis

IYLN = Length of y-axis in inches (0 defaults to 8 in.)

IOP1 = 0 - Different y-interval on each plot

IOP1 = 1 - Same y-interval on each plot

9. (STITLE(II,I), II=1, 4), NPLOT(I) (4A8, 3X, I5)

STITLE = Title of station

NPLOT = Net point number

(Repeat card 9 NOXS times)

10. ID, IBRNCH(I,1), IBRNCH(I,2), IBRS(I), ISED(I), IBC(I) (6I5)

ID = Branch number

IBRNCH(I,1) = First net point on branch

IBRNCH(I,2) = Last net point on branch

IBRS(I) = 1 - Branch has upstream outer boundary

IBRS(I) = 0 - Branch is an interior branch

IBRS(I) = -1 - Branch has downstream outer boundary

ISED(I) = 0 - Sediment at boundary computed internally

ISED(I) = 1 - Sediment at boundary input

IBC(I) = -1 - Rating curve will be used if this branch contains downstream outer boundary

IBC(I) = 0 - If this is an interior branch or discharge is input at its boundary

IBC(I) = 1 - Elevations will be input if this branch contains downstream outer boundary

(There will be one card 10 for each branch. All mainstem branches should be numbered before numbering tributaries.)

11. ID, (IJUN(I,K),K=1,3), AL(J), AL(J+1) (4I5, 10X, 2F10.0)

ID = Junction number

IJUN(I,1) = Number of upstream branch on main river

IJUN(I,2) = Number of tributary branch

IJUN(I,3) = Number of downstream branch on main river

AL(J) = Velocity head correction factor associated with junction of upstream main river and downstream main river

AL(J+1) = Velocity head correction factor associated with junction of tributary and downstream river

(There will be one card 11 for each junction.)

12. TDAM(I), HSET(I), NL(I), NVARY(I) (A8, 2X, F10.0, 2I5)

TDAM = Description of dam

HSET(I) = Elevation maintained by dam

NL(I) = Net point immediately upstream of dam

NVARY(I) = 0 - Normal dam

NVARY(I) = 1 - Time-varying elevations of pool will be input

NVARY(I) = 2 - Rating curve will be input for this dam

13. ISCON (I5)

ISCON = 0 - Sediment coefficients will be read in as constants

ISCON = 1 - Sediment coefficients will be spatially varying

(If ISCON = 1, skip card 14)

14. CKT, CMS, CNS (3F10.0)

See definitions below.

(If ISCON = 0, go to card 18)

15. (CKT(I),I=1,NX) (8F10.0)

(NX = Total number of net points)

CKT(I) = Sediment transport coefficient in $C_s = KV^{CM}D^{CN}$ where CKT = K . A value between 0.000005 and 0.000015 is appropriate in upper Mississippi River.

16. (CMS(I),I=1,NX) (8F10.0)

CMS(I) = CM in the equation above. Value of 3.4 is appropriate in upper Mississippi River.

17. (CNS(I), I=1, NX) (8F10.0)

CNS(I) = CN in the equation above. Value of -1.0 is appropriate in upper Mississippi River.

18. CP (F10.0)

CP = Initial volume of sediment per unit volume of bed material

19. IEDYHD (I5)

IEDYHD = 0 - Eddy head loss coefficients set to 0

IEDYHD = 1 - Eddy head loss coefficients read in

(If IEDYHD = 0, Skip card 20)

20. (CKE(I), I=1,NX) (8F10.0)

(NX = Total number of net points)

CKE(I) = Coefficient in eddy loss term

21. (HO(I),I=1,NX) (8F10.0)

HO(I) = Initial water-surface elevation in ft at each net point

22. (Q(I),1),I=1,NX) (8F10.0)

Q(I,1) = Initial discharge in cfs at each net point

23. NRCH,(IRCH(I),I=1,NRCH) (16I5)

NRCH = Total number of reaches containing lateral inflows

IRCH(I) = Numbers of the reaches containing lateral inflow

(If NRCH = 0, Skip the next card)

24. CONCL,(QL2P(K),K=1, NRCH) (8F10.0)

CONCL = Concentration of sediment in ft^3/ft^3 contained in the lateral inflow

QL2P(K) = Lateral inflow at the initial time line in cfs

25. NLEVEE, (ILEVEE(I),I=1,NLEVEE) (16I5)

NLEVEE = Number of reaches with levees

ILEVEE(I) = Upstream net points of reaches with levees

(If NLEVEE = 0, Skip next card)

26. (ELEVEE(K), K=1,NLEVEE) (8F10.0)

ELEVEE(K) = Average elevation of the top of the levee along this reach in feet

27. RANGE(I), XL(I), DUM, ZF(I), ZO(I), BETA(I) (A8,2X,5F10.0)

RANGE(I) = Description of I'th net point

XL(I) = River mileage of I'th net point. Tributary mileage is zero at the junction

DUM = Space for top width. Can leave blank

ZF(I) = Top bank elevation for I'th net point

ZO(I) = Bed elevation of I'th net point

BETA(I) = Momentum correction factor

28. HI(I,J), AI(I,J), TI(I,J), RNI(I,J) (4F10.0)

HI = Elevation of channel geometry

AI = Flow area

TI = Top width

RNI = Manning's n

(Card 28 is repeated ISTAGE times)

29. HF(I,J), AFI(I,J), RNIFP(I,J) (3F10.0)

HF = Elevation of floodplain geometry

AFI = Cross-sectional area of the floodplain at elevation HF(I,J)

RNIFP = Manning's n

(Card 29 is repeated IFPLN times)

(Cards 27, 28, and 29 are repeated in sequence for each net point. They are read from unit ILUG)

(If IBC(I) = 1, Cards 30 and 31 are omitted)

30. NSEG (I5)

NSEG = Number of linear segments approximating the rating curve

31. QRC(I), HRC(I), SEE(I) (3F10.0)

QRC = Discharge at the end of the I'th linear segment

HRC = Elevation of water surface corresponding to the end of the I'th linear segment

SEE = Elevation of channel bottom - intercept of this segment on the elevation axis.

(Card 31 is repeated for each linear segment)

(If NVARY(I) $\neq$ 2, Omit card 32)

32. KRC(I), QLIMIT(I), QCHECKO(I), ODRCF(I),
(QDRC(K,I),HDRC(K,I),K=1,KRC(I)) (I5,7F10.0/8F10.0)

KRC = Number of entries in rating curve table at the I'th dam

QLIMIT = Discharge below which a fixed water-surface elevation is prescribed

QCHECKO = Initial discharge of I'th dam

QDRCF = Discharge above which the falling portion of the rating curve will be used if the discharge is decreasing

QDRC = Discharge in rating curve table

HDRC = Water-surface elevation corresponding to QDRC

(Card 32 is repeated for each dam with NVARY = 2)

(Card 33 is omitted if NRCH = 0)

33. J, (QL2(K),K=1,NRCH) (I5,5X,7F10.0/8F10.0)

J = Number of time-steps before new lateral inflows will be input

QL2 = Lateral inflow in cfs

34. Q(I,2), IQCK(I) (F10.0,I5)

Q = New boundary discharge in cfs

IQCK = Number of time-steps before a new discharge will be input

35. QS(I,2), IQSCK(I) (F10.0,I5)

QS = New sediment discharge at boundary in cfs

IQSCK = Number of time-steps before a new sediment discharge will be input

(Cards 34 and 35 are repeated for each upstream boundary)

(If IBC(I) $\neq$ 1, Omit card 36)

36. H(I,2), IHCK(I) (F10.0,I5)

H = New downstream boundary water surface elevation

IHCK = Number of time-steps before a new elevation will be input

(If NVARY(K) = 1 for K = 1, NDAMS omit card 37)

37. HSET(K), IHSET(K) (F10.0,I5)

HSET = New water-surface elevation to be set upstream of the K'th dam

IHSET = Number of time-steps before a new HSET is read

(Repeat card 37 for each dam with NVARY = 1)

Remember, at each time-step the check is on lateral inflows first, then on boundary conditions, and finally on time-varying pools.

APPENDIX B: EXAMPLE OUTPUT FROM FLOWSED

COMPLETE OHIO RIVER BASIN MODEL

NUMBER OF REACHES = 951
NUMBER OF BRANCHES = 25
NUMBER OF JUNCTIONS = 12
NUMBER OF DAMS = 27

NUMBER OF DAYS OF COMPUTATIONS = 100.0
TIME STEP = 3600.0 SEC

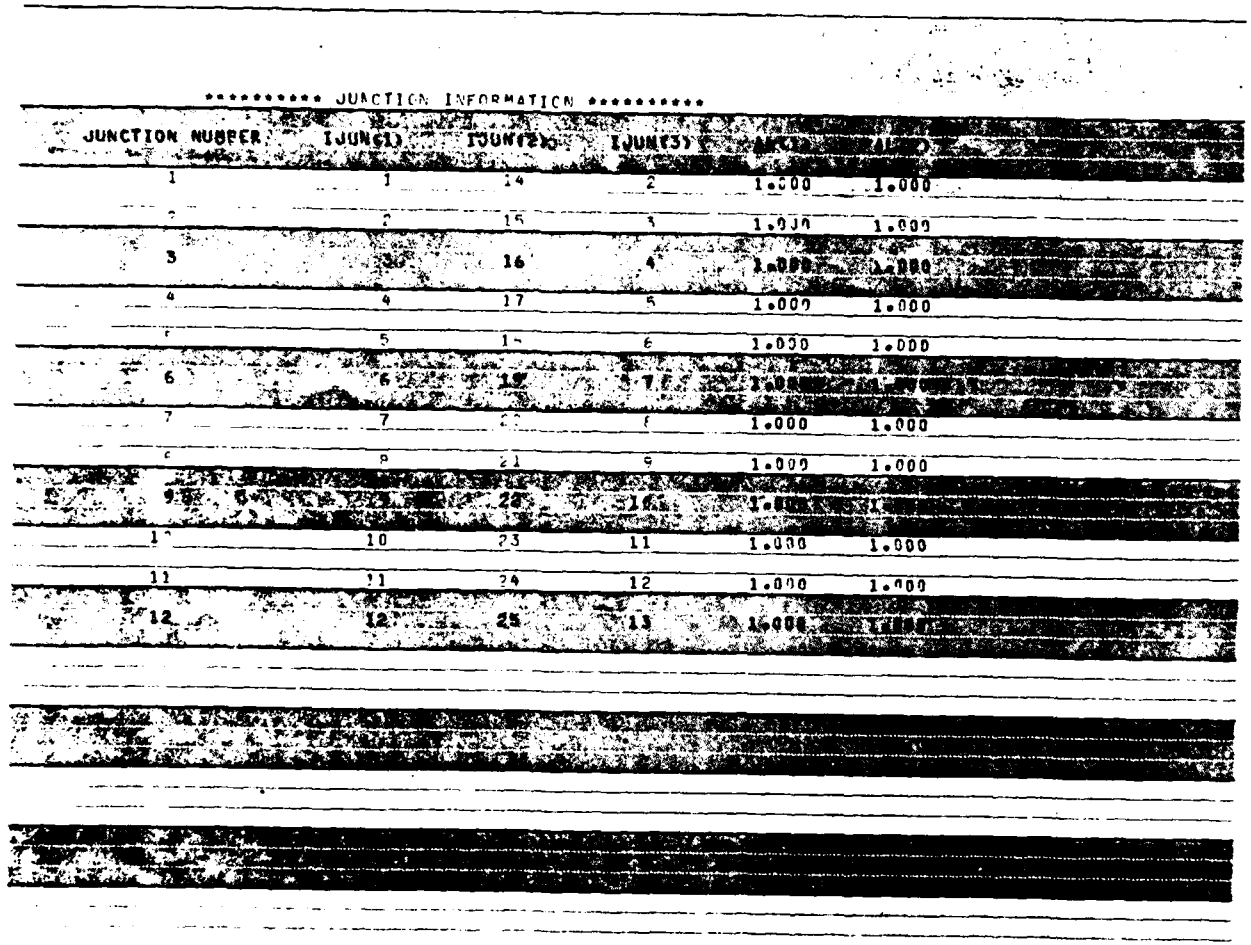

********** JUNCTION INFORMATION **********

JUNCTION NUMBER	IJUN(1)	IJUN(2)	IJUN(3)		
1	1	14	2	1.000	1.000
2	2	15	3	1.000	1.000
3	3	16	4	1.000	1.000
4	4	17	5	1.000	1.000
5	5	18	6	1.000	1.000
6	6	19	7	1.000	1.000
7	7	20	8	1.000	1.000
8	8	21	9	1.000	1.000
9	9	22	10	1.000	1.000
10	10	23	11	1.000	1.000
11	11	24	12	1.000	1.000
12	12	25	13	1.000	1.000

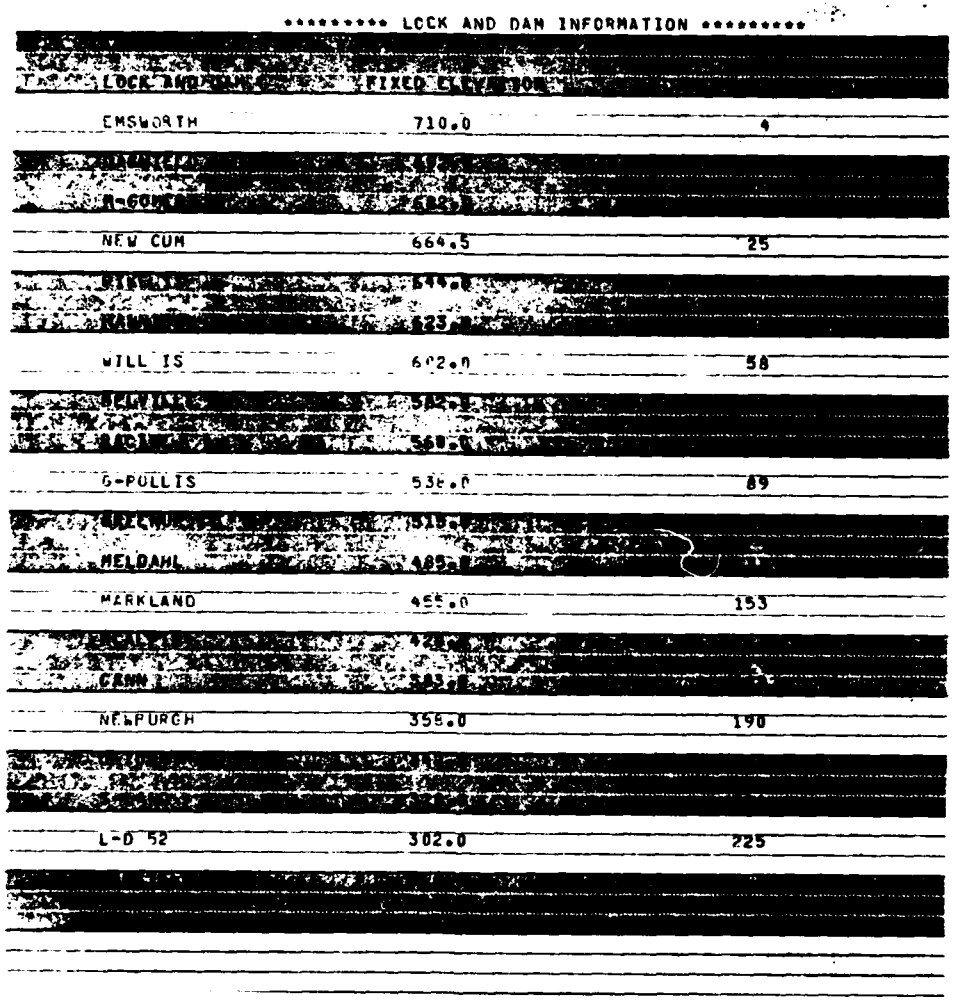

********** LOCK AND DAM INFORMATION **********

LOCK AND DAM	FIXED CREST ELEVATION	
EMSWORTH	710.0	4
[illegible]	[illegible]	
NEW CUM	664.5	25
[illegible]	[illegible]	
WILLIS	602.0	58
[illegible]	[illegible]	
G-PULLIS	538.0	89
[illegible]	[illegible]	
MARKLAND	455.0	153
[illegible]	[illegible]	
NEWBURGH	356.0	190
[illegible]	[illegible]	
L-D 52	302.0	225
[illegible]	[illegible]	

********** INITIAL CONDITIONS **********

NET POINT	ELEVATION	DISCHARGE	LATERAL FLOW	EDDY LOSS COEF
2	715.0	59400.		0.00
3	709.5	59400.	0.	0.00
5	697.5	59400.		0.00
6	697.0	59400.		0.00
8	696.3	59400.	0.	0.00
9	696.2	59400.		0.00
11	684.1	59400.		0.00
12	683.0	59400.		0.00
14	682.4	59400.		0.00
15	682.1	59400.		0.00
17	682.0	59400.		0.00
18	667.8	59400.		0.00
21	666.0	59400.	0.	0.00
21	665.9	59400.		0.00
23	665.1	59400.		0.00
24	664.7	59400.	0.	0.00
26	645.1	59400.		0.00
27	648.3	59400.		0.00
29	645.6	59400.		0.00
30	644.9	59400.		0.00

TIME STEPS = 36 TIME = 12.00 DATE 3/26/80

NET POINT									
1	OHIO R.	[illegible]							
2	OHIO R.	979.80	711.18	87321.	3.53	689.9966	1.4959	0.00001713	0.00	0.0
3	OHIO R.	977.80	[illegible]						
4	OHIO R.	975.80	[illegible]						
5	OHIO R.	975.40	699.23	87081.	2.67	679.9825	0.2681	0.00000308	0.00	0.0
6	OHIO R.	973.80	[illegible]						
7	OHIO R.	971.80	[illegible]						
8	OHIO R.	969.30	697.28	86237.	2.59	675.0032	0.5263	0.00000610	0.00	0.0
9	OHIO R.	[illegible]							
10	OHIO R.	[illegible]							
11	OHIO R.	965.80	685.88	85851.	3.52	664.9961	1.5151	0.00001765	0.00	0.0
12	OHIO R.	960.80	[illegible]		2.90	[illegible]				
13	OHIO R.	956.80	[illegible]		2.97	[illegible]				
14	OHIO R.	955.80	682.76	85014.	2.90	659.9984	0.6822	0.00000802	0.00	0.0
15	OHIO R.	953.80	[illegible]		2.97	[illegible]				
16	OHIO R.	951.80	[illegible]		2.97	[illegible]				
17	OHIO R.	950.30	682.00	84940.	1.55	650.0010	0.0582	0.00000069	0.00	0.0
18	[illegible]									
19	[illegible]									
20	OHIO R.	942.80	667.31	83901.	3.12	645.0039	0.8902	0.00001061	0.00	0.0
21	OHIO R.	[illegible]								
22	OHIO R.	[illegible]								
23	OHIO R.	935.80	665.68	83305.	2.52	640.0003	0.3655	0.00000438	0.00	0.0
24	OHIO R.	[illegible]	[illegible]	83151.	2.23	[illegible]				
25	[illegible]									
26	OHIO R.	926.50	651.80	83113.	3.42	629.9918	0.0695	0.00000084	0.00	0.0
27	[illegible]									
28	[illegible]									
29	OHIO R.	914.60	646.80	80936.	2.76	625.0007	0.5208	0.00000644	0.00	0.0

[illegible]	SCIOTO	3.90	500.5[illegible]	[illegible]	0.27	[illegible]	.0000	.000[illegible]	-0.00	0.0
295	SCIOTO	0.50	500.55	2751.	0.33	473.0000	0.0000	0.00000000	-0.00	0.0
296	LICKING	34.65	489.37	500.	1.94	466.6900	0.0392	0.00000785	0.00	0.0
297	LICKING	32.75	484.76	5000.	2.87	476.9967	0.1449	0.00002897	0.00	0.0
298	LICKING	29.80	471.20	5000.	1.81	470.0000	0.0361	0.00000722	0.00	0.0
299	LICKING	28.50	471.16	500.	7.14	465.0015	0.1282	0.00002563	0.00	0.0
300	LICKING	21.55	466.83	4999.	1.84	455.0033	0.0158	0.00000317	0.00	0.0
301	LICKING	17.50	465.64	4998.	1.15	450.0002	0.0029	0.00000057	0.00	0.0
302	LICKING	14.50	464.68	4994.	1.21	453.0000	0.0040	0.00000049	0.00	0.0
303	LICKING	8.32	463.74	4997.	0.98	450.0000	0.0021	0.00000042	0.00	0.0
304	LICKING	4.12	463.41	4978.	0.67	429.0000	0.0003	0.00000006	0.00	0.0
305	LICKING	0.50	467.50	4979.	0.72	429.0000	0.0003	0.00000006	0.00	0.0
306	G. MIAM	34.00	542.01	6335.	3.34	533.0265	0.5054	0.00007978	0.00	0.0
307	G. MIAM	31.50	532.16	6331.	2.49	522.0095	0.0780	0.00001232	0.00	0.0
308	G. MIAM	27.50	527.54	6331.	2.20	516.9765	0.0475	0.00000749	0.00	0.0
309	G. MIAM	23.50	511.65	6339.	4.90	501.0000	1.3182	0.00020795	0.00	0.0
310	G. MIAM	19.60	495.68	6339.	2.33	481.0208	0.0629	0.00000992	0.00	0.0
311	G. MIAM	16.10	487.45	6339.	3.04	477.9971	0.2537	0.00004004	0.00	0.0
312	G. MIAM	12.50	475.18	6335.	3.28	461.0003	0.2338	0.00003690	0.00	0.0
313	G. MIAM	8.50	462.89	6337.	3.00	451.0016	0.2381	0.00003761	0.00	0.0
314	G. MIAMI	4.00	459.16	6333.	0.63	443.0017	0.0006	0.00000009	0.00	0.0
315	G. MIAM	0.50	452.84	6324.	0.41	435.9983	0.0001	0.00000002	0.00	0.0
316	KENTUCK	30.00	7456.25	34200.	2.81	419.9983	0.2075	0.00000606	0.00	0.0
317	KENTUCK	27.05	455.54	34200.	2.80	417.9990	0.2551	0.00000746	0.00	0.0
318	KENTUCK	23.00	450.52	34200.	2.21	416.9998	0.2237	0.00000654	0.00	0.0
319	KENTUCK	19.00	448.47	34200.	0.49	416.9992	0.0491	0.00000143	0.00	0.0
320	KENTUCK	15.00	446.96	34200.	3.08	412.9966	0.3254	0.00000952	0.00	0.0
321	KENTUCK	11.00	446.16	34200.	1.43	411.9969	0.0983	0.00001437	0.00	0.0
322	KENTUCK	7.00	444.00	34200.	1.70	407.9925	0.6673	0.00001952	0.00	0.0
323	KENTUCK	3.00	443.475	34199.	4.13	404.9996	1.1255	0.00003291	0.00	0.0
324	[illegible]	[illegible]	[illegible]	34198.	[illegible]	[illegible]	[illegible]	[illegible]	[illegible]	[illegible]
325	[illegible]	[illegible]	[illegible]	[illegible]	2.80	350.9821	0.1718	0.00001571	[illegible]	[illegible]
326	GREEN	59.33	356.21	1260.	1.85	338.0008	0.0279	0.00000217	0.00	0.0

APPENDIX C: NOTATION

A	Total cross-sectional area of channel
A_f	Cross-sectional area of floodplain
A_x^y	Derivative of A with respect to channel distance at a constant flow depth
B	Top width of water surface
C_s	Average suspended sediment concentration
C_{WL}	Wash-load concentration
C_1, C_2, C_3	Coefficients in the sediment transport function
E	Coefficient in difference equations
f	General function
g	Acceleration due to gravity, general function
H	Height of water over a levee
h	Water-surface elevation
K	Coefficient in difference equations
K_e	Coefficient in eddy head loss term
L	Coefficient in solution scheme
M	Coefficient in solution scheme
n	Coefficient in Manning's equation
p	Porosity of bed layer
P	Wetted perimeter of a section
q	Unit lateral outflow from levee overtopping
q_ℓ	Unit lateral inflow rate of water
q_{ℓ_1}	Unit lateral outflow rate of water to the floodplain
q_{ℓ_2}	Unit lateral inflow rate of water from a tributary
q_s	Unit lateral inflow rate of sediment
q_{s_1}	Unit lateral inflow rate of sediment from a tributary
q_{s_2}	Unit lateral outflow rate of sediment to the floodplain
Q	Flow discharge
Q_s	Sediment discharge
Q_{WL}	Wash-load discharge

R	Hydraulic radius
S_e	Eddy head loss term
S_f	Friction slope
S_x	Slope of channel bed
t	Time
V	Average flow velocity
x	Longitudinal distance
y	Vertical distance
Y	Flow depth
Z	Elevation of channel bed
Δh	Change in water-surface elevation
Δt	Computational time-step
ΔZ	Bed layer thickness
ΔZ_f	Change in height of natural levees
ΔZ_{WL}	Change in height of wash load deposited on floodplain
α	Energy correction factor
β	Momentum correction factor
ρ	Density of sediment-water mixture
ρ_s	Density of sediment
ρ_w	Density of water
τ_o	Shear stress
$\partial/\partial t$	Derivative with respect to time
$\partial/\partial x$	Derivative with respect to channel distance
ϕ	Arbitrary variable
ϕ_i^n	Variable evaluated at i^{th} net point at the n^{th} time-step
ξ	Width function
η	Integration variable

In accordance with letter from DAEN-RDC, DAEN-ASI dated 22 July 1977, Subject: Facsimile Catalog Cards for Laboratory Technical Publications, a facsimile catalog card in Library of Congress MARC format is reproduced below.

Johnson, Billy H.
Development of a numerical modeling capability for the computation of unsteady flow on the Ohio River and its major tributaries / by Billy H. Johnson (Hydraulics Laboratory, U.S. Army Engineer Waterways Experiment Station). -- Vicksburg, Miss. : The Station ; Springfield, Va. ; available from NTIS, 1982.
154 p. in various pagings : ill. ; 27 cm. -- (Technical report ; HL-82-20)
Cover title.
"August 1982."
Final report.
"Prepared for U.S. Army Engineer Division, Ohio River."
Bibliography: p. 46.

1. Computer programs. 2. FLOWSED (computer program). 3. Mathematical models. 4. Ohio River. I. United States. Army. Corps of Engineers. Ohio River Division.

Johnson, Billy H.
Development of a numerical modeling capability : ... 1982.
(Card 2)

II. U.S. Army Engineer Waterways Experiment Station. Hydraulics Laboratory. III. Title IV. Series: Technical report (U.S. Army Engineer Waterways Experiment Station) ; HL-82-20.
TA7.W34 no.HL-82-20

END

FILMED